

Copyright
by
Gregory John Gabriel
2004

**The Dissertation Committee for Gregory John Gabriel certifies that this is
the approved version of the following dissertation:**

**Exploiting Aromatic Donor-Acceptor Recognition
in the Folding and Binding of Naphthyl Oligomers**

Committee:

Brent L. Iverson, Supervisor

Eric V. Anslyn

Michael J. Krische

Paul F. Barbara

Venkat Ganesan

**Exploiting Aromatic Donor-Acceptor Recognition
in the Folding and Binding of Naphthyl Oligomers**

by

Gregory John Gabriel, B.S.

Dissertation

Presented to the Faculty of the Graduate School of

The University of Texas at Austin

in Partial Fulfillment

of the Requirements

for the Degree of

Doctor of Philosophy

The University of Texas at Austin

August 2004

Dedication

To my family

Acknowledgments

I am indebted to my advisor, Professor Brent Iverson. His example was a constant motivation for me to conduct research meticulously and to improve as a teacher. I can recall many situations when his fairness, creativity, tact, business sense, etc, have shown me that opportunities to advance our ideas and science can be extracted from even the most frustrating of situations. I leave the Iverson group with this belief a permanent part of me.

I thank my defense committee members Professors Eric Anslyn, Michael Krische, Paul Barbara, and Venkat Ganesan for providing a refreshing new point of view of my work. I thank the wonderful people at NYU including Professor Jim Canary, Yu-Hung Chiu, and Lei Zhu. I deeply appreciate all the friendly people at UT and the talented Iverson lab members. “This crew is good.”

I want to thank several people in particular. Andy Zych and Mark Olsen for early lessons in constructive skepticism and for their continued friendship. Steve Sorey for his abundant patience. Yeonsuk Roh for our coffee breaks and six months of phone calls to get my behind moving. Joe Reczek for timely research suggestions and getting the aforementioned behind out of trouble (My apologies. You guys really weren’t hiding my final). Karl Griswold for his impressions (Prof. Mickey Mouse and Det. Whatman) and providing a nurturing environment for ridiculous conversations and uncomfortable situations. Jeeyeon Lee for being a great labmate and classmate. She supported my ideas at group meeting, challenged me in lab, gladly fed me humble pie when I deserved it, and always gave me a thoughtful, honest opinion. I was very fortunate.

I thank my brothers whose talks of escherchers, coelenterates, perpetual motion, etc, have inspired their older brother. Most of all, I thank my parents for their love and advice in all matters truly important to me.

Don't worry about people stealing your ideas.

If your ideas are any good, you'll have to ram them down people's throats.

Howard Aiken

Exploiting Aromatic Donor-Acceptor Recognition in the Folding and Binding of Naphthyl Oligomers

Publication No. _____

Gregory John Gabriel, Ph.D.

The University of Texas at Austin, 2004

Supervisor: Brent L. Iverson

Biomolecules, for example, DNA and enzymes, perform nearly all the chemical processes essential for life. Their functions are dependent though on their ability to fold and bind into precise three-dimensional conformations and assemblies. A variety of oligomers that adopt compact conformations in solution, termed foldamers, have been synthesized to elucidate strategies to control folding and binding akin to biomolecules.

The Iverson group has been developing a class of foldamers, called aedamers, which employ the aromatic-aromatic complexation between electron-rich 1,8-dialkoxy-naphthalene (Dan) and electron-deficient 1,4,5,8-naphthalene-

tetracarboxylic diimide (Ndi) “building blocks”. It is expected that further work with these naphthyl oligomers will help establish aromatic interactions as a reliable tool for the construction of water-stable assemblies with tunable and predictable properties not found in nature.

Overall, this dissertation describes the group’s first attempts to test the structural “designability” of naphthyl oligomers of previously unexplored sequences. Bottomline is that these studies have utilized the Dan:Ndi interaction to dictate *intra*- and *inter*- molecular associations to afford distinct folding topologies and achieve selective binding, respectively.

Chapter 2 reports the observation that a previously studied amphiphilic aedamer happens to be an effective refolding inhibitor of RNase thus introducing the prospect of aedamer-protein interactions, a long-standing aim for these molecules. Chapter 3 presents the “shuffling” of the aedamer sequence $(\text{DanNdi})_n$ to afford naphthyl oligomers, of the form $\text{Dan}_{n+1}\text{Ndi}_n$, that adopt turn structures. The results here demonstrate the ability of foldamers to access various secondary structures through changes to their primary sequence analogous to proteins. Chapter 4 details the first hetero-duplex system to operate via aromatic interactions in aqueous solutions. Dan_n and Ndi_n complementary strands exhibit high binding affinities and chain discrimination. The ability of the Dan:Ndi association to direct binding is expected to be extensively used by the laboratory to create discrete assemblies.

As a whole, these projects probe the folding and binding of naphthyl oligomers in a variety of situations to demonstrate the wide reach of directed aromatic interactions to create various architectures. With this level of control established, surface patterning for microarrays, functional artificial proteins, biomolecule-aedamer ensembles, and other application-driven pursuits using naphthyl oligomers are possible in the near future.

Table of Contents

Acknowledgments	v
Abstract	vii
List of Figures	xii
List of Tables	xxii

Chapter 1

From Aedamers to Aromatic Interactions to Naphthyl Oligomers	1
1.1 Foldamers as Models of Higher-Order Structure	1
1.1.1 β -Peptides	7
1.1.2 Peptoids	9
1.1.3 Oligo(<i>meta</i> -Phenylene Ethynylene)s	10
1.1.4 Aedamers	11
1.2 Update: Foldamers with Aedamer-Like Designs	15
1.3 Closer Examination of Aedamer Aromatic Interactions	17
1.3.1 Forces that Dictate Folding	17
1.3.2 Detailed Picture of Folding	22
1.4 Overview of Naphthyl Oligomer Projects	26

Chapter 2

Intriguing Heat-Triggered Behavior of an Amphiphilic Aedamer	33
2.1 Chapter Summary	33
2.2 Background: A Foldamer that Forms Stable Gels in Water	35
2.3 Results and Discussion	40
2.3.1 Synthesis of Aedamer Derivatives	40
2.3.2 UV-Vis, NMR, and LS Comparisons at 25° C	42
2.3.3 Evaluation of UV-Vis, NMR, and LS Data	48

2.3.4 Concentration Dependent Gelling Studies	49
2.3.5 Discussion of Thermal Gelling Data	51
2.3.6 Exploring Aedamer-Protein Interactions	51
2.3.7 Fluorometric Assay of RNase Activity	55
2.3.8 Discussion of Refolding Inhibition Data	59
2.4 Chapter Conclusions	61
2.5 Ideas for Future Investigations	62
2.6 Experimental Section	64

Chapter 3

Altering the Folding Patterns of Naphthyl Oligomers	73
3.1 Chapter Summary	73
3.2 Background: Mimics of Biological Hairpin Structures	75
3.3 Results and Discussion	79
3.3.1 Synthesis of Non-Alternating Naphthyl Trimers	79
3.3.2 UV-Vis Spectroscopy	82
3.3.3 Evaluation of UV-Vis Data	83
3.3.4 Unfolding Studies by UV Spectroscopy	90
3.3.5 NMR Techniques for Proton Assignment	92
3.3.6 NOESY Spectroscopy	95
3.3.7 Computer Modeling	98
3.3.8 Evaluation of NMR Data and Computer Modeling	101
3.3.9 Preliminary Studies of a Potential Hairpin Pentamer	105
3.4 Chapter Conclusions	107
3.5 Ideas for Future Investigations	107
3.6 Experimental Section	109

Chapter 4

Naphthyl Oligomers that Form Hetero-Duplexes	122
4.1 Chapter Summary	122
4.2 Background: Self-Assembly of Molecular Strands	124
4.3 Results and Discussion	131
4.3.1 Synthesis of Homo-Naphthyl Oligomers	131
4.3.2 NMR Job Plots and Titrations	132
4.3.3 Evaluation of One-to-One Binding	134
4.3.4 Isothermal Titration Calorimetry (ITC)	135
4.3.5 Summary of Binding Data	141
4.3.6 Examination of Heat Capacity	144
4.3.7 Size Exclusion Chromatography (SEC)	147
4.3.8 Polyacrylamide Gel Electrophoresis (PAGE)	150
4.3.9 Discussion of SEC and PAGE Results	152
4.4 Chapter Conclusions	154
4.5 Ideas for Future Investigations	154
4.6 Experimental Section	156

Chapter 5

Final (Personal) Remarks	176
References	178
Vita	192

List of Figures

Chapter 1

Figure 1.1	A ribbon representation of a hemoglobin complex and a diagram of the unwinding of a chromosome (adapted from http://www.psc.edu/MetaCenter/MetaScience/Articles/Ho/Ho-hemoglobin.html , Copyright 1993 University of Pittsburgh Supercomputing Department and http://www.accessexcellence.org/AB/GG/chromosome.html , Copyright 2004 the National Human Genome Research Institute.	2
Figure 1.2	Examples of the different types of foldamer architectures. Boxed are the most prevalent natural secondary structures (adapted from Hill 2001).	6
Figure 1.3	A) A sampling of various nonnatural amino acids. B) Helical conformation of a representative β -peptide from crystallography data (from Appella 1996). C) β -peptide studied for its biological activity.	8
Figure 1.4	A) General structure of peptoids and side chain examples. B) Cationic 36-mer peptoid effective as a gene delivery reagent.	9
Figure 1.5	A) Example of an oligo(<i>m</i> -PE). B) Proposed helical folding (from Hill 2001). C) Terpene examples used in molecular recognition studies.	11
Figure 1.6	A) Chemical structure of an aedamer hexamer designed by Lokey and Iverson (Lokey 1995). B) Idealized model of the pleated folding pattern and absorption signatures (in the UV and visible range) that support face-centered stacking of aromatics. Dotted arrows indicate the change in the spectrum upon the denaturing of the aedamer hexamer caused by CTAB addition.	13

Figure 1.7	Cartoon representations of recent foldamers reminiscent of the aedamer design. A) Stacked structure using water-solubilizing guanidine linkers. (Tanatani 1998) <i>B</i> = <i>m</i> - or <i>p</i> -substituted benzene. B) System using hexasubstituted benzenes (Zhang 2003). <i>CA</i> = crowded aromatic. C) Zipper-type system (Zhao 2004). <i>D</i> = donor, <i>A</i> = acceptor. D) Aromatic stacking polymer with cation binding (Ghosh 2004).	16
Figure 1.8	Compounds used in the monomer study and their associations (M^{-1}) in a few of the solvents reported (Cubberley 2001b).	18
Figure 1.9	Calculated electrostatic surface potentials and chemical structures of compounds used to obtain X-ray quality crystals (adapted from Cubberley 2001b). From inspection the expected desolvation driving force is strongest in an equimolar mixture of Dan and Ndi.	20
Figure 1.10	Early model systems to study aromatic interactions. A) Bicyclic cyclophane host/pyrene guest (from Smithrud 1991). B) Diarylnaphthalene system. <i>X</i> = various electron withdrawing and donating groups (Cozzi 1992). C) Diarylcarboxylate models. <i>R</i> = naphthalene or adenine (Newcomb 1994).	21
Figure 1.11	Aromatic region of the NMR spectra for a few of the compounds used for conformational analysis (Zych 2000).	23
Figure 1.12	Illustrated concept of conformational modularity and chart showing the high accuracy of chemical shift prediction when this concept is applied to larger aedamers (Zych 2001, 2002).	25
Figure 1.13	Projects in the Iverson laboratory designed to explore aromatic interactions. All work can trace its beginnings to Lokey's aedamer paper. Results detailed in chapter 2, 3, and especially 4 have led to several new research directions.	28
Figure 1.14	Cartoon representation of the naphthyl oligomers studied and the main question each project aimed to answer. Arrows indicate direction of growth for longer oligomers.	30

Chapter 2

Figure 2.1	Cartoon representation of the modular aedamer design showing the potential to decorate the periphery of the structure with chosen residues. X = amino acid side chain. SPPS = solid phase peptide synthesis.	34
Figure 2.2	Chemical structure of the original aedamer hexamer (Lokey 1995) and an amphiphilic derivative (Nguyen 1999).	36
Figure 2.3	Cartoon representation of the folded conformation. Graph of the kinetics of the conformational transition (dotted line) of the amphiphilic aedamer upon heating at 80° C, as monitored at the charge-transfer band absorbance of 526 nm (from Nguyen 1999). Solid line shows the kinetics of an identical solution except 10% of pregelled material was added before heating.	37
Figure 2.4	Proposed scheme for the thermal conversion of an aedamer solution to the tangled aggregate state (adapted from Nguyen 1999).	38
Figure 2.5	Compounds synthesized for the gelling study. A.A. 1-6 represents the amino acid linker positions along the backbone.	40
Figure 2.6	Dan and Ndi amino acid adducts synthesized and used in the standard solid phase oligo synthesis cycle. Full structures can be found in the Experimental Section. Fmoc = 9-fluoronylmethyloxycarbonyl. SPPS = solid phase peptide synthesis. LC = liquid chromatography.	42
Figure 2.7	Aromatic region of ¹ H-NMR spectra. Concentrations were 1.5 in mM D ₂ O. Even dilute solutions (0.1 mM) of 2.1 failed to give resolved spectra.	45
Figure 2.8	Scattering ratio, S ₉₀ , as a function of molality for penicillin in water. Dotted line below 0.04 m indicates the theoretical line for unassociated monomers and arrows denote the critical concentrations (Varela 1999).	46

Figure 2.9	Scattered light intensity as a function of concentration. The failure to describe data from solutions of 2.1 with a linear fit is normally indicative of a shift in solute size but at this point the discontinuity cannot be interpreted as a critical concentration.	47
Figure 2.10	Kinetics of the conformational transition of 2.1 and 2.2 at different concentrations. The loss of the CT band absorbances for 2.1 was a consequence of aedamer unfolding and "entangling" as a gel formed. For 0.1 mM solutions of 2.1 , a 1 cm cuvette was necessary to increase the CT signal above baseline noise while a 0.1 cm cuvette was used for the other solutions. 5.0 mM solutions of 2.2 had a CT corrected absorbance of 0.23 ± 0.04 at all times (not shown). Photographs of 2.1 and 2.2 after 150 min of heating are also included.	50
Figure 2.11	Primary structure of ribonuclease (RNase) indicating polar (green), hydrophobic (orange), basic (blue), and acidic (red) residues. Schematic of fluorometric assay adapted from the manual of the <i>RNaseAlert</i> kit sold by Ambion.	54
Figure 2.12	Compounds tested in the RNase inhibition study.	55
Figure 2.13	Fluorescence data of 2.1 at 120-0.15 μ M concentrations measured at 30 minute time intervals. Runs with 2.1 afforded moderate refolding inhibition. Neg = negative control. <i>Secure</i> = Ambion's commercially available RNase inhibitor, <i>RNasecure</i> . Pos = positive control.	57
Figure 2.14	Fluorometric assay results for 2.1 , 2.4 , and SDS with and without preheat treatment measured at 105 minutes. Only the 2.1 heat trial gave dramatically different results (~75% inhibition for 30 μ M solutions) than the other compounds and conditions.	58
Figure 2.15	Conditions to determine if a preformed tangled aggregate of 2.1 can enhance inhibition in the same manner that gelled 2.1 enhances gelation through a product promoted mechanism.	60

Chapter 3

Figure 3.1	Cartoon representation of two different folding patterns. Arrows indicate direction of growth with longer oligomers.	74
Figure 3.2	Hairpin peptides synthesized by Waters and co-workers (Tatko 2002, 2004). X = various sidechains to explore aromatic-aromatic and C-H $\cdots\pi$ interactions.	77
Figure 3.3	Donor-acceptor δ -peptides synthesized by Li and co-workers and a cartoon representation of their asserted “zipper” structure (Zhao 2004).	78
Figure 3.4	Design of a proposed hairpin pentamer.	80
Figure 3.5	Compounds synthesized for folding studies.	81
Figure 3.6	Cartoon representation showing A) the likelihood of some type of intermolecular stacking for 3.2 driven by the Dan:Ndi association and B) that intermolecular Dan:Ndi associations are not available if 3.1 , 3.3 , and 3.4 fold in the asserted manner. Double-headed arrows represent repulsion of the electron-rich π -clouds of two Dan units. C) Possible explanation of how trimers 3.5 and 3.6 could afford UV spectra similar to dimers.	86
Figure 3.7	Compounds analyzed by 2D NMR and idealized cartoon representations of possible solution conformations. Letter designation for NMR peak assignments for the Dan and Dan* units are given. Also shown is a design of a hairpin structure incorporating an intercalative fold (dotted boxed).	89
Figure 3.8	Unfolding curves displayed in two different forms.	90
Figure 3.9	Proton NMR spectra of the aromatic region representing 16 hydrogens for each spectrum. Spectra were taken at 1 mM concentrations in 50 mM Na phosphate D ₂ O.	93

Figure 3.10	Method of “walking” from the terminus of 3.4 in order to assign the Dan and Dan* hydrogen chemical shifts. Examples of key through-space (solid line) and through-bond (dotted line) H-H correlations are marked.	94
Figure 3.11	Expansion of NOESY spectrum for 3.1	96
Figure 3.12	Expansion of NOESY spectrum for 3.4	97
Figure 3.13	Expansion of NOESY spectrum for 3.6	98
Figure 3.14	Side view of the lowest energy conformers of 3.1 and 3.4 and axis view of the same conformers showing the general topology of the linkers. Arrows indicate the Dan/Dan* linkage. Hydrogens omitted (except for the aromatic of the side views) for clarity.	100
Figure 3.15	The assignment of the AA'BB' Ndi protons shown in a partial spectrum and chemical structure of 3.4	104
Figure 3.16	Pentamers used for preliminary studies on hairpin structures.	105
Figure 3.17	Aromatic region of NOESY spectrum.	106
Figure 3.18	Proposed oligomers for future study.	108
Figure 3.19	“Water” ROESY spectrum of 3.1	115
Figure 3.20	Expansion of “water” ROESY spectrum of 3.1	116
Figure 3.21	“Water” TOCSY spectrum of 3.4	117
Figure 3.22	Expansion of “water” TOCSY spectrum of 3.4	118
Figure 3.23	NOESY spectrum of 3.1	119
Figure 3.24	NOESY spectrum of 3.4	120
Figure 3.25	NOESY spectrum of 3.6	121

Chapter 4

Figure 4.1	Cartoon representation of a proposed hetero-duplex formed to maximize Dan:Ndi associations in an intermolecular fashion and critical questions answered in this project.	123
Figure 4.2	Aromatic π - π stacking system from Stoddart's laboratory (Ashton 1992).	127
Figure 4.3	X-ray crystal structure of Lehn's oligopyridinecarboxamide ($R^1 = R^2 = H$, $R^3 = O^tBu$) showing interstrand aromatic stacking and hydrogen bonding which includes two bridging NH-O hydrogen bonds. Crystals grown from $CH_3CN/DMSO$. (Berl 2000).	128
Figure 4.4	Proposed structure of zipper complex between two different aromatic amide oligomers showing hydrogen bonding and edge-to-face aromatic interactions (Bisson 2000).	129
Figure 4.5	A donor-acceptor tetrameric hetero-duplex formed with comb-type naphthyl oligomers (Zhou 2003).	130
Figure 4.6	Compounds synthesized and studied in Chapter 4. 13-atom linkers between naphthyl moieties were used.	131
Figure 4.7	Computer generated space-filled model (right structure is rotated by 90°) of the duplex formed from truncated 4.3 (black) and 4.4 (white). Linker atoms not along backbone path omitted for clarity.	132
Figure 4.8	NMR Job plots and titration curves for evaluating the complexation of monomers (4.1:4.2) and dimers (4.3:4.4) at $T = 318\text{ K}$	134

Figure 4.9	Binding isotherms for the titration of 4.7 with 4.8 at two different temperatures. Top panels display, the raw isotherm or the total heat evolved ($\mu\text{cal/sec}$) per injection of 4.8 (40 injections total). Data points in the bottom panels represent the heat evolved (kcal/mol) after correcting for heats of dilution. ITC data collected at $T = 298\text{ K}$ did not fit theoretical curves (line in bottom panels). Data collected at $T = 318\text{ K}$ on the other hand fitted predicted curves well according to a chi-square error analysis (Wiseman 1989, Microcal, Inc. 1999).	137
Figure 4.10	Representative binding isotherms at $T = 318\text{ K}$. Three trials were performed for each system. Fitted line was based on 40 injection data points but only every other point is shown for clarity.	139
Figure 4.11	Graph of the thermodynamic parameters taken from ITC experiments of 4.3:4.4 binding and table of the corresponding free energies.	145
Figure 4.12	UV chromatograph (270 nm) showing that solutions of 4.7 are aggregated (at the SEC conditions) but are effectively broken up by the addition of 4.8 as seen by the trace give the 1:1 molar mixture. Also the 1:1 mixture results in a complex with a distinctly different retention volume than either strand.	149
Figure 4.13	Photograph of gel from PAGE experiments. Arrow indicates direction of band migration.	151
Figure 4.14	Representative HOSTEST output for (4.1:4.2) binding at $T = 318\text{ K}$	162
Figure 4.15	Representative HOSTEST output for (4.3:4.4) binding at $T = 318\text{ K}$	163
Figure 4.16	Typical buffer into buffer titration that results in extremely small heats ($0.05\text{-}0.30\text{ kcal/mole}$) released per injection. For comparison the first couple of injections (same volume) in a tetramer run released 20 kcal/mole of heat.	166

Figure 4.17	Typical tetra-Dan injections into buffer. The small heats absorbed were taken into account when processing the tetramer runs where tetra-Dan 4.8 was injected into tetra-Ndi 4.7 . For all ITC data reported, heats of dilutions were subtracted from the titration runs to afford the heats associated with binding.	167
Figure 4.18	Unsuccessful reverse titration at T = 298 K where tetra-Ndi 4.7 was injected into tetra-Dan 4.8 . Even a two-sites binding model could not accurately describe the experimental data. All reported ITC data used a one-site binding model where the N value was allowed to vary.	168
Figure 4.19	A representative trimeric system run at T = 298 K. Though the chi-square value is 55,000 the fit appeared to be fairly accurate. On average the K_a (4.5:4.6) was $1.1 \times 10^5 \text{ M}^{-1}$ for the trimeric system at T = 298 K, more than twice as large as that measured at T = 318 K.	169
Figure 4.20	A tetrameric system run at T = 298 K. A chi-square value of 250,000 indicated an inability to describe the binding with a one sites model. Only about three-fourths of the curve fit the model possibly indicating a switch in binding stoichiometry at excess titrant (tetra-Dan 4.8) at room temperature.	170
Figure 4.21	Representative isotherm that afforded excellent results for the tetrameric system (T = 318 K). Notice the chi-square value was below 50,000 and the N value was within a 10% error of 1.0.	171
Figure 4.22	90 degree light scattering chromatograms of individual components and 1:1 molar mixture. Note that the intensity of the aggregate peak (1.5 mL) for the 1:1 mixture is less than half that of sample 4A, implying that some of the aggregates are broken during complex formation.	173

Figure 4.23 90 degree light scattering chromatograms of 1:1 molar complex
 10 minutes after preparation (15 minute of heating, 60°C)
 (green), 24 min (cyan), 79 min (red), 93 min (blue). The peak at
 1.5 mL is attributed to aggregates; peak at 2.7 mL is from the
 complex. (Author's comments – magnitude of 90 degree light
 scattered is dependent on size of aggregate or complex. See
 Figure 4.12 for a better quantitative idea of the amount of
 presumed 1:1 complex to aggregate.) 174

List of Tables

Table 2.1	Analyses at 25 °C for 2.1-2.4	43
Table 3.1	UV-Vis data for 3.1-3.6	83
Table 4.1	Summary of hetero-duplex binding data.	141
Table 4.2	NMR data for Job plots and titrations.	161
Table 4.3	Complete hetero-duplex binding data.	165

CHAPTER 1

From Aedamers to Aromatic Interactions to Naphthyl Oligomers

1.1 FOLDAMERS AS MODELS OF HIGHER-ORDER STRUCTURE

Although biological molecules such as proteins and DNA are inherently complex due to the wide range of cellular functions they carry out, their primary architecture is surprisingly not at all that intricate. Most proteins and DNA are simply long chain molecules synthesized in the cell from a set of monomeric building blocks, twenty amino acids for proteins and a mere four nucleic acids for DNA. As shown in Figure 1.1, these string-like molecules can be thought of as necklaces in a way, with each amino acid residue (R) or nucleic acid base (B) acting as a bead along a strand. Though the linear (or primary) sequence of beads is important, these chain molecules are only functional after they adopt a three-dimensional structure through specific folding and binding. For instance hemoglobin, a transport protein that delivers oxygen, is made up of four polypeptide chains that are folded and bound together. In another example, uncoiling a human chromosome, which is about five micrometers long, results in a piece of DNA 10,000 times that length. This piece of DNA can then be recognized as having the familiar double-helix conformation formed by two complementary strands. It is this higher-order structure (the precise folding and binding) that positions functional groups properly and endows biomolecules with their important properties.

Biological Molecules Resemble Strands of Beads

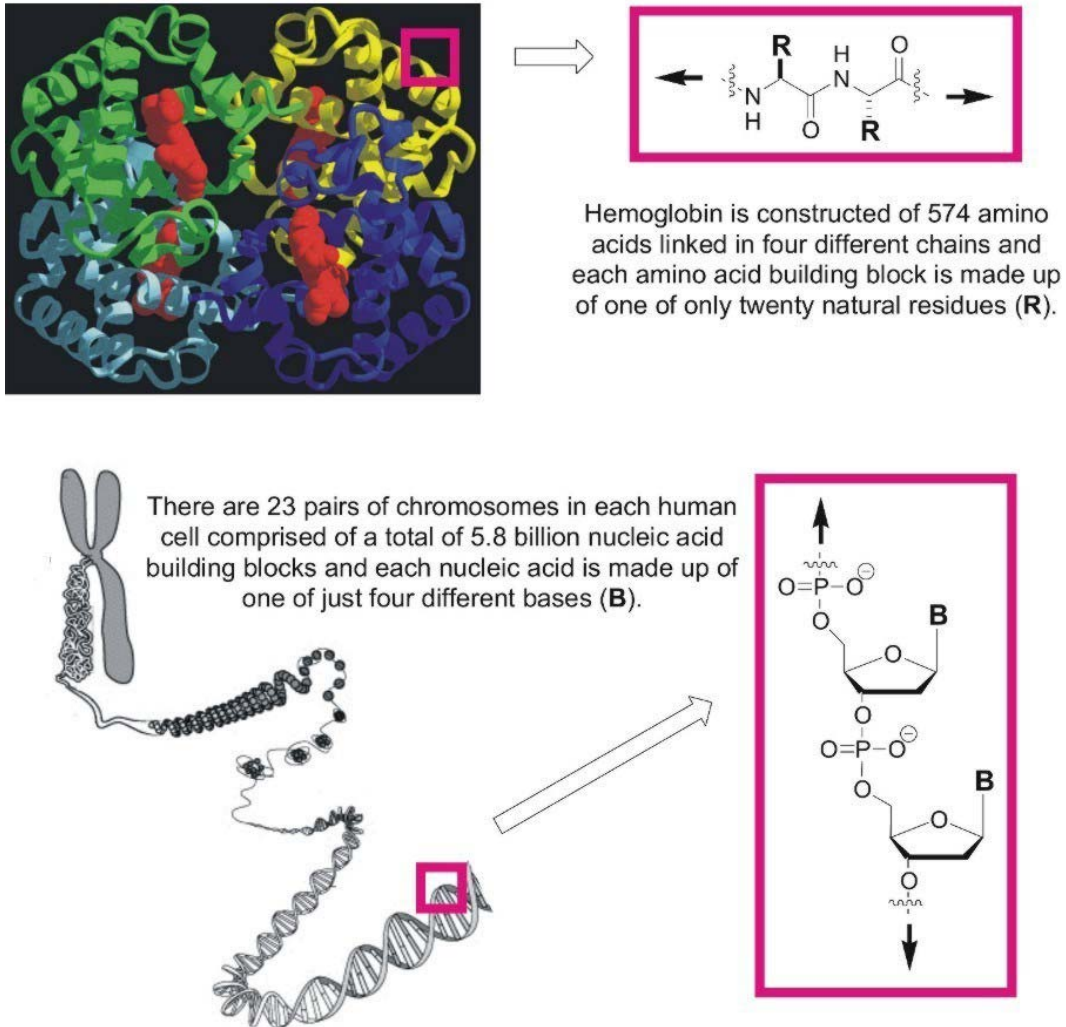


Figure 1.1 A ribbon representation of a hemoglobin complex and a diagram of the unwinding of a chromosome (adapted from <http://www.psc.edu/MetaCenter/MetaScience/Articles/Ho/Ho-hemoglobin.html>, Copyright 1993 University of Pittsburgh Supercomputing Department and <http://www.accessexcellence.org/AB/GG/chromosome.html>, Copyright 2004 the National Human Genome Research Institute.

The necessity for *specific folding* and *selective binding* in order to arrange the numerous functional groups of biomolecules into precise and chemically useful positions can hardly be overstated. To sum up: *Structure is crucial for function in all biopolymers*. Without the many types of noncovalent molecular attractions (hydrogen bonding, ionic interactions, metal-complexation, and aromatic stacking to name a few), which constitute the driving forces for folding and binding, a cell would closely resemble a disordered jewelry box of tangled necklaces.

There have been significant efforts to understand the folding of natural biomolecules in relationship to its structure along with its function and malfunction (i.e. disease). More reliable three-dimensional structure prediction from the primary sequences of proteins may ultimately lead to widespread use of enzymes and antibodies with tailored activities. Scientists are also motivated to elucidate the folding mechanisms of particular proteins to provide a better understanding of illnesses such as Alzheimer's and Creutzfeldt-Jakob's disease, both of which are neuro-degenerative diseases involving irreversible protein-*misfolding* events (Buxbaum 2000).

Rather than constructing derivatives of known proteins and natural DNA to create and study molecules with biological complexity, several chemistry research groups, both in academia and industry, are using a complementary approach to develop macromolecules possessing well-defined folding and in a growing number of cases, designed functions. Organic chemists have synthesized artificial folding chain-like molecules that promise to open up avenues to new

types of self-organizing polymers in part because they are not constrained to use the limited set of natural building blocks mentioned above (Hill 2001, Cubberley 2001a). Also the reliance on reversible noncovalent interactions rather than covalent bonds to drive assembly allows for exploring many different chain conformations and could lead to distinct abiotic folding motifs, which may afford activities not necessarily evolved in nature.

In classifying these folding molecules, Gellman first coined the term “foldamer” in a 1998 article “to describe any polymer with a strong tendency to adopt a specific compact conformation” (Gellman 1998). While proteins and DNA are by definition natural foldamers and their general structures have been elucidated more than fifty years ago, this account was extremely timely considering that *nonnatural* foldamers were emerging as useful tools for investigating the use of noncovalent interactions to access supramolecular structures. Since then there has been increased activity in the field and Moore, and co-workers have published a comprehensive review in 2001 entitled “A Field Guide to Foldamers” (Hill 2001). Here, they updated the definition of foldamers to, “any oligomer that folds into a conformationally ordered state in solution, the structures of which are stabilized by a collection of noncovalent interactions between nonadjacent monomer units. There are two major classes of foldamers: single-stranded foldamers that only fold (peptidomimetics and their abiotic analogues) and multiple-stranded foldamers that both associate and fold (nucleotidomimetics and their abiotic analogues).” The above definition is

appropriate for the purposes of this dissertation and the use of the term foldamer(s) will explicitly refer only to the synthetic, nonnatural variety.

Research in foldamers has attracted scientists from many different fields. What engages scientists in organic and computational chemistry, biology, physics, engineering and many other disciplines is the mix of projects spanning basic research and applied science and the often serendipitous interplay between these two motivations. Whether the aims of these research programs are the basic understanding of interesting phenomena or the application of foldamers such as for molecular recognition, the foremost goal is to synthesize novel chain molecules that possess some type of stable secondary structure in solution based on noncovalent interactions. Natural biomolecules use this organizational strategy and provide a seemingly infinite number of examples of how to use secondary structures to tune chemical properties and impart function (Wang 2001, Venkatraman 2001, Anfinsen 1967). The prevalent secondary structures found in nature are the α -helices and the β -sheets along with the B-form helix of DNA. Illustrated in Figure 1.2 are a couple of the topologies (natural and artificial) that have been achieved by foldamers.

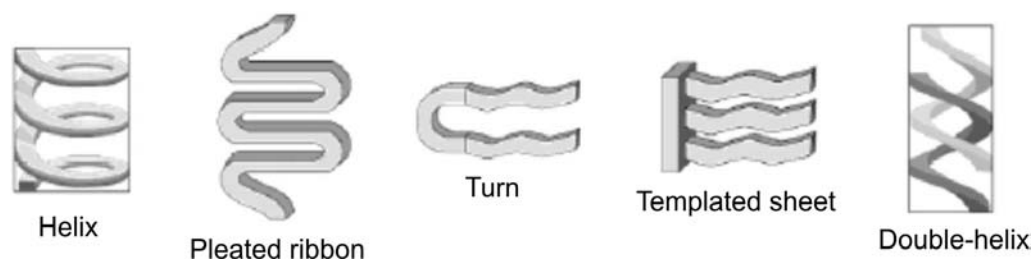


Figure 1.2 Examples of the different types of foldamer architectures. Boxed are the most prevalent natural secondary structures (adapted from Hill 2001).

Reprinted with permission from Hill, D. J.; Mio, M. J.; Prince, R. B.; Hughes, T. S.; Moore, J. S. *Chem. Rev.* **2001**, *101*, 3893. Copyright 2001 American Chemical Society.

Currently, the most widely studied foldamers include the β -peptides, the peptoids, and the oligo(*m*-phenylene ethynylene)s which all display helical secondary structure. The Iverson group has also been developing foldamers, called aedamers (described in detail later), constructed of electrostatically-paired naphthalenes that adopt not a spiral but a “pleated ribbon” pattern (Figure 1.2). These four systems represent a broad sampling of foldamer research since they 1) make use of several types of noncovalent interactions to control solution structure, 2) can exhibit well-defined conformations in organic and/or aqueous solutions, 3) give examples of three classes of foldamers as first outlined by Zych: the biomimetic, transitional and bio-inspired foldamers (Zych 2001) and 4) span a wide range of properties and functions dependent on their secondary structure.

Before examining each of these four foldamers briefly, it should be noted that the majority of the successes in this area of chemical research deal directly with the detailed characterization of secondary structure and the basic understanding of how different attractive forces add up and contribute to this

structure. Initial attempts though at tertiary structure (an association of distinct secondary structures on one strand) are beginning to be reported. By extension, quaternary structures (an ordered bundle made up of more than one strand like hemoglobin) are also being pursued. Finally, as this field matures and as chemists become more adept at fine-tuning folding and binding properties, more uses for foldamers will be discovered. Examples of these higher-order structures and published applications will be included in the descriptions of these four foldamers below.

1.1.1 β -Peptides

The artificial β -amino acids that make up β -peptides are structurally similar to natural α -amino acids and therefore have the benefit of well-established characterization techniques provided by decades of protein research. (Ramachandran 1968, Brandon 1999). The synthesis of many types of β -amino acids, including those with R groups identical to natural amino acids and those incorporating rigid *cis* or *trans* rings (Figure 1.3A), make it possible to construct a wide variety of β -peptides. The majority of β -peptide research has come independently from the Seebach (Seebach 1998) and Gellman (Appella 1996) groups and an informative review by DeGrado and Gellman entitled " β -Peptides: From structure to function" was published in 2001 (Cheng 2001).

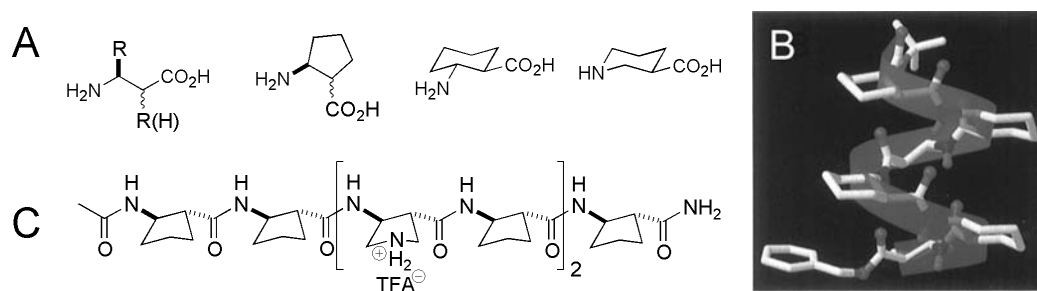


Figure 1.3 A) A sampling of various nonnatural amino acids. B) Helical conformation of a representative β -peptide from crystallography data (from Appella 1996). C) β -peptide studied for its biological activity.

Reprinted with permission from Appella, D. H.; Christianson, L. A.; Karle, I. L.; Powell, D. R.; Gellman, S. H. *J. Am. Chem. Soc.* **1996**, *118*, 13071. Copyright 1996 American Chemical Society.

In terms of folding propensities, exquisite control of stable helix formation via hydrogen bonding (Figure 1.3B) has been demonstrated, originally in organic solvents. Even the number of units per turn (from 3.4 residues per turn to more compact turns) can be designed into the oligomer (Appella 1997). Because of the their close relation in chemical structure and conformation to naturally occurring peptides, β -peptides have been categorized as biomimetic foldamers (Zych 2001). Considering this, it is not surprising that β -peptides have been reported showing strong helix formation in aqueous solutions (Appella 2000). Additionally, groups are starting to rationally design β -peptides to mimic turns (Langenhan 2004), β -sheet secondary structures (Seebach 1999), and tertiary structures (Cheng 2001) using exclusively β -amino acids. The ability of β -peptides to resist general enzymatic degradation (Frackenhohl 2001) makes them potential bioactive agents as well and animal studies have shown promising results (Weigard 2002). Other biological activities include inhibition of cholesterol and fat adsorption (Werder

1999) and antibiotic effects (Liu 2001) (Figure 1.3C). Lastly, γ - and δ -peptides, though first studied long before Gellman's introduction of the term foldamer, have been recently reinvestigated in the context of foldamer development (Brenner 2001).

1.1.2 Peptoids

In 1992, the Zuckermann research team from the Chiron Corporation introduced oligomers constructed of *N*-substituted glycines termed peptoids, (Simon 1992). Since then, many different pendant side groups have been attached to the amide nitrogen including those that incorporate chirality (Figure 1.4A).

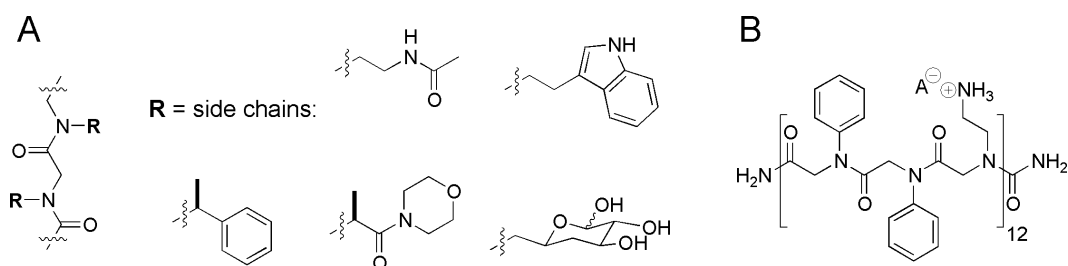


Figure 1.4 A) General structure of peptoids and side chain examples. B) Cationic 36-mer peptoid effective as a gene delivery reagent.

Zuckermann's group has shown that peptoids adopt helical conformations in both aqueous and organic solvents (Kirshenbaum 1998). This helix formation occurs without the stabilization benefits of amide hydrogens participating in intramolecular hydrogen-bonding found in natural helical peptides and β -peptides. Secondly, low energy conformations of the tertiary amides along the backbone exist in both the *cis* and *trans* isomer states, while peptide bonds that connect natural amino acids are almost exclusively in the *trans* state which aids in

the structural organization of natural peptides. It has been postulated that the steric limitations of peptoids with chiral bulky side chains limit the set of available conformations and general solvophobic interactions also contribute to the stability of peptoids (Armand 1997, Wu 2001a, b). These key differences from both α and β -peptides place peptoids in the transitional class of foldamers. Just as the β -peptides though, peptoids are resistant to proteases and analogues of natural peptide ligands have shown effective biological activity (Simon 1992). Peptoids have even been shown to have good transfection (specifically lipofection) activity, which is useful for gene delivery therapies (Murphy 1998, Figure 1.4B).

1.1.3 Oligo(*meta*-Phenylene Ethynylene)s

Moore and co-workers have published extensively on oligo(*meta*-phenylene ethynylene)s, also known as oligo(*m*-PE)s (Figure 1.5A). These foldamers also adopt helical conformations employing solvophobic interactions and local geometric constraints along the backbone to stabilize folding (Hill 2001) (Figure 1.5B). These molecules are considered to be in the bio-inspired class of foldamers in which there is little relation to any natural system and many times applications lean towards material science rather than protein emulation (Mio 2000). The first generation of oligo(*m*-PE)s varied in length and pendant groups and demonstrated the manipulation of the conformational transition via changes in solvent and temperature (Nelson 1997). Additionally, twist-sense preferences by means of a chiral perturbation in the side chains (Prince 2000a) or backbone (Gin 1999) have also been reported.

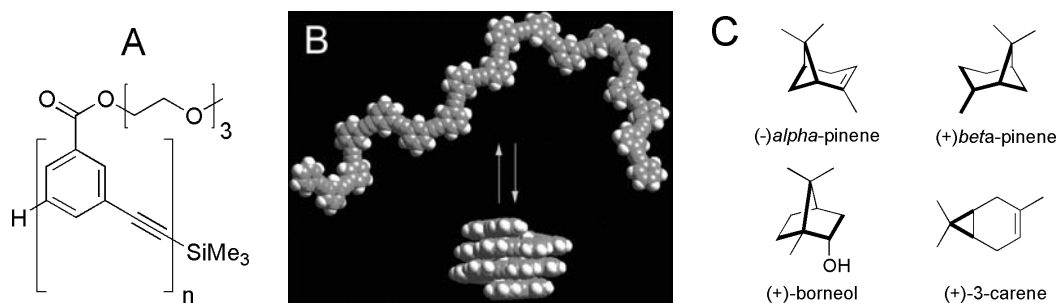


Figure 1.5 A) Example of an oligo(*m*-PE). B) Proposed helical folding (from Hill 2001). C) Terpene examples used in molecular recognition studies.

Reprinted with permission from Hill, D. J.; Mio, M. J.; Prince, R. B.; Hughes, T. S.; Moore, J. S. *Chem. Rev.* **2001**, *101*, 3893. Copyright 2001 American Chemical Society.

Numerous analytical studies (UV-Vis, fluorescence, circular dichroism, and NMR spectroscopy) support the proposed helical conformation and observed twist-sense. These studies have even led to the design of properly sized cavities for molecular recognition. 12-mers can function as receptors for various monoterpenes displaying association strengths in the 10^3 M^{-1} range and modest selectivities in polar solvents (Prince 2000b, Figure 1.5C). Other oligo(*m*-PE)s have been derivatized to accept rodlike guests as well, such as diphenylpiperazines, in order to template the growth of chains of specific length (Tanatani 2001). Finally, Moore and co-workers have recently published the synthesis of a new water-soluble oligo(*m*-PE) (Stone 2004).

1.1.4 Aedamers

In 1995 Lokey and Iverson described the first foldamers to make use of aromatic stacking interactions in water to direct folding (Lokey 1995). These molecules utilize the hydrophobically-driven face-to-face complexation between

electron-rich 1,5-dialkoxynaphthalene (Dan) and electron-deficient 1,4,5,8-naphthalenetetracarboxylic diimide (Ndi) units to attain a compact conformation (Figure 1.6A). When these two moieties were linearly connected with appropriately flexible linkers, and in an alternating fashion, the resulting oligomer adopted an entirely abiotic secondary structure, a pleated fold conformation, in water (Figure 1.6B, Lokey 1995). These molecules were termed aedamers after the aromatic electron donor-aceptor interactions that direct folding, and just as the oligo(m-PE)s, these aromatic containing foldamers belong also to the bio-inspired class of foldamers.

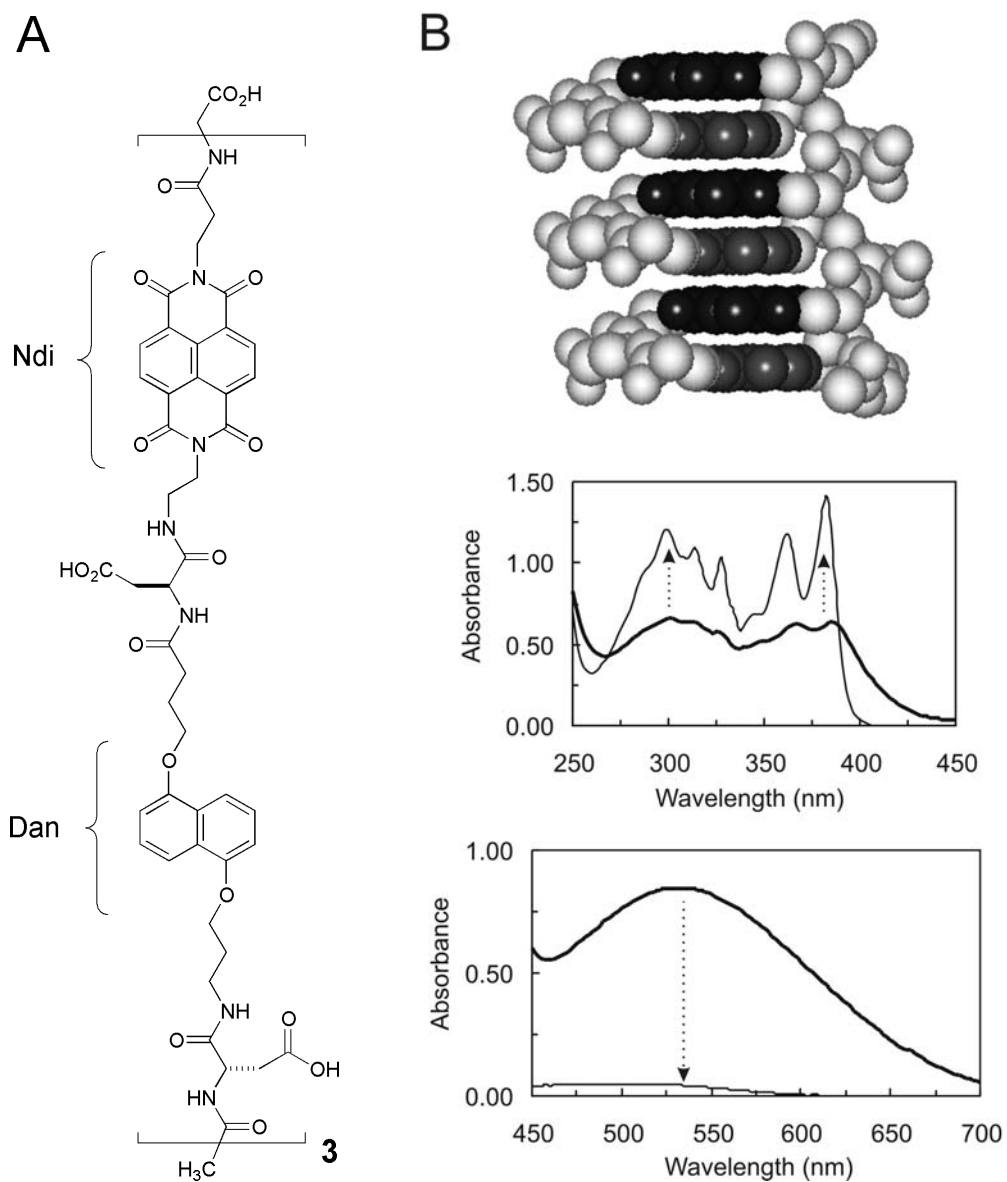


Figure 1.6 A) Chemical structure of an aedamer hexamer designed by Lokey and Iverson (Lokey 1995). B) Idealized model of the pleated folding pattern and absorption signatures (in the UV and visible range) that support face-centered stacking of aromatics. Dotted arrows indicate the change in the spectrum upon the denaturing of the aedamer hexamer caused by CTAB addition.

A prominent feature of aedmaers is the modular design that allows facile solid-phase synthesis plus the incorporation of a wide variety of linkers that might possibly be used to modify folding and binding properties. There are also useful spectroscopic handles that are consistent with aedamers adopting a folded conformation in solution. Hypochromism (such as that found with DNA base stacking) and the existence of a charge transfer band are consistent with face-to-face ring stacking arrangements (Lokey 1995, 1997, Cantor 1980, Figure 1.6B). Under denaturing conditions such as with the addition of the cationic detergent cetyltrimethylammonium bromide (CTAB), these spectroscopic signatures are significantly altered to reflect approximately the superposition of the spectra of isolated Dan and Ndi monomer solutions (Figure 1.6B). Also, ring current effects caused by stacked π -systems, results in characteristic upfield chemical shifts of the Dan and Ndi aromatic hydrogens relative to the signals given by Ndi and Dan monomers separately (Zych 2000, 2002).

Finally, the space-fill model in Figure 1.6B suggests that the adopted conformation creates a hydrophobic column with the potential to display functional groups along its periphery. Couple this well-defined scaffold and its ability to be easily derivatized with the fact that these foldamers are most stable in water, it is envisaged that aedamers that interact with biological systems can be constructed.

1.2 UPDATE: FOLDAMERS WITH AEDAMER-LIKE DESIGNS

Since the original publication of aedamers appeared in 1995, several foldamers based on aromatic interactions have been reported. The use of aromatic interactions, in particular donor-acceptor type interactions, is emerging as a reliable strategy to build molecular scaffolds complementary to other non-covalent forces.

Figure 1.7 shows schematic representations of the most recent of these systems, all of which are reminiscent of the aedamer design. The *N*-methylated phenylguanidines developed by the Kagechika group is the only system of the four presented that operates in aqueous solutions (Tanatani 1998, Figure 1.7A). Impressively, x-ray crystal structures were obtained for both pentamers whose benzene rings were either attached at the *meta* or *para* positions, plus several derivatives afforded chiral crystals. The folded columnar superstructures of the Nuckolls group were an extension of their work on discotic-like liquid crystals (Zhang 2003, Figure 1.7.B). Their pleated-ribbon secondary structure is driven by a combination hydrogen bonding and π -stacking. A δ -peptide foldamer was developed using Dan and pyromellitic diimide (Pdi) units (Zhao 2004, Figure 1.7C). Further description on this system from the Li group can be found in Chapter 3 in the context of peptide-turn mimics. Lastly, the Ramakrishnan group was able to polymerize Dan and Pdi units in an alternating fashion with hexa(ethylene oxide) linkages (Ghosh 2004, Figure 1.7D). They assert that charge-transfer, solvophobic, and metal binding effects leads to a strongly folded

state. This particular report is sure to be well cited as one of the first studies on polymeric foldamers.

OTHER FACE-TO-FACE AROMATIC STACKING FOLDAMERS

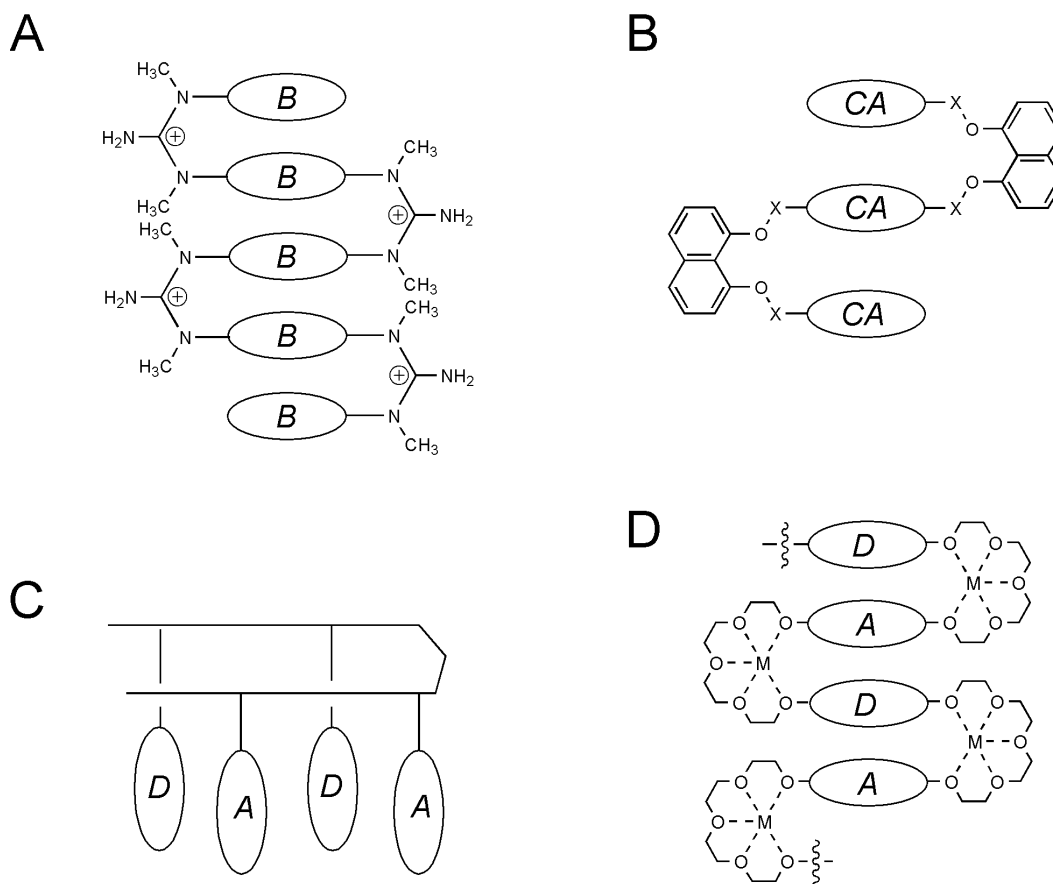


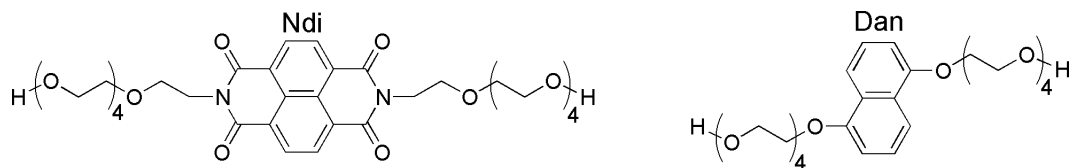
Figure 1.7 Cartoon representations of recent foldamers reminiscent of the aedamer design. A) Stacked structure using water-solubilizing guanidine linkers. (Tanatani 1998) *B* = *m*- or *p*-substituted benzene. B) System using hexasubstituted benzenes (Zhang 2003). *CA* = crowded aromatic. C) Zipper-type system (Zhao 2004). *D* = donor, *A* = acceptor. D) Aromatic stacking polymer with cation binding (Ghosh 2004).

1.3 CLOSER EXAMINATION OF AEDAMER AROMATIC INTERACTIONS

1.3.1 Forces that Dictate Folding

After reporting on a hexameric aedamer as a novel abiotic folding molecule (Lokey 1995), the Iverson group found it beneficial to study models at the monomer (Cubberley 2001) and dimer (Zych 2000) level to expound a much better description of aedamer folding. These investigations aimed to answer two important questions: 1) What are the fundamental forces responsible for Dan:Ndi association in aedamer folding? and 2) Can methods be developed to better describe the inter-ring orientations to give a more comprehensive picture of aedamer folding? Ultimately, these necessary fundamental studies paved the way for much of the work described in this dissertation.

To elucidate the driving forces of aromatic stacking, Cubberley performed ^1H -NMR binding titrations to measure association constants of the complexation of Dan and Ndi neutral monomers as well as Ndi:Ndi and Dan:Dan associations (Cubberley 2001b, Figure 1.8). A sampling of the calculated association constants (M^{-1}) in deuterated solvents covering a broad polarity range is shown in Figure 1.8. The data in the solid-line box pointed to a strong desolvation (in particular a hydrophobic) effect for Dan:Ndi complexation since the strength of this association is 2-3 orders of magnitude greater in D_2O than in organic solvents. This result is not surprising for the stacking of flat molecules with relatively nonpolar faces that self-organize to minimize contact with polar solvents.



solvent	Dan:Ndi	Ndi:Ndi	Dan:Dan
D ₂ O	2045	245	20
CD ₃ OD	30	8	1
CD ₃ CN	11	3	1
DMSO- <i>d</i> ₆	3	2	1
CDCl ₃	2	negligible	negligible

Boxed data argues for desolvation as the driving force for binding while the data in the dotted box is consistent with an electrostatic motive.

Figure 1.8 Compounds used in the monomer study and their associations (M^{-1}) in a few of the solvents reported (Cubberley 2001b).

Unanticipated though was the data (in the dotted box, Figure 1.8) that revealed Ndi:Ndi and Dan:Dan association was 10 and 100 times less stable than Dan:Ndi complexation, respectively. If desolvation were the lone important factor for association then it would be predicted that Dan:Ndi, Ndi:Ndi, and Dan:Dan associations would all be comparable due to the similar sizes of the hydrophobic aromatic surfaces of the Dan and Ndi rings. Therefore, this trend argued for an electrostatic driving force in which matching the electrostatic surface potentials would predict Dan:Ndi complexation to be the strongest scenario.

Inspection of the X-ray crystal structures (Figure 1.9) nicely explained how hydrophobics and electrostatics act in concert. It appeared that the low

stability of Dan self-association stemmed from its inability to stack in a face-centered manner due to putative repulsion of the electron-rich π -cloud of one Dan face with another. The resulting herringbone orientation thus tempers the extent of the desolvation driving force for Dan self-complexation. To explain the intermediate strengths of Ndi self-association, Cubberley and Iverson postulated that the preferred stacking geometry of Ndi also tempers desolvation effects. Ndi crystal data displayed a face-to-face but off-set stacking likely due to the electron repulsion of the electron-rich oxygen atoms of the carbonyl groups. Interestingly, the Hunter and Sanders model for aromatic stacking had previously described, albeit in a different context, edge-to-face geometries for electron-rich aromatics and slipped face-to-face stacking for electron-deficient aromatics that contain electron-rich heteroatoms (Hunter 1990, 2001). In summary, the dominant driving force was found to be the desolvation of the aromatic faces. However Cubberley and Iverson emphasized that “the magnitude of desolvation is modulated significantly by stacking geometry, which, in turn, is dictated by the electrostatic complementarity in predictable fashion (Cubberley 2001b).”

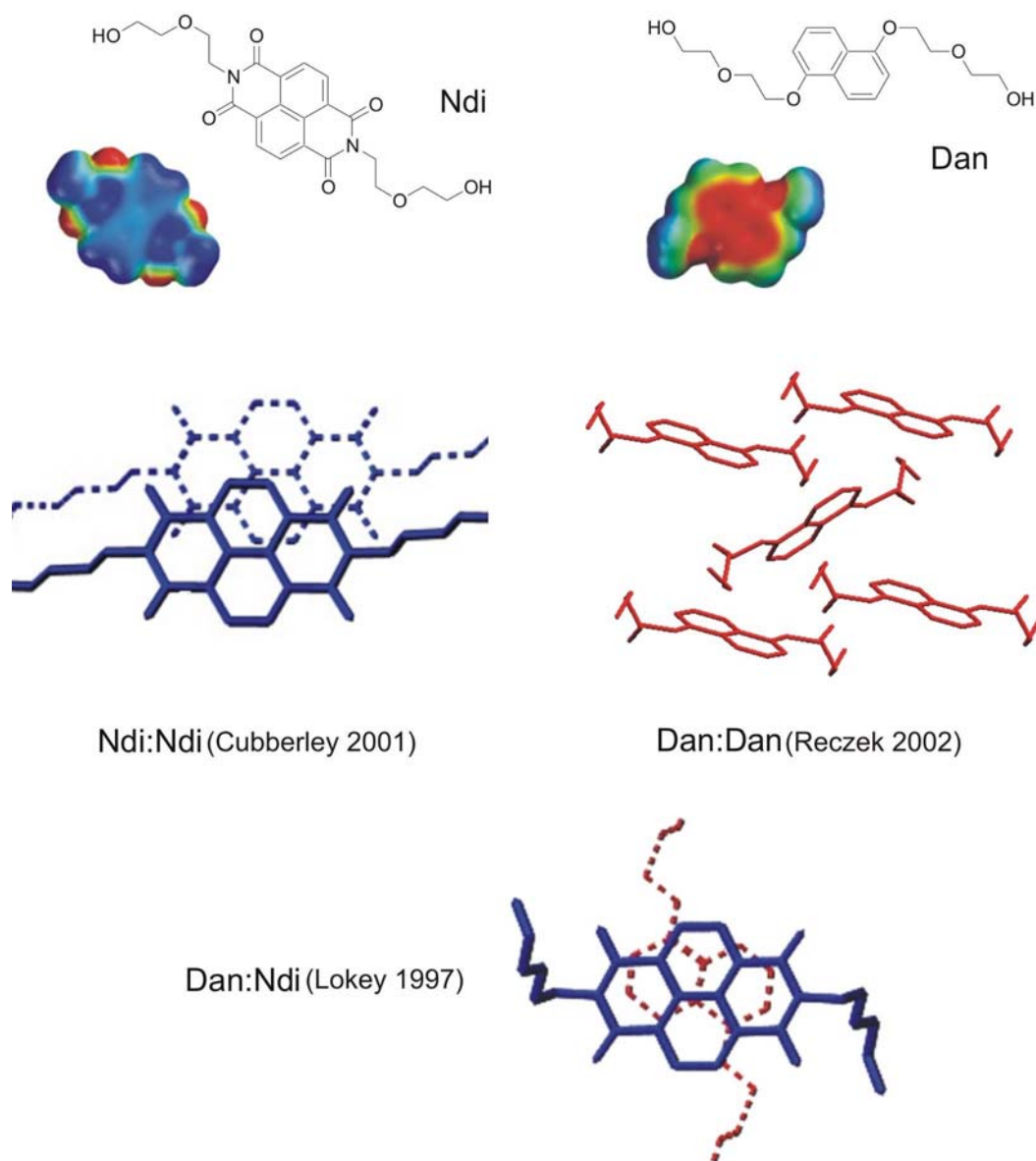


Figure 1.9 Calculated electrostatic surface potentials and chemical structures of compounds used to obtain X-ray quality crystals (adapted from Cubberley 2001b). From inspection the expected desolvation driving force is strongest in an equimolar mixture of Dan and Ndi.

Reprinted with permission from Cubberley, M. S.; Iverson, B. L. *J. Am. Chem. Soc.* **2001**, 123, 7560. Copyright 2001 American Chemical Society.

In general, many factors can contribute to aromatic interactions including Van der Waal's, charge-transfer, desolvation and electrostatic forces (Hunter 2001). The findings of Cubberley and Iverson, coupled with seminal work from several other groups studying synthetic models, have added greatly to the understanding of aromatic interactions, which also includes π - π stacking. Figure 1.10 briefly highlights three examples that have influenced how scientists view the fundamental basis of aromatic interactions.

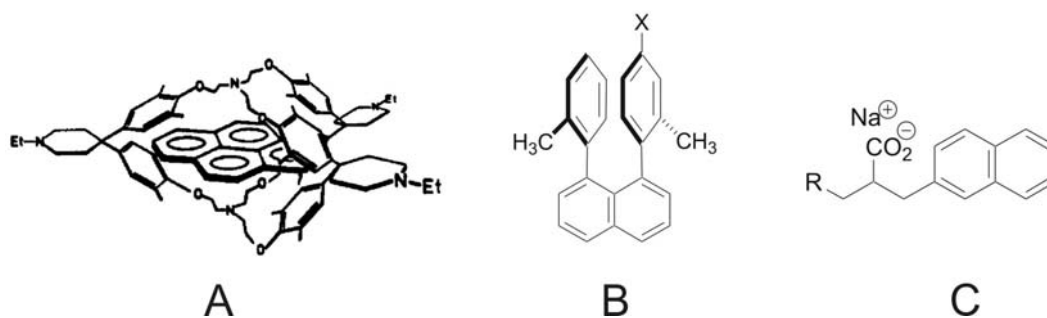


Figure 1.10 Early model systems to study aromatic interactions. A) Bicyclopentaphane host/pyrene guest (from Smithrud 1991). B) Diarylnaphthalene system. X = various electron withdrawing and donating groups (Cozzi 1992). C) Diarylcarboxylate models. R = naphthalene or adenine (Newcomb 1994).

Reprinted with permission from Smithrud, D. B.; Wyman, T. B.; Diederich, F. *J. Am. Chem. Soc.* **1991**, *113*, 5420. Copyright 1991 American Chemical Society.

Diederich's group examined the stability of pyrene-cyclophane complexes in water and organic solvents by NMR and calorimetry (Smithrud 1990, 1991, Figure 1.10A). A model of solvation effects on apolar binding resulted from their work and interestingly they found that the strength of the complexation for their system could be predicted and controlled by solvent polarity. In an ingenious

method to probe aromatic interactions, Siegel and co-workers measured the barrier to rotation of 1,8-diarylnaphthalenes and showed that their system was sensitive to through-space polar interactions (Cozzi 1992, Figure 1.10B). Another intriguing study came from the Gellman group who gave a partial charge attraction explanation for the intramolecular stacking observed for the adenine-naphthyl carboxylate but surprisingly stacking was not observed for the dinaphthyl carboxylate (Newcomb 1994, Figure 1.10C). This report also put forth the curious concept of a nonclassical hydrophobic effect where it was postulated that water is not well suited to the solvation of partially charged atoms if those atoms are in an extended planar array.

In the years following these early studies, it has become increasingly apparent that depending on the system, Van der Waal's, charge-transfer, desolvation, electrostatic forces and other effects can subtly alter each other's contributions to aromatic stacking. This complexity though is encouraging because it provides compelling evidence that aromatic interactions have the potential to be highly controllable in chemical (Waters 2002) and biological (Meyer 2003) systems.

1.3.2 Detailed Picture of Folding

To explore in-depth the degree of folding for aedmaers, Zych characterized the conformations of a diverse set of dimers (representing the minimal aedamer folding unit). This was accomplished by using modeling, NMR spectra analysis, and spectra prediction calculations applying a computer algorithm that was developed (Zych 2000, 2001). The impetus for this detailed

conformational analysis was the unique chemical shifts, displayed by the aromatic protons of dimers having different Dan/Ndi linkers of varying lengths and flexibilities. In effect, these shifts, upfield from the monomer aromatic signals (Figure 1.11), gave a distinct spectral fingerprint associated with specific ring-stacked conformations that Zych was able to predict by considering the many subtle ring current and carbonyl effects taking place with Dan:Ndi complexation.

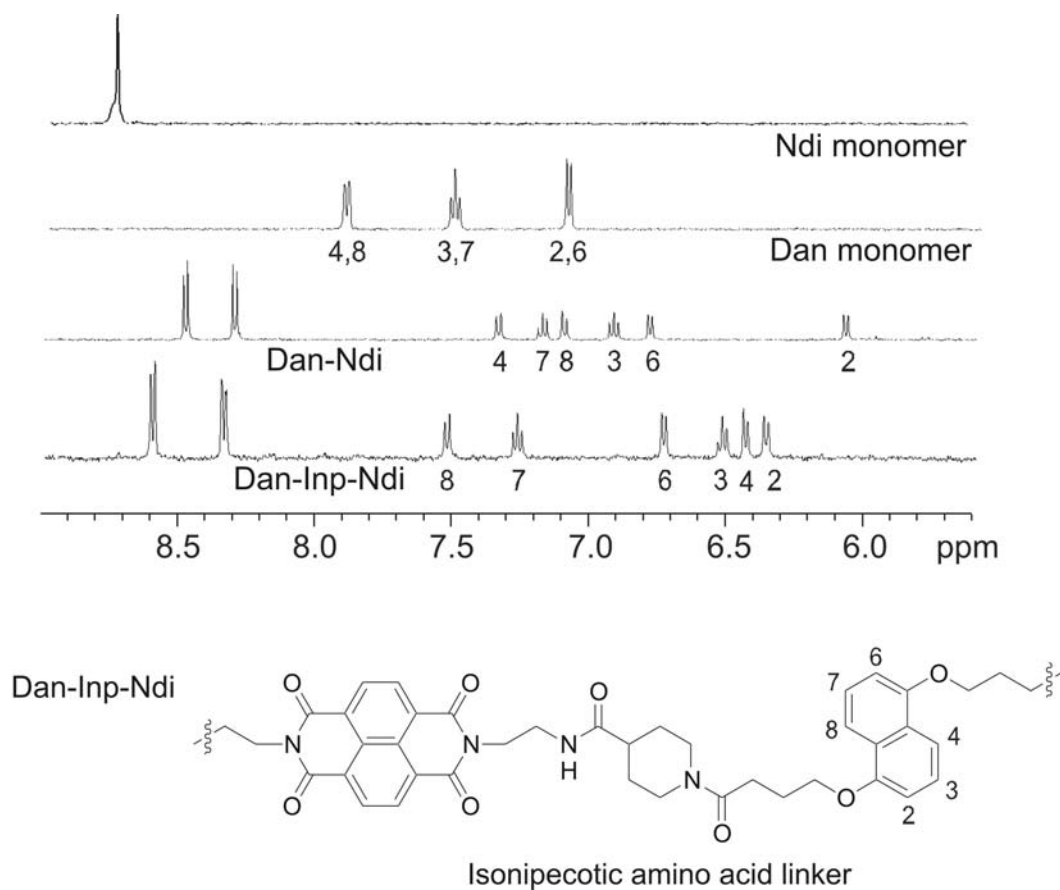


Figure 1.11 Aromatic region of the NMR spectra for a few of the compounds used for conformational analysis (Zych 2000).

A total of eleven dimers were investigated and for each, 100 computer-model conformations were generated from molecular dynamics simulation and geometry optimization. After 1) constructing conformational “maps” for all conformers and 2) applying equations to predict their chemical shifts, Zych found that, in most instances, an ensemble of predicted low-energy structures as opposed to one definitive conformer best described the experimentally acquired spectra. Thus, Zych and Iverson concluded that “folding” does not appear to follow a two-state unfolded/folded model with a rigid, unique conformation but follows a more dynamic model in which all the different folded conformers are related by having a face-to-face stacking arrangement. (Zych 2000).

This study also revealed that the aedamer pleated structure was tolerant of a wide range of linkers. On the other hand, it has been proven difficult to substitute amino acids without inadvertently disrupting the structure of proteins (LaBrenz 1995, Quinn 1994). Thus, this may prove beneficial for the development of functional aedamers since ideally one could decouple properties from the overall architecture of the molecule (Zych 2001).

Ultimately, larger aedmaers will have to be used to approach the size and functionality found in proteins but the type of detailed conformational analysis performed with dimers becomes prohibitive with increasing size. Therefore, in follow-up work, Zych and Iverson looked at the possibility that the conformations of larger aedamers are actually the “sum” of their component dimers (Zych 2002). Figure 1.12 illustrates the concept of this behavior that was designated as conformational modularity. For instance the Dan region of the NMR spectrum of

a Dan-Inp-Ndi-Dan trimer could be closely predicted by the chemical shifts found for its component dimers, Dan-Inp-Ndi and Ndi-Dan (Figure 1.12). In another situation, if a Dan unit was sandwiched in between two Ndi units in an assumed pleated fold stack, conformational modularity still held fairly true but only when ring current effects were considered to be additive. For instance, the delta chemical shifts found for the Dan unit in the tetramer, Dan-Asp-Ndi-Dan-Asp-Ndi, nearly matched the sum of the delta chemical shifts for the Dan unit of Ndi-Dan and Dan-Asp-Ndi.

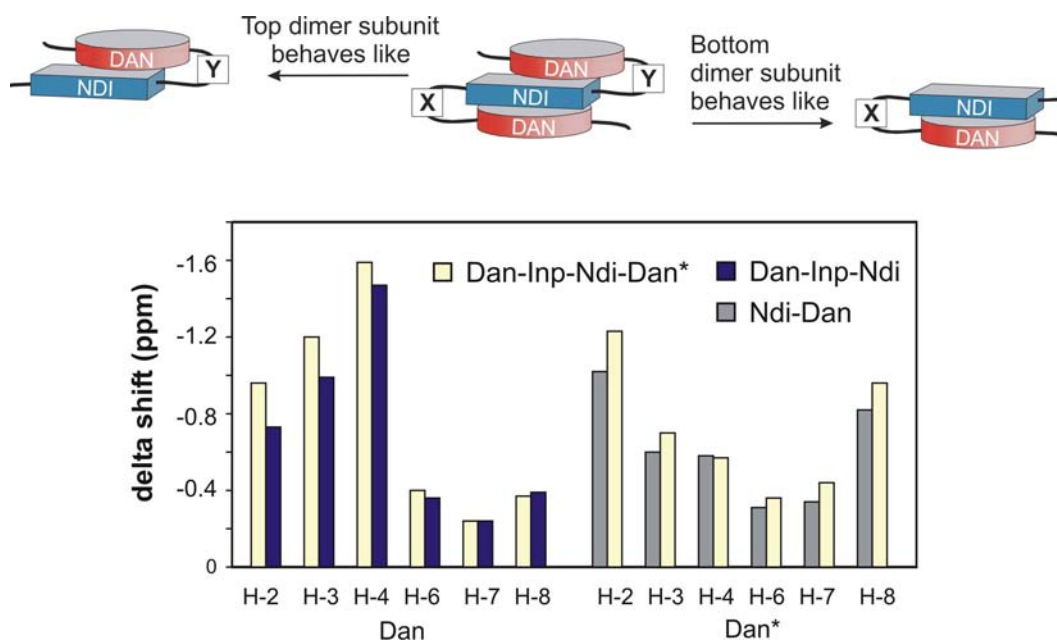


Figure 1.12 Illustrated concept of conformational modularity and chart showing the high accuracy of chemical shift prediction when this concept is applied to larger aedamers (Zych 2001, 2002).

Certain trimers and tetramers were found though that did not follow the conformational behaviors of their component dimers. It was proposed that for

some aedamers steric clashes between the linkers shifted the expected orientations of the rings. Zych and Iverson pointed out that this insight would have been dramatically more difficult to obtain if a *de novo* conformational analysis of the larger structures were attempted. Nonetheless, most of the trimers and tetramers studied displayed this highly desirable feature of conformational modularity. Further refinement of this feature could greatly aid in the design of larger folding systems with predictable structure and function.

As a whole, the meticulous studies into the fundamental basis of folding, done independently by Cubberley and Zych, laid a foundation for future aedamer work and their findings will probably increase in importance as aedamer research moves towards applications. In fact, only after these basic science studies were performed did this dissertation research begin to significantly move forward; where the reported strengths and directionality of the “directed” interactions of Dan and Ndi moieties could be utilized in previously unexplored ways.

1.4 OVERVIEW OF NAPHTHYL OLIGOMER PROJECTS

The projects in the Iverson laboratory dealing with aromatic interactions can all trace their beginnings to the original aedamer paper (Lokey 1995). Since then, research utilizing Dan and Ndi moieties has diversified to investigate varied aromatic interactions phenomena in areas spanning from molecular biology to materials science. Figure 1.13 organizes these projects roughly based on the size of the Dan/Ndi compounds synthesized and the general focus of the study. As presented above, several significant results have come from exploring monomer associations and dimer conformations. Currently the Iverson group is well

involved with studying systems at the oligomeric size regime and has even recently started investigating polymeric materials containing Dan and Ndi building blocks.

Research in the Iverson Group Focused on the Varied Interactions of Naphthyl Compounds

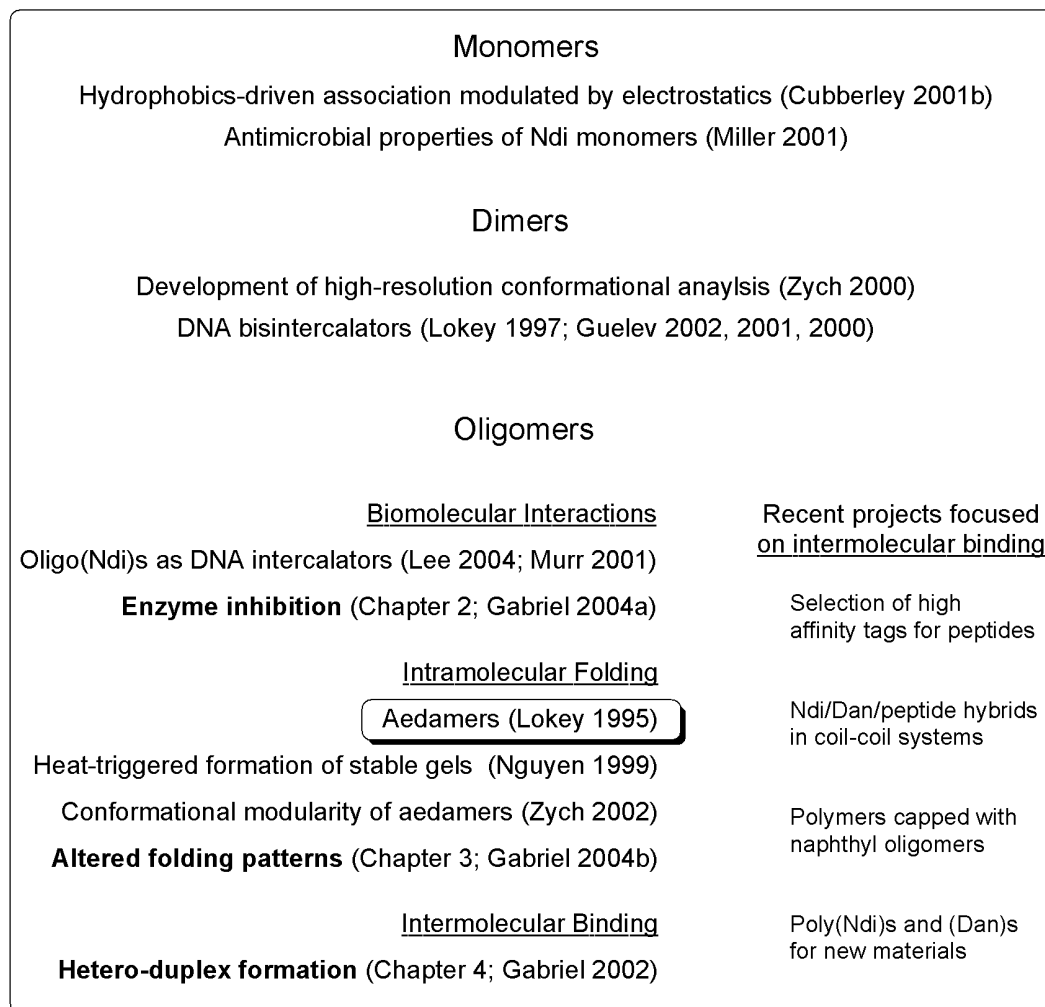


Figure 1.13 Projects in the Iverson laboratory designed to explore aromatic interactions. All work can trace its beginnings to Lokey's aedamer paper. Results detailed in chapter 2, 3, and especially 4 have led to several new research directions.

The focus of this dissertation is to illustrate the ability to exploit the Dan:Ndi interaction for creating novel folding and binding properties not previously accessed with naphthyl oligomers of the original “alternating” **(Dan-Ndi)_n** dimer design. Quite simply, this dissertation documents the group’s initial attempts to extend the Dan:Ndi interaction to controlling other behaviors beyond driving a pleated fold conformation. Figure 1.14 is a cartoon illustrating this basic premise using “non-alternating” naphthyl oligomers, for example, compounds of such sequences as, **Dan_{n+1}-Ndi_n**, **Dan_n** and **Ndi_n**.

Shuffling the Naphthyl Units to Create Different Architectures

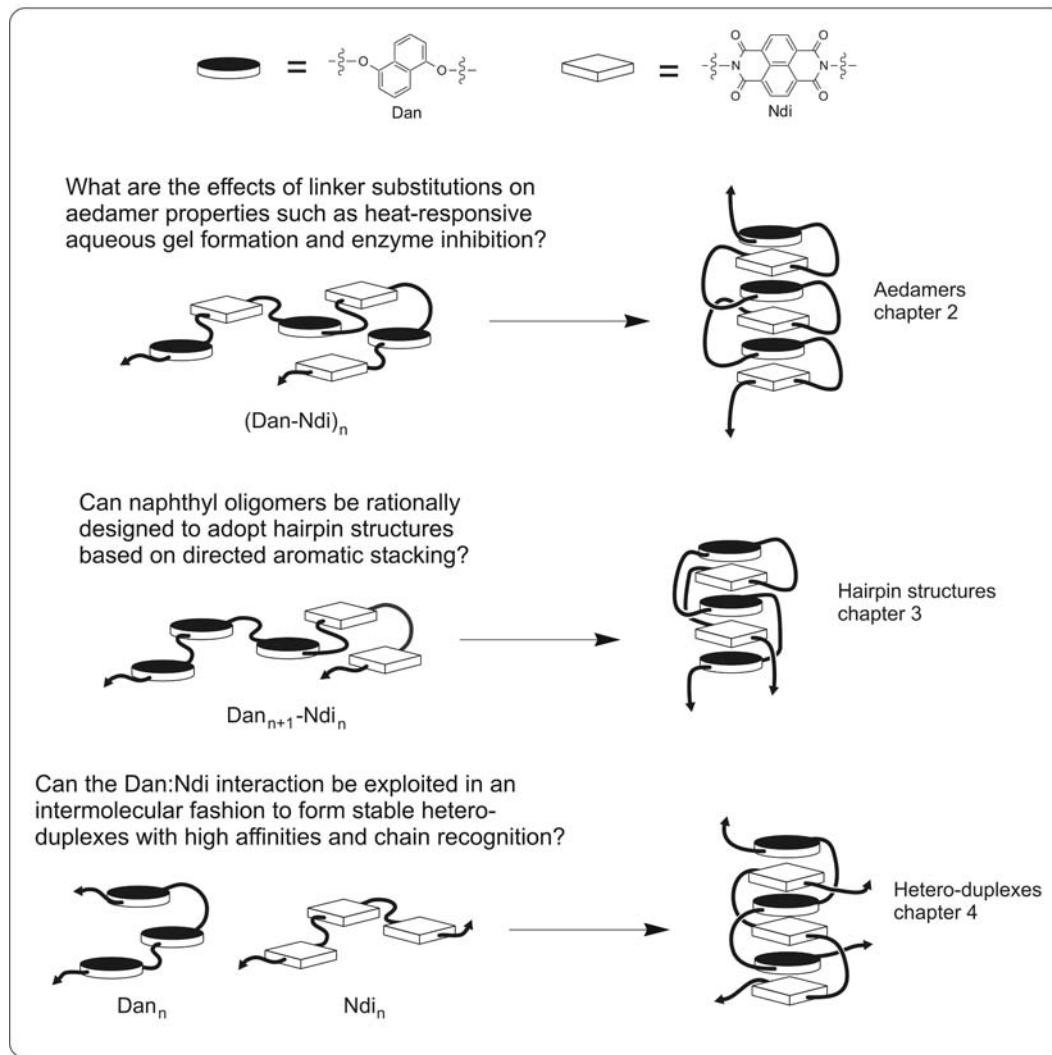


Figure 1.14 Cartoon representation of the naphthyl oligomers studied and the main question each project aimed to answer. Arrows indicate direction of growth for longer oligomers.

The project described in **Chapter 2: Intriguing Heat-Triggered Behavior of an Amphiphilic Aedamer** involves work initiated by Nguyen, who discovered that amphiphilic aedamers could be thermally triggered to irreversibly

form stable aqueous gels (Nguyen 1999). Studies were done with a derivatized aedamer set to probe whether residue substitutions could modulate gelling properties. The amphiphilic aedamer (ungelled) was also shown to act as an effective refolding inhibitor of RNase. Inhibition studies testing several compounds and conditions were thus tested. Of interest to the Iverson group are the potentially selective interactions between the aromatic moieties of aedamers and the aromatic amino acids of proteins. This work represents the group's first steps towards identifying aedamer-protein interactions.

Many groups working with foldamers have shown that the secondary structures of their synthetic strands remain unchanged and are thus remarkably stable to a wide array of residue substitutions. The project described in **Chapter 3: Switching the Folding Patterns of Naphthyl Oligomers** reports the first successful demonstration of a foldamer accessing *significantly different abiotic secondary structures* in water simply by rearranging their primary sequence analogous to proteins. Here synthetic strands of the new type ($\text{Dan}_{n+1}\text{-Ndi}_n$) were synthesized and found to adopt hairpin-type turn structures. The results presented in this chapter represent another checkmark on a list of properties that are possessed by natural biomolecules that foldamers can now emulate. The designability of these naphthyl oligomers is not only useful to create different folding topologies but is expected to provide a facile route to the development of larger, extremely stable hairpin structures with useful properties.

Lastly, this dissertation will account the group's entrance into the growing field of designed, synthetic duplexes. The project described in **Chapter 4:**

Naphthyl Oligomers that Form Hetero-Duplexes details several analytical methods that provided evidence of the first hetero-duplex system to form via aromatic interactions and operate in aqueous solutions. This system uses complementary Dan_n and Ndi_n strands to form robust artificial duplexes that exhibited high chain discrimination. Noteworthy was that even though these chains each possess substantial negative charge, they still associate with substantial affinities regardless of potential charge repulsion. This work, which was also the first to demonstrate the strength and directionality of the Dan:Ndi association in an *intermolecular* format, has opened up several research paths dealing with orthogonal self-assembly of complementary species (Figure 1.13).

CHAPTER 2

Intriguing Heat-Triggered Behavior of an Amphiphilic Aedamer

2.1 CHAPTER SUMMARY

Introduction. Due to the modular design of aedamers (Figure 2.1), synthesizing an amphiphilic aedamer with three aspartate and three leucines residues, instead of with six aspartates as in the original aedamer (Chapter 1), was straightforward. While studying this new aedamer, Nguyen and Iverson discovered unusual gelling properties in which an aqueous solution of this compound is irreversibly converted thermally to a viscous gel accompanied by a color change from purple to pale pink (Nguyen 1999). The original aedamer on the other hand was found to be resistant to this change in physical state. This chapter will describe aggregation studies on a set of different aspartate/leucine containing aedamers evaluated for their gelling propensities. It also appeared that heat-induced aggregation related to aqueous gel formation plays a role in the inhibition of the enzyme RNase (folding, not active-site, inhibition). It is proposed that RNase cannot refold properly after heat denaturation in the presence of the amphiphilic aedamer. When the original aedamer was tested, RNase recovered its full catalytic activity. This proof-of-concept study evaluating the possibility of strong aedamer-protein interactions will be discussed in the second half of this chapter.

Can easily create diversity by substituting X for any amino acid

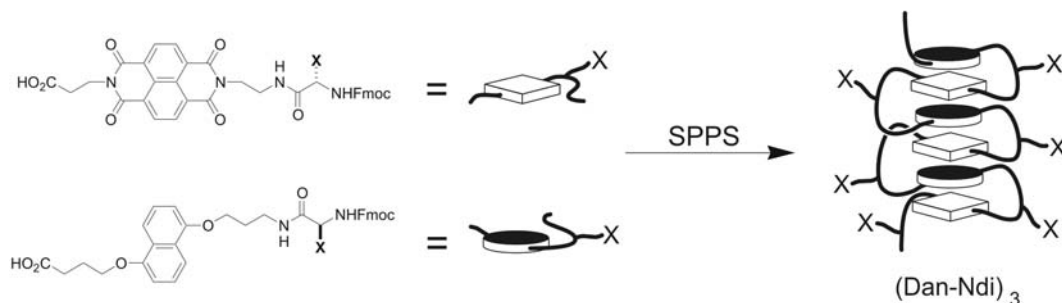


Figure 2.1 Cartoon representation of the modular aedamer design showing the potential to decorate the periphery of the structure with chosen residues. X = amino acid side chain. SPPS = solid phase peptide synthesis.

Goals. Experiments described in this chapter aimed to answer the question: *What are the effects of linker substitutions on aedamer properties such as heat-responsive aqueous gel formation and enzyme inhibition?* The short-term goal of this work was to investigate the structure-activity relationship of a set of aedamers by measuring their gelling kinetics and RNase refolding inhibition under different conditions. The long-term objective of this research is to gain a working knowledge of how to design naphthyl oligomers for use as materials with tunable properties.

Approach. The aggregation state of four aedamers of varying aspartate/leucine content was analyzed at 25 and 80 °C using UV-Vis, NMR, and light scattering (LS) spectroscopy. Gelling curves were also constructed. The enzyme inhibition studies utilized a commercially available fluorometric assay to monitor the activity of RNase under different conditions.

Results. It was found that only a solution of the amphiphilic aedamer was able to undergo a conformational transition to form aqueous gels, while the aedamers with less than three leucine residues were unchanged when heated. At room temperature the amphiphilic aedamer exhibited a highly aggregated, yet soluble, state (by NMR and LS) but still displayed characteristics of being well-folded in the expected pleated ribbon fashion (by UV-Vis). When heated, insoluble gels formed after an initial slow period followed by a rapid gelling phase. In the RNase studies, again the amphiphilic aedamer was found to exhibit unique properties. Only when RNase was heated in the presence of the amphiphilic aedamer did refolding inhibition occur (Gabriel 2004a). The original aedamer and even detergent had little effect. This result is encouraging for long-term studies of selective aedamer-protein interactions. Mechanisms were thus proposed to explain both the unique gelling and enzyme inhibition properties of the amphiphilic aedamer.

2.2 BACKGROUND: A FOLDAMER THAT FORMS STABLE GELS IN WATER

Nguyen and Iverson previously reported on an aedamer hexamer in which three of the aspartate linkers in the original aedamer developed by Lokey and Iverson were replaced with hydrophobic leucine residues (Nguyen 1999, Lokey 1995) (Figure 2.2). This facially amphiphilic aedamer, once folded, presents one side with hydrophobic side chains and the other with hydrophilic aspartate side chains (Figure 2.3). Characterization of this compound gave unresolved NMR spectra and an apparent molecular weight of $400,000 \text{ g}\cdot\text{mol}^{-1}$ by dynamic light scattering indicating extensive aggregation in solution. When heated, in an

attempt to break up aggregates, the NMR sample, initially a purple aqueous solution, surprisingly became a pale pink gel.

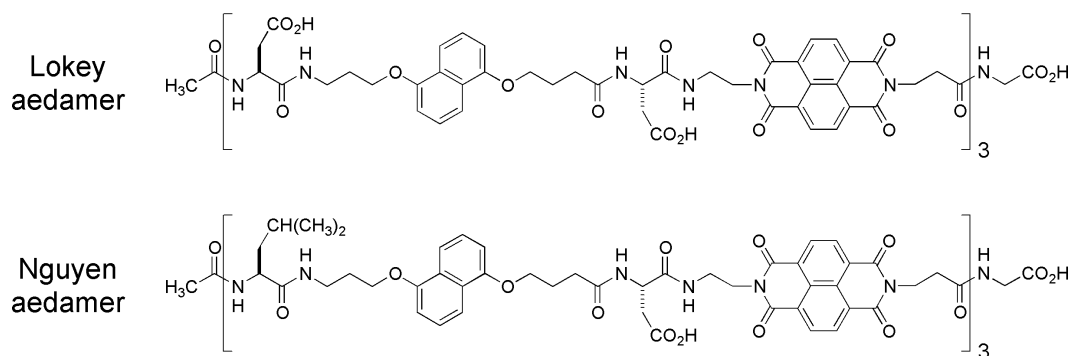


Figure 2.2 Chemical structure of the original aedamer hexamer (Lokey 1995) and an amphiphilic derivative (Nguyen 1999).

The resulting gel was quite stable in the sense that upon cooling and standing at room temperature for weeks it did not revert back to the properties of the original solution. Mass spectrometry and reverse phase liquid chromatography ascribed these properties to conformational changes and not covalent transformations of the chemical structure. The kinetics of the conformational transition is shown in Figure 2.3 showing the loss of the charge-transfer (CT) absorbance at 526 nm and loss of its intense purple color as the solution became more viscous. Interestingly, there was a lag period followed by a relatively rapid gelation phase suggesting that this transition is product promoted. This behavior was confirmed when 10% of pregelled aedamer was added to a solution before heating which resulted in complete transformation of the solution within 15 minutes rather than 70 minutes (Figure 2.3).

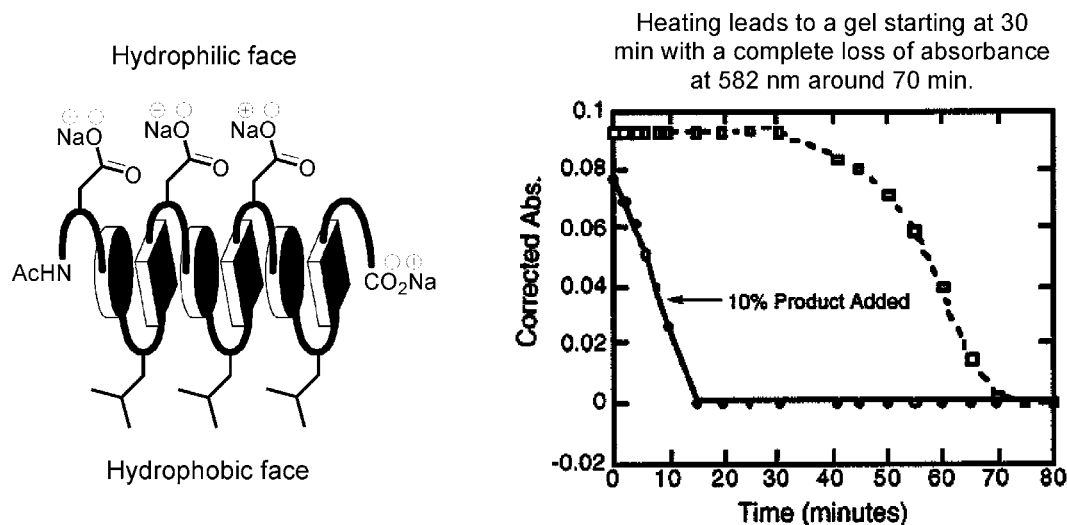


Figure 2.3 Cartoon representation of the folded conformation. Graph of the kinetics of the conformational transition (dotted line) of the amphiphilic aedamer upon heating at 80°C , as monitored at the charge-transfer band absorbance of 526 nm (from Nguyen 1999). Solid line shows the kinetics of an identical solution except 10% of pregelled material was added before heating.

Reprinted with permission from Nguyen, J. Q.; Iverson, B. L. *J. Am. Chem. Soc.* **1999**, *121*, 2639. Copyright 1999 American Chemical Society.

A proposed mechanism of this behavior is shown in Figure 2.4. In brief, heating causes partial unfolding of the aedamer that promotes a new type of hydrophobics-driven interaction where the aromatics screen their relatively non-polar surfaces from water by forming tangled aggregates instead of refolding. Most importantly, this type of aggregation proceeds slowly at first because the concentration of unstacked molecules is initially low and collisions between these unstacked molecules are rare. It was proposed that the tangled aggregate becomes more and more efficient at capturing unstacked molecules as it increases in size, hence the relatively rapid gel phase after a perceived lag period. It was assumed

that the final viscous material is composed of a randomly tangled aggregate absent of the ordered face-to-face stacking of chromophore units responsible for the CT absorbance, hence the loss of color. It was also pointed out that the irreversibility of this transition stems from the near impossibility of untangling this aggregate, at least through temperature changes or dilution (Nguyen 1999).

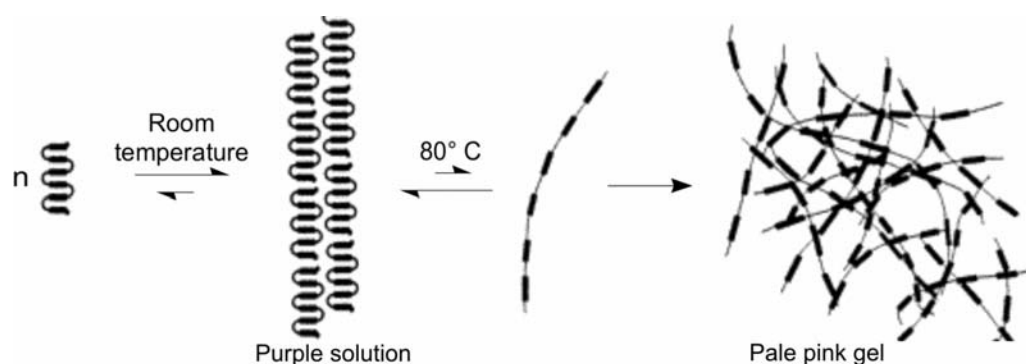


Figure 2.4 Proposed scheme for the thermal conversion of an aedamer solution to the tangled aggregate state (adapted from Nguyen 1999).

Reprinted with permission from Nguyen, J. Q.; Iverson, B. L. *J. Am. Chem. Soc.* **1999**, *121*, 2639. Copyright 1999 American Chemical Society.

The data emphasized that an initial folded state at ambient temperatures should be assumed since any substantial population of significantly unfolded aedamer would lead to gel formation at room temperature. Also Nguyen and Iverson drew comparisons between the behavior of this aedamer and collagen, a biological polymer that forms gelatin when heated but is more than 40 times larger than the amphiphilic aedamer. As Gellman commented, “[this] behavior establishes a link between synthetic folding systems and materials science (Rouhi 1999),” thus presenting a new motivation for foldamers which were previously

studied mainly with emulating proteins in mind. Ironically, the initial aim of Nguyen's amphiphilic aedamer was to design a mimic of leucine zipper motifs for biological and not materials investigations.

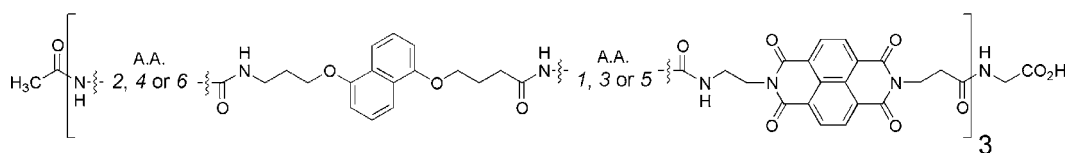
The Iverson group has been intent on understanding and hopefully controlling conformation-dependent behavior of these foldamers. In broader terms, the general field of hydrogels is finding applications in tissue engineering (for instance as biocompatible scaffolds), controlled drug delivery, bioadhesives (for wound healing), glucose sensors, and other biomaterials such as soft contact lenses and kidney dialyzers (Langer 2003). Hydrogels have been constructed from molecules of varying sizes from short oligopeptides (Pochan 2003) to polymers (Aamer 2003). Also there is a report of a thermally coaxed gel system developed by Tirrell and co-workers that interestingly employs two short leucine zipper domains (Petka 1998). Most recently, a coordination gelator that exhibits a chromatic and sol-gel transition for both thermal and chemical stimuli, has been reported as well (Kawano 2004). Even with these numerous examples, there is still a need for better modulation of hydrogel properties, including texture, strength, and water content. These issues were addressed in a comprehensive review published by Langer and Peppas (Langer 2003).

With such activity currently in the hydrogel field it seemed logical to explore the possibility of tunable gels with the aedamer system. Specifically, the kinetic curves for gel formation in Figure 2.3 piqued the Iverson group's interest in modulating such gelling parameters as the onset temperature, speed of transition, and overall strength of the resulting gel.

2.3 RESULTS AND DISCUSSION

2.3.1 Synthesis of Aedamer Derivatives

New aedamer hexamers, **2.2** and **2.3**, were synthesized, as well as **2.1** and **2.4** from previous studies, in order to probe how varying the number of aspartate and leucine side chains and thus changing the hydrophilic/phobic content, affects aqueous gel formation (Figure 2.5).



Compound	Asp	Leu
2.1 (Nguyen 1999)	1, 3, 5	2, 4, 6
2.2	1-3, 5	4, 6
2.3	1-5	6
2.4 (Lokey 1995)	1-6	

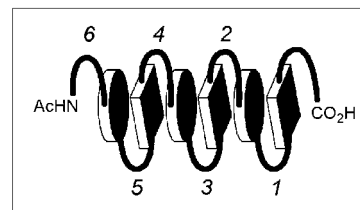
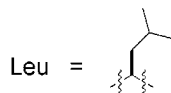
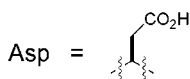
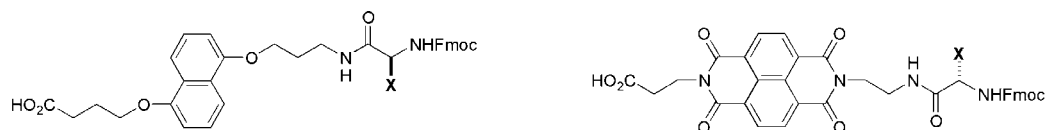


Figure 2.5 Compounds synthesized for the gelling study. A.A. 1-6 represents the amino acid linker positions along the backbone.

Fmoc-based solid-phase peptide protocols (Chan 2000) were followed (Figure 2.6) to synthesize **2.1-2.4**. Also shown in Figure 2.6 are the three amino acid adducts **2.5-2.7** synthesized in solution phase following analogous procedures previously described (Zych 2000 - **2.5**, [**2.6** by an analogous

procedure], Guelev 2001c - **2.7**). These amino adducts were coupled sequentially onto Wang resin using PyBOP (Benzotriazole-1-yl-oxy-tris-pyrrolidino-phosphonium-hexafluorophosphate) with Fmoc deprotections using piperidine/DMA (*N,N*-Dimethylacetamide) between each coupling step. After the last Fmoc deprotection, the oligomer was then capped, in this case using acetic anhydride, to provide a *N*-terminal acetyl group. Aedamers were then fully deprotected and cleaved off the resin with 95/5 w/w TFA (Trifluoroacetic acid) /phenol. Purification by FPLC (Fast protein liquid chromatography) using an aqueous ammonium acetate and CH₃CN gradient afforded homogeneous samples in 40-50% yield based on the mmol/mg loading capacity of the resin. All compounds were soluble in 50 mM Na phosphate buffer, pH = 7 at up to 2.0 mM for **2.1** and up to 5.0 mM concentrations for **2.2-2.4** before a precipitate formed. Each compound gave satisfactory HPLC (High performance liquid chromatography) and mass spectrometry analysis.



2.5 X = protected aspartic acid side chain

2.7 X = protected aspartic acid side chain

2.6 X = leucine side chain

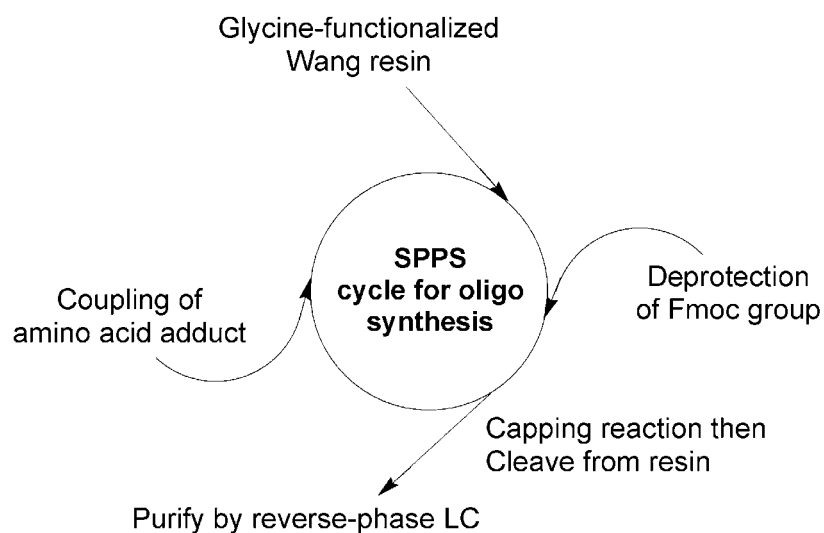


Figure 2.6 Dan and Ndi amino acid adducts synthesized and used in the standard solid phase oligo synthesis cycle. Full structures can be found in the Experimental Section. Fmoc = 9-fluoronylmethyloxycarbonyl. SPPS = solid phase peptide synthesis. LC = liquid chromatography.

2.3.2 UV-Vis, NMR, and LS Comparisons at 25° C

UV-Vis, NMR, and light scattering (LS) experiments were carried out at room temperature (25° C) to possibly gain insight into the aggregation state of **2.1-2.4** prior to heat-triggered gelation. Nguyen's report had already asserted that even though **2.1** is extensively aggregated, it still formed a stack of aromatics in an intramolecular fashion at room temperature with UV-Vis characteristics

indicative of the pleated folded structure attributed to aedamers (Nguyen 1999). Table 2.1 shows that solutions of all four compounds exhibited marked hypochromism (48-54%) that is fully consistent with substantial face-centered π -stacking (Lokey 1995, Cantor 1980). The CT band absorbances (526-540 nm) for each compound that resulted in the solutions being purple to reddish purple in color indicated donor-acceptor aromatic stacking and were also seen previously with folded aedamers (Zych 2002, Lokey 1995).

Table 2.1 Analyses at 25 °C for **2.1-2.4**.

	UV data	Vis data		NMR data
Compound	Hypo (%) ^a	λ_{CT} (nm) ^b	ϵ_{CT} (M ⁻¹ ·cm ⁻¹) ^c	Linewidth (Hz) ^d
2.1	54	540	1400	NS
2.2	51	538	1500	10.8
2.3	48	536	1500	5.3
2.4	51	526	1500	2.8

^a Solutions at 40 μ M concentrations. Hypo(chromism) = [1 - (absorbance at 382 nm without CTAB \div with excess CTAB)] \times 100%. ^b λ_{CT} = wavelength of charge-transfer band. Concentrations at 1 mM ^c ϵ = extinction coefficient. ^d Solutions at 1.5 mM concentrations. Linewidth of singlet of the Gly methylene at the C-terminus. NS = no discernable signal.

It could not be ruled out rigorously that the hypochromism and CT bands are derived entirely from intramolecular interactions because of aggregation. It is reasonable to believe though that these UV-Vis spectroscopic signatures were predominantly due to intramolecular interactions since the CT bands exhibited linear Beer's law behavior below 2.0 mM. Likewise, Nguyen and Iverson contended that the spectral similarities between **2.1** and **2.4** argue against

intermolecular stacking effects playing a major role in the UV-Vis spectra for **2.1** (Nguyen 1999).

While the UV-Vis data suggested that the intramolecular interactions for **2.1-2.4** are comparable, it was clear from NMR data that **2.1** was significantly aggregated compared to **2.2-2.4** as evidenced by the NMR spectra in Figure 2.7 and the linewidth data in Table 2.1. Figure 2.7 shows that a solution of **2.1** failed to give resolved spectra diagnostic of a highly aggregated state (albeit a soluble aggregated state). On the other hand, although line broadening was observed, spectra of **2.2-2.4** gave distinguishable signals. Linewidths of NMR resonances have been shown to be sensitive to aggregate size (Whitford 1991). For instance, the methylene linewidths from spectra of phospholipid vesicles increase in a roughly linearly fashion with vesicle radius (Liao 1980). In spectra of 1.5 mM solutions of **2.2-2.4** the linewidths of the singlet assigned to the C-terminal methylene roughly doubles with the sequential replacement of aspartates on **2.4** with leucines (Table 2.1). Thus, the effect of increasing leucine content on aggregation appeared to be somewhat additive for the series **2.4-2.2** with a dramatic jump in signal broadening for aedamer **2.1**.

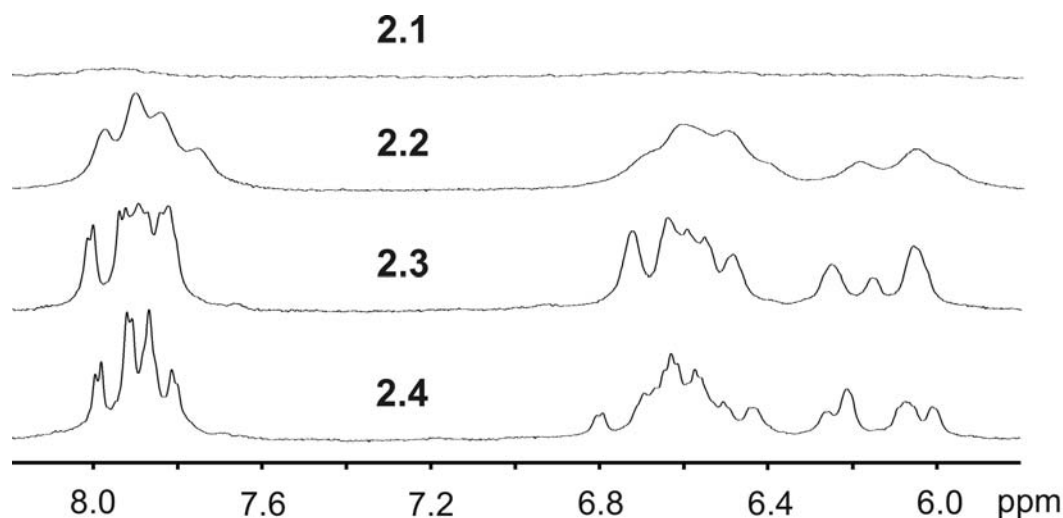


Figure 2.7 Aromatic region of ¹H-NMR spectra. Concentrations were 1.5 in mM D₂O. Even dilute solutions (0.1 mM) of **2.1** failed to give resolved spectra.

Light scattering (LS) has been shown to be an effective tool for studying the aggregation properties of self-associating molecules including polymers (Nolan 1997), detergents (Perez-Rodriguez 1998), and bioactive molecules (Varela 1999). The use of LS is sure to expand as pharmaceutical companies examine more closely how aggregation enhances or decreases the effectiveness of certain drug formulations (Seidler 2003). A classic LS experiment is to probe for discontinuities in the amount of light scattered as a function of concentration to identify critical aggregation concentrations (CACs). An example is shown in Figure 2.8 from a study of the self-association of penicillin. For penicillin, 0.04 and 0.25 m (molality) were identified by Mosquera and co-workers as critical concentrations for an observed monomer/trimer transition and a trimer/12-mer transition, respectively (Varela 1999).

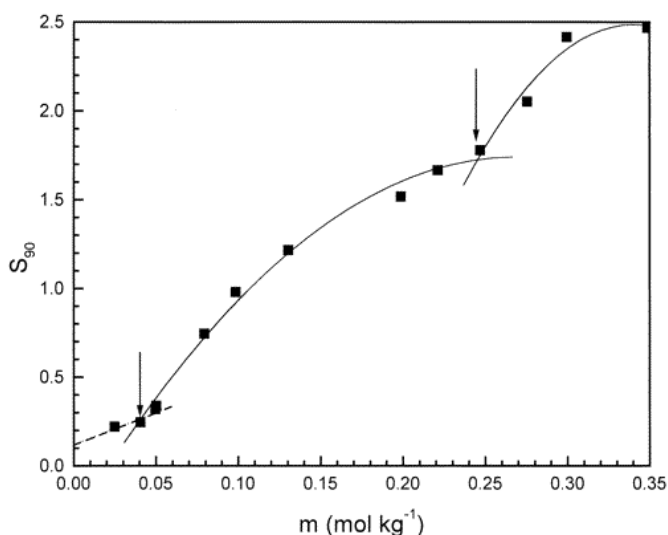


Figure 2.8 Scattering ratio, S_{90} , as a function of molality for penicillin in water. Dotted line below 0.04 m indicates the theoretical line for unassociated monomers and arrows denote the critical concentrations (Varela 1999).

Reprinted with permission from Varela, L. M.; Rega, C.; Suarez-Fillooy, M. J.; Ruso, J. M.; Prieto, G.; Attwood, D.; Sarmiento, F.; Mosquera, V. *Langmuir* **1999**, 15, 6285. Copyright 1999 American Chemical Society.

Analogous graphs (Figure 2.9) were created for compounds **2.1** and **2.2**, two compounds that differ by only one residue yet seemingly have drastically different room temperature aggregation states by NMR. The “discontinuity” shown by **2.1** was judged to be too slight and not compelling to suggest a CAC while the data for **2.2** fit a linear model well ($R^2 = 0.996$) for all concentrations indicating size homogeneity (Figure 2.9). What was quite striking is that the scattered light intensity of **2.1** was more than an order of magnitude greater than **2.2** corroborating NMR data implying the presence of large aggregates of **2.1** even at low concentrations.

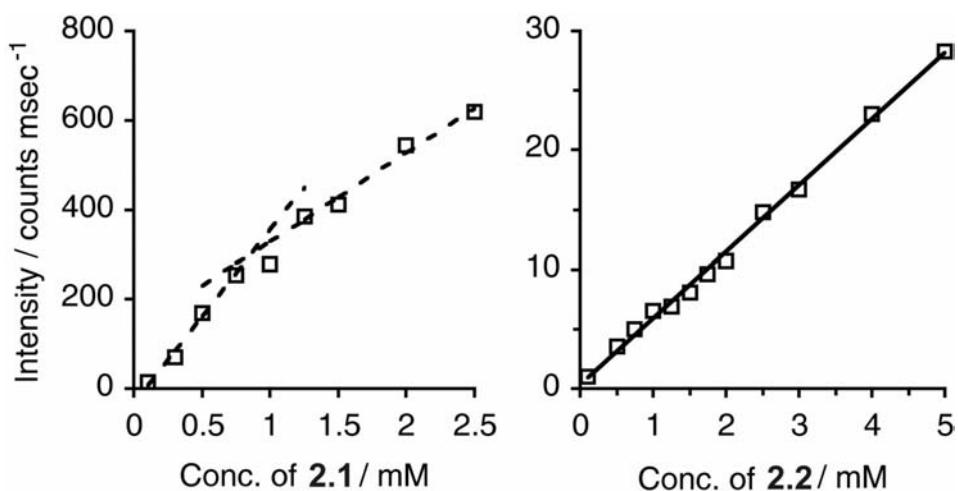


Figure 2.9 Scattered light intensity as a function of concentration. The failure to describe data from solutions of **2.1** with a linear fit is normally indicative of a shift in solute size but at this point the discontinuity cannot be interpreted as a critical concentration.

The above graphs measured the time-average intensity of scattered light also known as static scattering. Dynamic light scattering (DLS) on the other hand measures the movements of isolated particles. With a large collection of measurements DLS can afford estimated molecular weights and yield hydrodynamic radii (Ruso 2000, Pecora 1985). Unfortunately, DLS results varied too much between separate measurements from trial to trial and even within single runs to allow for any confidence in the data acquired. This was likely due to the available fitting models that limit analyses to only systems with well-defined monomodal or bimodal weight distributions. The aggregated state of **2.1** at room temperature therefore likely spans a wide range of sizes and may be quite variable over time and sensitive to how solutions are handled. Future studies

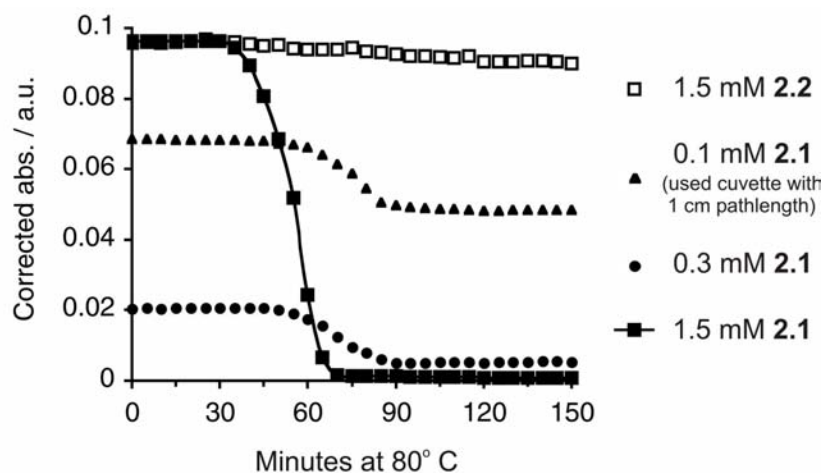
obtaining sedimentation equilibrium data via analytical ultracentrifugation might lead to better descriptions of these aggregates of **2.1** (Raguse 2001).

2.3.3 Evaluation of UV-Vis, NMR, and LS Data

UV-Vis spectroscopy fully supported that all compounds had a similar folding pattern in solution, where the aromatics are stacked face-centered at 25 °C. While the intramolecular folding of **2.1-2.4** appeared to be comparable to each other, it was clear from NMR and LS that **2.1** was drastically aggregated but in such a way that the Dan:Ndi intramolecular stacking appeared mostly unaffected. This suggests that intermolecular interactions were significantly different between **2.1** and **2.2-2.4**. Possibly there are enough leucine-leucine intermolecular interactions to cause aggregation for **2.1**. One must also consider charge effects as an explanation for the apparent differences between **2.1** and **2.2** whose five carboxylates in solution may have presented adequate intermolecular charge repulsion to prevent the rapid capture of partially unfolded aedamers. To address these parameters it would be worthwhile to synthesize hexamers with identical charges as **2.1** but with less hydrophobic residues, such as glycine, to probe whether the hydrophobicity of the linker side chains could truly be used to modulate aggregation properties. Finally, although **2.1** existed as large soluble aggregates in solution, HPLC and mass spectrometry conditions seemed to break up these aggregates for measurements of presumably monomeric species during these analyses. This observation indicates that the intermolecular interactions responsible for this aggregation state at ambient conditions are fairly weak and reversible.

2.3.4 Concentration Dependent Gelling Studies

While it was important to characterize the aggregation state at room temperature, the main inquiry of this study is whether compounds **2.2-2.4** gel at elevated temperatures such as **2.1**. Thermally-induced gelling experiments were performed and the data for **2.1** and **2.2** is shown in Figure 2.10 (compounds **2.3** and **2.4** gave near identical results as **2.2**). The gelling of **2.1** (1.5 mM) reproduced the results found previously (Nguyen 1999) while solutions of **2.2** at the same concentration did not gel. Attempts to “turn off” the gelling propensity of **2.1** by dilution were unsuccessful where even 0.1 mM solutions became viscous and pale pink although the onset of gelling was slightly delayed (Figure 2.10). Likewise, raising the concentration of **2.2** up to 5.0 mM did not “turn on” the propensity for gelling. Originally it was thought that dilute solutions of **2.1** could limit the intermolecular interactions that caused a highly aggregated state at room temperature, which in turn would inhibit gel formation. Also it was thought that **2.2** could be forced to mimic the leucine intermolecular associations supposedly occurring for **2.1** at room temperature just by increasing its concentration. At this point, these two compounds, whose aggregation properties appeared to be dictated by just one residue substitution, are resistant to any attempts to switch their gelling behaviors.



1.5 mM **2.1**
after 150 min



1.5 mM **2.2**
after 150 min

Figure 2.10

Kinetics of the conformational transition of **2.1** and **2.2** at different concentrations. The loss of the CT band absorbances for **2.1** was a consequence of aedamer unfolding and "entangling" as a gel formed. For 0.1 mM solutions of **2.1**, a 1 cm cuvette was necessary to increase the CT signal above baseline noise while a 0.1 cm cuvette was used for the other solutions. 5.0 mM solutions of **2.2** had a CT corrected absorbance of 0.23 ± 0.04 at all times (not shown). Photographs of **2.1** and **2.2** after 150 min of heating are also included.

2.3.5 Discussion of Thermal Gelling Data

Although the hope was to modulate gelling properties through residue substitution it appeared that gelation by aedamers was an all-or-none proposition with no gray area in which to observe intermediate differences in the time course of the slow and rapid phases of the conformational transition. Encouraging though, was that a lone residue substitution (Asp→Leu) was identified that in effect converted **2.2**, which did not form aqueous gels, into **2.1**, an effective gelator. A report from Rotello and co-workers may provide clues as to how to modulate the gelling properties of aedamers (Ilhan 1999). That report illustrated the use of small molecule intercalators to control the solution structures of their globular polymers via intra- and intermolecular aromatic stacking under varying temperatures. A more thorough knowledge of both the intra- and intermolecular interactions at play in the gel formation of aedamers would be indispensable in achieving the control of structure demonstrated by Rotello and co-workers. Direct measurements of the physical properties of the aedamer gels formed at different conditions would also advance this research. Worthwhile future experiments may include variable-temperature rheology (to calculate gel strengths and water loss/recovery while stressed) and transmission electron microscopy (to visualize gel morphology) (Menger 2003).

2.3.6 Exploring Aedamer-Protein Interactions

The ability of aedamers to adopt well-defined conformations in water stimulated the group to pursue aedamers that have useful interactions with natural molecules in biological systems. Recent papers, extending the seminal work of

Lokey and Iverson (Lokey 1997), have exquisitely shown that oligo(Ndi)s can intercalate different DNA sequences with remarkable specificity (Lee 2004, Guelev 2000, 2001b, 2002). The strength and selectivity of binding was attributed in part to a) the aromatic interactions of the electron-deficient Ndi with the DNA bases and b) the linkers which were amenable to combinatorial library synthesis to create a diverse set of intercalators to screen. Aedamers might also have the same attributes in the context of protein binding especially considering that a) most proteins contain aromatic amino acids and b) aedamer folding remains robust with a wide range of linkers (Zych 2000) making combinatorial libraries possible. Therefore, in light of the group's success investigating oligo(Ndi)-DNA interactions, a strong motivation grew to explore the possibility of oligo(Dan-Ndi)s (i.e. aedamers) interacting with proteins.

The proposed gelling mechanism shown in Figure 2.4 sparked thoughts of a proof-of-concept experiment in which enzyme capturing (and putative refolding inhibition) by **2.1** would be a good indicator of aedamer-protein interactions. It was expected that **2.1** would be most effective as an inhibitor under heating conditions (80 °C) in which its exposed hydrophobic aromatic units could trap a thermally denatured enzyme before both could properly refold back when the solution cooled to room temperature. Any aromatic interactions in proteins would be between residues with relatively electron-rich aromatics (phenylalanine, tyrosine, histidine, and tryptophan). It is reasonable to believe that donor-acceptor interactions between an Ndi moiety of an unfolded aedamer and a natural amino

acid would be very competitive with the donor-donor aromatic interactions found in proteins.

Also proposed was to test aedamer **2.4**, which remains highly folded at 80 °C, on the off chance it would be able to capture unfolded enzyme just due to the availability of its terminal aromatic units or linker carboxylate functionalities. Lastly, it was not known whether aedamers inherently have elements that might endow these molecules with active site recognition capabilities in which case inhibition may not even require a heat-induced denature/trap route.

It was decided that the enzyme RNase would present an interesting challenge because of its robust structure and its ability to renature efficiently even after heating to above 60 °C (Figure 2.11). Plus, fluorometric assay kits called *RNaseAlert* can be purchased from Ambion (Austin, TX). These kits are used often by molecular biology laboratories to monitor RNase activity and to detect RNase contamination in solutions containing susceptible oligonucleotides. The RNase substrate probe emits a green fluorescence when cleaved (Figure 2.11). Lastly and most intriguing is that Ambion does indeed provide a storage solution called *RNaseSecure* that inhibits present RNase only when heated to above 60 °C. Once cooled this solution does not produce any measurable downstream enzyme inhibition. The solution contains proprietary ingredients therefore the active molecules and mode of action cannot be speculated on.

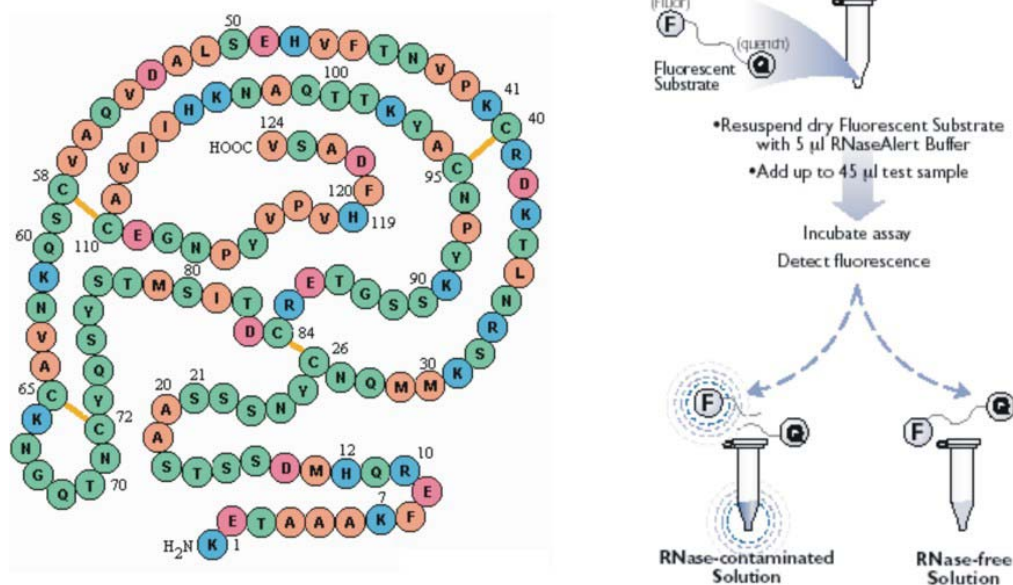


Figure 2.11 Primary structure of ribonuclease (RNase) indicating polar (green), hydrophobic (orange), basic (blue), and acidic (red) residues. Schematic of fluorometric assay adapted from the manual of the *RNaseAlert* kit sold by Ambion.

Compounds **2.1** and **2.4** at different concentrations were tested for their ability to inhibit RNase with and without a preheat treatment (Figure 2.12). Sodium dodecyl sulfate (SDS), an anionic detergent, was also tested. The general procedure for a “heat trial” involved heating the RNase enzyme solution (5 μL , activity = 0.01 U/mL) in the presence of aedamer or SDS (40 μL , various known concentrations) in (45 μL Na phosphate buffer) for 1 hour at 80 $^{\circ}\text{C}$. Once the solution had cooled, probe (10 μL , 5 mM) was added. Solutions were then transferred to a 96-well plate and fluorescence measured (Ex/Em 485/516 nm) at 30 minute time intervals. “Non-heat trials” were identical except the compound and RNase were mixed and left standing at room temperature for 1 hour before

the probe was added. High fluorescence readings indicate that RNase activity still remained and little inhibition had taken place (Figure 2.11). Negative controls contained only test compound, while positive controls contained only added RNase before probe was added. Lastly, it was observed that fluorescence quenching of the fully cleaved probe by Dan (**2.8**) or Ndi (**2.9**) monomers is insignificant.

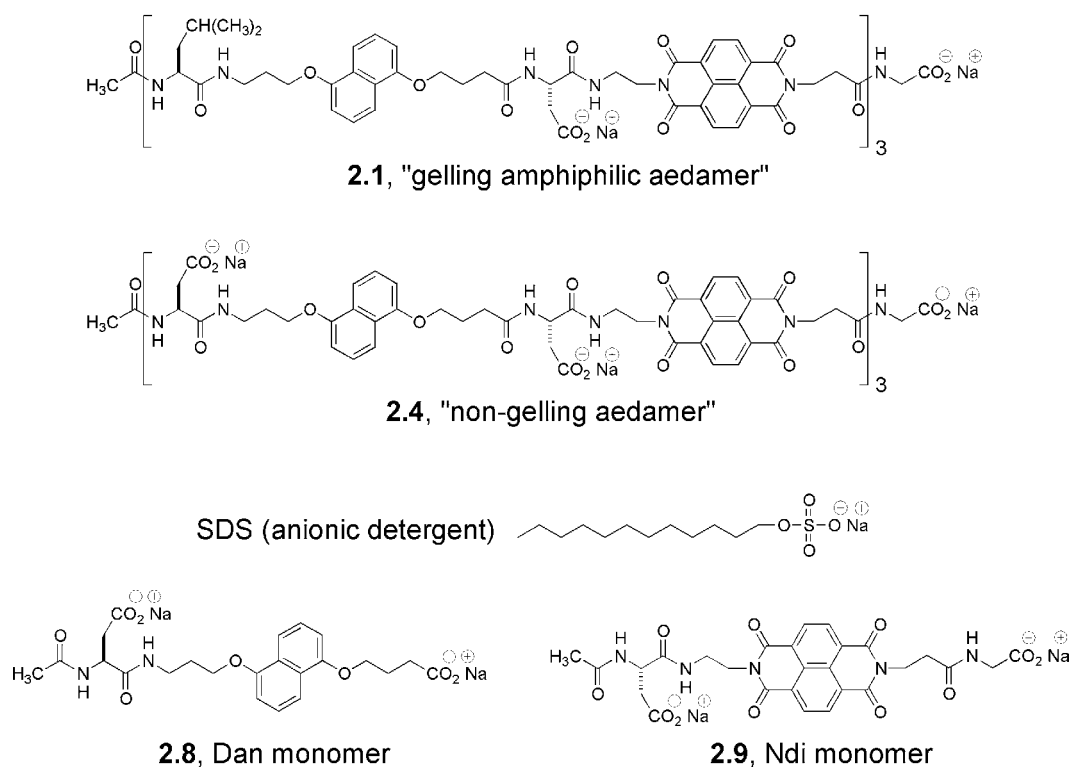


Figure 2.12 Compounds tested in the RNase refolding inhibition study.

2.3.7 Fluorometric Assay of RNase Activity

Figure 2.13 shows the fluorometric assay data obtained when **2.1** was used in the heat trial protocol described above. Keeping in mind that fluorescence is

proportional to enzyme activity, several trends from the bar graph are noteworthy. First, *RNasecure* was astonishingly effective at RNase inhibition giving readings near identical to the negative control. Second, while 30 μ M concentrations of **2.1** exhibited moderate inhibitory effects, attempts to completely wipe out RNase activity with higher concentrations of **2.1** surprisingly did not translate into greater inactivation of RNase. Lastly, since full inhibition was not reached in the runs with **2.1**, it is reasonable to assume that any active RNase remaining would demonstrate catalytic turnover and continue to cleave the probe leading to the observed rise in fluorescence with time. The positive control also showed this rise in fluorescence with time. Measurements after 48 hours gave readings of about 250 emission units (judged to represent complete cleavage of probe) for all plate wells except for the “Neg” and “*Secure*” wells. Based on the promising results from this heat trial using **2.1**, similar assays were carried out with the other test compounds, and without preheat treatments as well (Figure 2.4).

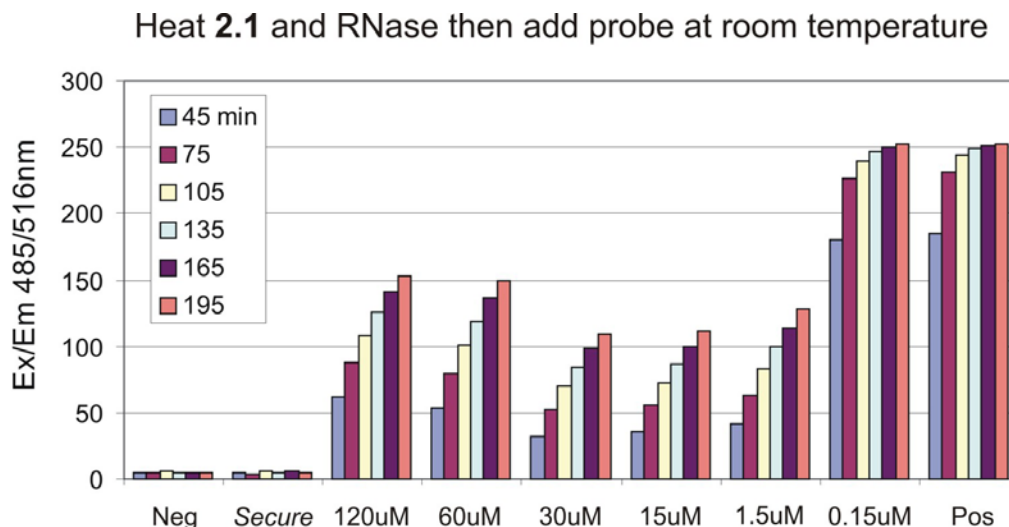


Figure 2.13 Fluorescence data of **2.1** at 120-0.15 μM concentrations measured at 30 minute time intervals. Runs with **2.1** afforded moderate refolding inhibition. Neg = negative control. *Secure* = Ambion's commercially available RNase inhibitor, *RNasecure*. Pos = positive control.

Figure 2.14 exhibits more extensive data; specifically the heat and non-heat trials using **2.1**, **2.4**, and SDS at different concentrations. Results at 105 minutes were reported at which time cleavage of the probe was judged to have reached near completion for the positive control. Three runs were performed for each of the conditions and results were reproducible (within 10%). Overall, the results comparing **2.1**, **2.4**, and **SDS** can be simply summarized: RNase activity was significantly decreased only by **2.1** and only when RNase was heated in the presence of **2.1**. Compound data from the other five bar graphs (grayed in Figure 2.14) gave similar emission numbers as their respective positive controls. Data for monomers **2.8** and **2.9** and a 1:1 mixture at all concentrations studied had limited inhibition effect as well. This monomer data indicates that there is probably a

strong dependence on the structural elements of **2.1** rather than purely aromatic-aromatic recognition events when **2.1** inhibits RNase.

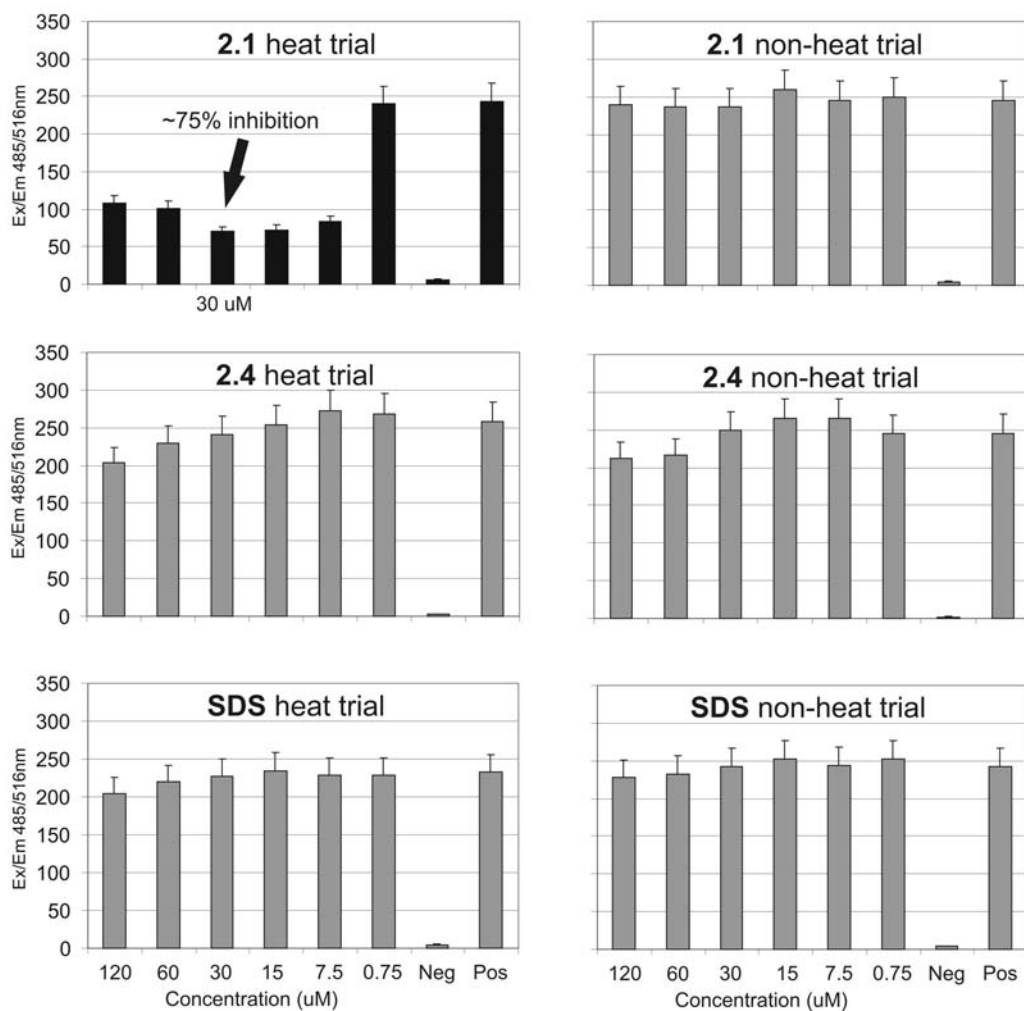


Figure 2.14 Fluorometric assay results for **2.1**, **2.4**, and **SDS** with and without preheat treatment measured at 105 minutes. Only the **2.1** heat trial gave dramatically different results (~75% inhibition for 30 μ M solutions) than the other compounds and conditions.

2.3.8 Discussion of Refolding Inhibition Data

Results shown in Figure 2.13 indicate that heating RNase in the presence of **2.1** certainly does decrease its activity but still the fact that a 120 μM solution of **2.1** performed worse than a 30 μM solution needed to be addressed. A possible explanation is that at higher concentrations the presumably aggregating aedamer in effect “gets in its own way” and entangles itself more efficiently than trapping the unfolding RNase. It follows to argue that 30 μM solutions of **2.1** possibly allowed better contact between unfolded aedamer and unfolded RNase at elevated temperatures while at higher concentrations unfolded **2.1** traps itself before having a chance to capture unfolded RNase. Still one has to remember that a 120 μM solution of **2.1** gave a modest 66% inhibition (a 30 μM solution gave ~80% inhibition) as compared to the positive control at 45 and 75 minutes (Figure 2.13).

In additional experiments related to the proposed explanation above, heating RNase with “gelled” **2.1** inhibited RNase but was slightly less effective than when heating RNase with “ungelled” **2.1** (Figure 2.15). (Aedamer solutions, at these 30 μM concentrations, were determined as “gelled” when the purple color of the solution faded after heating. Recall, that to physically confirm a viscous gel as in experiments described in section 2.3.4 required solutions 100 times more concentrated.) The results in Figure 2.15 suggested that an aggregated **2.1** surface might not be required for capturing unfolded RNase. Unlike the Nguyen study where gel formation was accelerated by the addition of pregelled material (Nguyen 1999), it did not seem this was the case for RNase inhibition. In Nguyen’s study, unfolded **2.1** was trapped much more efficiently when the

solution contained initially 10% gel product suggesting a high affinity of unfolded **2.1** for the tangled aggregate (Graph in Figure 2.3 and schematic in Figure 2.4). In sum, unfolded RNase did not appear to have this same high affinity. Instead it appeared that when RNase and **2.1** unfold in the presence of each other this led to greater enzyme inhibition than when RNase unfolds in the presence of pregelled **2.1** (Figure 2.15). Together, the results shown in Figures 2.13 and 2.15 imply that inhibition by **2.1** proceeded by a different mechanism than *RNase*secure. Also it is clear that more investigation is required to approach the outstanding inhibitory effects of Ambion's heat-activated RNase inhibitor solution.

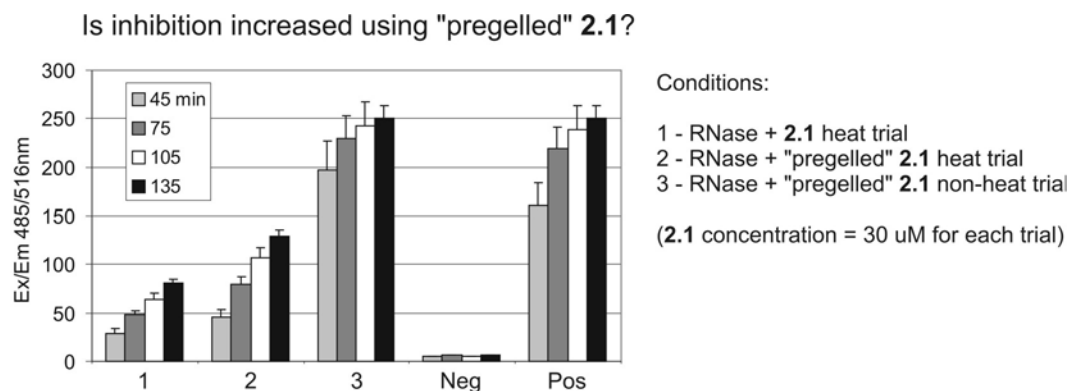


Figure 2.15 Conditions to determine if a preformed tangled aggregate of **2.1** can enhance inhibition in the same manner that gelled **2.1** enhances gelation through a product promoted mechanism.

The results in Figure 2.14 comment quite persuasively on the special inhibitory properties of **2.1**, but only when heated, as compared to **2.4**, SDS, and unheated **2.1**. This data bodes well for slight differences in aedamer chemical structure to modulate its physical properties and functions. A proposed mechanism of heat-triggered inhibition by **2.1** invokes a general, non-specific

association between the hydrophobic residues of the aedamer (in particular the electron-deficient Ndi moiety) and the RNase (and probably its electron-rich aromatics). Interestingly Ndi monomer **2.9** had no effect so it may be a combination of conformational effects and aromatic associations that ultimately give **2.1** its properties. The ability of **2.1** to aggregate appears to be important since **2.4**, **2.8**, and **2.9** (each of which do not form gels) had no significant effect. Still even with this proposed non-specific mode-of-action, one can envision future work taking advantage of the selective and opportunistic interactions between natural aromatic amino acids (phenylalanine, tyrosine, histidine, and tryptophan) and the naphthyl moieties of aedamers. In related research, screening of a peptide library has commenced to select sequences that strongly interact with a set of aedamers to identify high-affinity peptide tags. Hopefully these selection experiments will yield new insights into specific recognition elements and naphthyl oligomer-natural protein interactions.

2.4 CHAPTER CONCLUSIONS

Overall, the effects of linker substitutions on aedamer properties such as heat-responsive gelling and enzyme inhibition can be quite profound. Structure-activity relationship studies on gelling showed that while **2.1** has essentially the same intramolecular structure as aedamers **2.2-2.4**, apparently its intermolecular aggregation endows it with a propensity to form gels at elevated temperatures. This aqueous gel formation appeared to be an all-or-none situation where **2.1** gels but **2.2**, which differed by only a leucine to aspartate residue change, did not, even at high concentrations. This study also demonstrated that intramolecular folding

could be decoupled from bulk properties. This potential attribute could aid in designing highly derivatized aedamers (to target different properties) but with folding features that make the placement of functional groups fully predictable in the final conformation.

The investigation of **2.1** as an enzyme inhibitor further corroborated the unusual aggregation properties of **2.1** and emphasized that simple residue changes can have interesting effects. Only when RNase was heated in the presence of **2.1** was enzyme inhibition observed. This inhibition is a strong indication that there exist considerable interactions between unfolded **2.1** and unfolded RNase, enough to affect its activity. Lastly, this study is encouraging for future experiments probing aedamer-protein interactions.

2.5 IDEAS FOR FUTURE INVESTIGATIONS

Future investigations focused on the in-depth characterization of aedamer aqueous gels would advance both the gelling and the enzyme inhibition project. A couple of experiments are proposed below with this goal in mind along with the fact that SPPS makes it easy to synthesize a range of aedamer/peptide hybrids.

Constitutional isomers of the gelling aedamer and engineering techniques for hydrogel characterization. There is currently strong motivation to understand how to tune the properties of hydrogels to create biomaterials for tissue engineering and other applications (Langer 2003). Thus compounds **2.1-2.4** with varied hydrophobicity/philicity were tested. Other hydrophobic residues besides leucine though could be employed in future analogues. It would also be worthwhile to take **2.1**, which was the only aedamer shown to gel, and scramble

its primary sequence to see if leucine/aspartate position along the hydrophobic column could afford subtle differences in properties. Important for the success of these future studies though would be precise analytical techniques to monitor properties of these molecules in a wide range of conditions. The Chemical Engineering department at the University of Texas at Austin has such instruments as variable-temperature rheometers, light scatterers designed for large gels rather than proteins, and specialized microscopes that should prove to be extremely useful for this proposed study.

Investigation of new aedamer-protein interactions. As stated before aedamer-peptide affinity studies have been initiated. Another related project that has been kicked around is to use the Dan:Ndi interaction to create pseudocyclic peptides. An example would be a tetrapeptide capped on one end with a Dan unit and the other end with a Ndi unit which might induce a molecular turn via the Dan:Ndi association. This potentially would create a new set of compounds with flexibilities in between that of linear and covalently looped cyclic peptides. Peptide-based enzyme inhibitors have been explored testing how rigidification affects their binding and it is possible that intermediate flexibilities may be most effective for some tetrapeptide drugs. With this being the case, aedamer/tetrapeptide hybrids may act favorably as protein ligands. The feasibility of this proposed study will become more apparent after the description of naphthyl oligomer turns (Chapter 3) and artificial hetero-duplexes (Chapter 4), both of which demonstrate the strength and specificity of the Dan:Ndi interaction to cause the formation of structures beyond a pleated-ribbon fold.

2.6 EXPERIMENTAL SECTION

Solid phase peptide synthesis. A typical synthesis started with 0.10g (0.060 mmol) Fmoc-Gly-Wang resin (Advanced ChemTech, 100-200 mesh, 0.6 mmol/g) placed in a 5 mL fritted polypropylene syringe (Torviiq) and swelled in 4 mL DMA (*N,N*-dimethylacetamide) using a wrist-action shaker at low speed for 30 min. The DMA was drained and the Fmoc group removed by shaking with 4 mL deprotection solution (25 vol% piperidine in DMA) for 20 min, drained and repeated. The resin was then rinsed with DMA (3 × 4 mL), *i*PrOH (3 × 4 mL), and again with DMA (3 × 4 mL) and this wash was repeated after each step. Coupling reactions consisted of 3 equivalents (0.18 mmol) of the particular amino acid adduct dissolved in 3 mL DMA and taken up by the syringe followed by 3 equivalents (0.18 mmol) coupling reagent, PyBOP, (benzotriazole-1-yl-oxy-tris-pyrrolidino-phosphonium-hexafluorophosphate) (Novabiochem) in 1 mL DMA and 6 equivalents (0.36 mmol) base (*N*-methylmorpholine). The resin was shaken for 60 min for each coupling reaction. Rinsing, deprotection, rinsing, and coupling were repeated until the desired length was obtained. Either a rotary or orbital shaker was used for long periods of shaking/agitation but each time new solvent or solution was added to the resin the reaction syringe was capped and vortexed for a couple of seconds to break up clumps of resin. This seemed to improve overall yields by at least 10%.

After the last Fmoc deprotection the *N*-terminus of the oligomer was capped with an acetyl group by addition of 15 equivalents (0.9 mmol) DIEA (*N,N*-diisopropylethylamine) in 1.5 mL of DMA followed by 15 equivalents (0.9

mmol) acetic anhydride in 1.5 mL of DMA and shaken for 45 min. The oligomer was cleaved off the resin by shaking for 60 min with 4 mL TFA with 0.1g phenol as a cation scavenger and this solution also removed the *t*-butyl protecting group on the aspartate side chains. The TFA solution was collected and the resin was rinsed with additional TFA and CH₂Cl₂. The rinses were combined with the TFA solution and evaporated to an oil under reduced pressure at 60 °C. The oil was sonicated with heptane for 10 min and once again evaporated. The residue was then sonicated with diethyl ether for 5 min and cooled to 0 °C resulting in a granular precipitate that was collected by a glass fritted funnel and washed with additional cold diethyl ether. Crude solids were then dissolved through the vessel filter with a minimum amount of 50 mM sodium phosphate buffer, pH = 7.0 and subjected to fast protein liquid chromatography (FPLC) purification (details follow). Fractions judged pure by high performance liquid chromatography (HPLC) (details follow) were lyophilized and afforded **2.1-2.4** as airy purple solids.

Purification by FPLC. Crude oligomers dissolved in 50 mM sodium phosphate buffer (pH = 7) were purified on a Pharmacia FPLC system equipped with LKB P-500 pumps, a GP250 Plus programmer, and 254 nm UV detection using a Pharmacia column filled with Source™ 15RPC reverse-phase media from Amersham Pharmacia. A solvent gradient of 95% 0.1 mM ammonium acetate / 5% CH₃CN to 50% 0.1 mM ammonium acetate / 50% CH₃CN over 60 min was used. Solvents were degassed, filtered and were of high purity (double distilled H₂O and spectrograde acetonitrile from EM Science). Purity of the collected

fractions was judged by HPLC using a 50×4.6 mm “Luna” 5 micron C18 column from Phenomenex and a Beckman Coulter HPLC system equipped with a photodiode array detector scanning between 190 nm and 600 nm. A solvent gradient of 95% 0.1 mM ammonium acetate / 5% CH₃CN held for 1 min then ramped to 50% 0.1 mM ammonium acetate / 50% CH₃CN over 14 min was used and gave good resolution. Appropriate fractions were pooled and lyophilized for 48 hrs under a vacuum of < 10 microns. Pure compound was dissolved in H₂O and desalted by adsorption onto a C18 Sep-Pak® Plus cartridge from Waters followed by a H₂O wash and recovery with a H₂O/CH₃CN mixture and then lyophilized again for 48 hrs prior to experiments.

The recipe for the 50 mM sodium phosphate buffer, pH = 7.0, used in most experiments follows: Dissolve 8.16 g Na₂HPO₄·7H₂O and 2.70 g NaH₂PO₄·H₂O in 1L of dd H₂O.

Compound characterization (1D-NMR general methods). Samples were readily soluble in 50 mM sodium phosphate, pH = 7.0 D₂O. Routine spectra of monomers and precursors were obtained on a Varian UNITY+ 300 MHz spectrometer. Spectra were recorded on a Varian INOVA 500 MHz spectrometer at 1 mM concentrations of compound and TSP-*d*₄ (3-trimethylsilyl-propionic-2,2,3,3-*d*₄ acid, sodium salt) was used as a reference (δ = 0.00 ppm). Chemical shifts reported in ppm and abbreviations used are singlet (s), doublet (d), doublet of doublet (dd), triplet (t), quartet (q), multiplet (m) and complex multiplet of non-equivalent protons (comp). J coupling constants (*J*) reported in Hz.

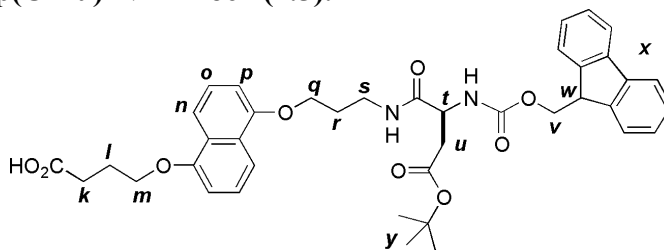
“AcHN-(LeuDanAspNdi)₃Gly-OH” (2.1). (SPPS yield = 40%) ¹H NMR (500 MHz, D₂O) Spectra gave prohibitively broadened signals. MALDI MS calcd for C₁₄₂H₁₅₁N₁₉NaO₃₉ [MH]⁺ 2771.8, found 2770.8.

“AcHN-(LeuDanAspNdi)₂AspDanAspNdiGly-OH” (2.2). (45% yield) ¹H NMR (500 MHz, D₂O) δ = 8.01-7.82 (12H), 6.80-6.42 (12H), 6.31-6.09 (6H), 4.68-4.64 (4H), 4.26-4.05 (13H), 3.83-3.92 (26H), 2.83-2.54 (15H), 2.48-2.34 (6H), 2.09-1.80 (15H), 1.55-1.46 (4H), 0.83 (d, *J* = 6.1, 3H), 0.78 (d, *J* = 6.1, 3H); FAB MS calcd for C₁₄₀H₁₄₆N₁₉O₄₁ [MH]⁺ 2749.0, found 2749.0.

“AcHN-LeuDanAspNdi(AspDanAspNdi)₂Gly-OH” (2.3). (49% yield) ¹H NMR (500 MHz, D₂O) δ = 8.05-7.83 (12H), 6.71-5.81 (18H), 4.66-4.64 (3H), 4.34-3.95 (14H), 3.69- 3.30 (26H), 2.82-2.39 (20H), 2.02-1.89 (16H), 1.65-1.40 (8H), 0.92-0.81 (12H); FAB MS calcd for C₁₃₈H₁₄₀N₁₉O₄₃ [MH]⁺ 2752.7, found 2752.7.

“AcHN-(AspDanAspNdi)₃Gly-OH” (2.4). (50% yield) ¹H NMR (500 MHz, D₂O) δ = 8.00-7.65 (12H), 6.81-6.59 (18H), 4.70-4.60 (5H), 4.52 (dd, *J* = 8.8, 5.0, 1H), 4.25-4.40 (12H), 3.87-3.77 (6H), 3.73 (s, 2H), 3.70-3.40 (18H), 2.47-2.37 (6H), 2.07-1.85 (6H), 1.93 (s, 3H); MALDI MS calcd for C₁₃₆H₁₃₃N₁₉NaO₄₅ [MH]⁺ 2775.6, found 2775.7.

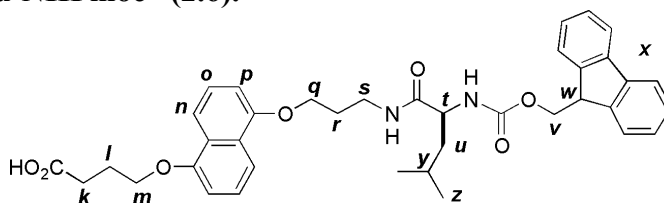
“HO-Dan-Asp(O^tBu)-NHFmoc” (2.5).



¹H NMR (300 MHz, DMSO-*d*₆) δ = 12.17 (s, 1H *OH*), 8.03 (t, *J* = 5.4, 1H *NH*), 7.86 (d, *J* = 7.5, 2H *x*), 7.73-7.67 (comp, 2H *x*, 2H *n*), 7.6 (d, *J* = 8.3, 1H *NH*),

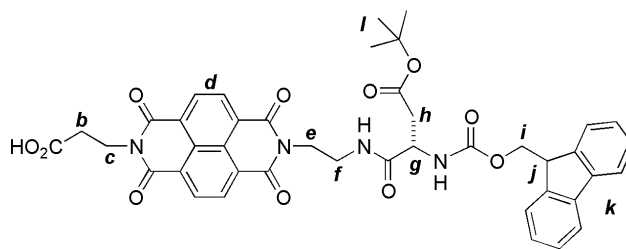
7.41-7.28 (comp, 4H *x*, 2H *o*), 6.94 (d, $J = 7.6$, 1H *p*), 6.91 (d, $J = 7.6$, 1H *p*), 4.35-4.28 (comp, 1H *t*, 1H *w*), 4.25-4.18 (m, 2H *v*), 4.15-4.10 (comp 2H *m*, 2H *q*), 3.38-3.31 (comp, 2H *s*, 2H *u*), 2.65 (dd, $J = 10.3$, 5.7 1H *k*), 2.45 (m, 1H *k*), 2.10-1.97 (comp, 2H *l*, 2H *r*), 1.35 (s, 9H *y*); ^{13}C NMR (300 MHz, DMSO- d_6) $\delta = 174.1, 170.4, 169.4, 155.7, 153.9, 153.8, 143.8, 143.7, 140.7, 127.6, 127.0, 126.0, 125.9, 125.3, 125.2, 120.1, 113.6, 113.5, 105.7, 80.0, 66.9, 65.7, 65.4, 64.9, 51.6, 46.6, 37.7, 35.8, 30.4, 28.8, 27.6, 24.3, 15.1$; CI HRMS calcd for $\text{C}_{40}\text{H}_{45}\text{N}_2\text{O}_9$ $[\text{MH}]^+$ 697.313, found 697.312.

“HO-Dan-Leu-NHFmoc” (2.6).



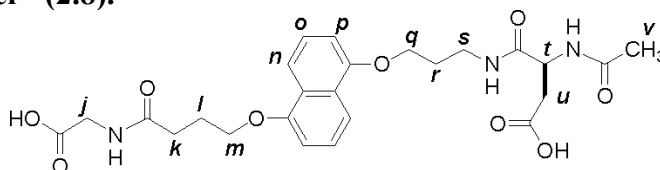
^1H NMR (300 MHz, D_2O) $\delta = 12.15$ (s, 1H *OH*), 8.01 (t, $J = 5.5$, 1H *NH*), 7.87 (d, $J = 7.5$, 2H *x*), 7.73-7.69 (comp, 2H *x*, 2H *n*), 7.4 (d, $J = 8.3$, 1H *NH*), 7.41-7.28 (comp, 4H *x*, 2H *o*), 6.95 (d, $J = 7.3$, 1H *p*), 6.91 (d, $J = 7.3$, 1H *p*), 4.28 (m, 1H *w*), 4.20 (m, 2H *v*), 4.15-4.11 (comp 2H *m*, 2H *q*), 3.99 (m, 1H *t*), 3.39-3.29 (comp, 2H *s*, 2H *u*), 2.49-2.48 (m, 2H *k*), 2.10-1.95 (comp, 2H *l*, 2H *r*), 1.60-1.55 (m, 1H *y*), 1.50-1.37 (m, 2H *u*), 0.84 (dd, $J = 13.3, 6.6$, 6H *z*); ^{13}C NMR (300 MHz, DMSO- d_6) $\delta = 174.1, 172.3, 155.9, 153.9, 153.8, 143.9, 143.7, 140.7, 127.6, 127.0, 126.0, 125.9, 125.3, 120.0, 113.6, 113.5, 105.7, 66.9, 65.5, 65.3, 53.1, 46.7, 40.8, 35.6, 30.4, 28.8, 24.3, 24.2, 22.9, 21.5$; CI HRMS calcd for $\text{C}_{38}\text{H}_{43}\text{N}_2\text{O}_7$ $[\text{MH}]^+$ 639.307, found 639.306.

“HO-Ndi-Asp(O^tBu)-NHFmoc” (2.7).



^1H NMR (300 MHz, D_2O) δ = 12.39 (s, 1H *OH*), 8.58 (s, 4H *d*), 8.05 (t, J = 5.9 1H *NH*), 7.83 (d, J = 4.2, 1H *k*), 7.82 (d, J = 4.2, 1H *k*), 7.61 (d, J = 7.6, 1H *k*), 7.58 (d, J = 7.6, 1H *k*), 7.44 (d, J = 8.5, 1H *NH*), 7.37 (t, J = 7.6, 1H *k*), 7.36 (t, J = 7.6, 1H *k*), 7.25 (t, J = 6.9, 1H *k*), 7.23 (t, J = 7.6, 1H *k*), 4.26-4.17 (comp, 1H *g*, 1H *j*, 2H *i*), 4.14-4.03 (comp, 2H *c*, 2H *f*), 3.54-3.35 (m, 2H *e*), 2.61 (t, J = 7.6, 2H *h*), 2.55-2.31 (m, 2H *b*), 1.31 (s, 9H *l*); ^{13}C NMR (300 MHz, $\text{DMSO}-d_6$) δ = 172.3, 170.8, 169.3, 162.7, 162.3, 155.6, 143.7, 143.5, 140.6, 140.5, 130.2, 127.6, 127.5, 127.0, 126.9, 126.4, 126.1, 126.0, 125.9, 125.2, 125.1, 120.0, 119.9, 127.6, 127.5, 127.0, 126.9, 126.4, 126.1, 126.0, 125.9, 125.2, 125.1; 80.0, 65.7, 51.4, 46.4, 37.4, 37.3, 36.6, 36.0, 32.0; CI HRMS calcd for $\text{C}_{42}\text{H}_{39}\text{N}_4\text{O}_{11}$ $[\text{MH}]^+$ 775.262, found 775.261.

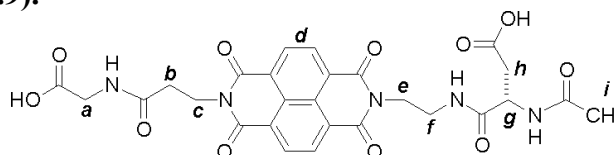
“Dan monomer” (2.8).



3-acetylamino-*N*-(3-{5-[3-(carboxymethyl-carbamoyl)-propoxy]-naphthalen-1-yloxy}-propyl)-succinamic acid (2.8). (SPPS yield = 91%) ^1H NMR (300 MHz, D_2O) δ = 7.88 (d, J = 8.4, 1H *n*), 7.84 (d, J = 8.6, 1H *n*), 7.50 (m, J = 2H *o*), 7.07 (t, J = 7.6, 2H *p*), 4.47 (dd, J = 5.2, 3.4, 1H *t*), 4.29-4.25 (comp, 2H *m*, 2H *q*), 3.69 (s, 2H *j*), 3.50 (t, J = 6.7, 2H *s*), 2.60 (dd, J = 5.2, 7.8, 1H *u*), 2.58 (t, J = 7.0,

2H *k*), 2.50 (dd, $J = 8.6, 7.4$, 1H *u*), 2.24 (m, 2H *l*), 2.13 (m, 2H *r*), 1.89 (s, 3H *v*); ^{13}C NMR (300 MHz, D_2O) $\delta = 178.2, 176.5, 174.6, 174.2, 154.5, 126.7, 126.6, 114.8, 114.6, 107.7, 107.3, 52.7, 47.1, 43.9, 39.5, 37.2, 33.6, 28.6, 25.4, 22.3$; CI HRMS calcd for $\text{C}_{25}\text{H}_{32}\text{N}_3\text{O}_9$ $[\text{MH}]^+$ 518.214, found 518.213.

“Ndi monomer” (2.9).



3-acetylamin-*N*-(2,{7-[2-(carboxymethyl-carbamoyl)-ethyl]-[1,3,6,8-tetraoxo-3,6,7,8-tetrahydro-1*H*-benzo[*lmn*][3,8]phenanthrolin-2-yl]}-ethyl)-succinamic acid (2.9). (94% yield) ^1H NMR (300 MHz, D_2O) $\delta = 8.56$ (AA'BB' $J = 7.6, 5.6$, 4H *d*), 4.43 (t, $J = 7.1$, 2H *c*), 4.36 (dd, $J = 4.8, 4.4$, 1H *g*), 4.30 (m, 2H *f*), 3.73 (s, 2H *a*), 3.61 (t, $J = 5.7$, 2H *e*), 2.74 (t, $J = 7.1$, 2H *b*), 2.45 (dd, $J = 4.8, 11.2$, 1H *h*), 2.33 (dd, $J = 9.2$ and 6.8 , 1H *h*), 1.86 (s, 3H *i*); ^{13}C NMR (300 MHz, D_2O) $\delta = 177.4, 176.4, 173.9, 173.6, 173.2, 163.9, 163.7, 131.1, 131.0, 125.9, 125.8, 125.6, 51.6, 42.3, 39.6, 38.6, 37.3, 33.9, 21.6$; CI HRMS calcd for $\text{C}_{27}\text{H}_{26}\text{N}_5\text{O}_{11}$ $[\text{MH}]^+$ 596.163, found 596.163.

UV-Vis spectroscopy. UV-Vis spectra were taken on a temperature regulated Hewlett Packard 8452A diode array spectrophotometer. Concentration of stock solutions used for UV studies was initially determined by NMR integration of a known concentration of TSP- d_4 added to an aliquot. Solutions of compound (40 μM in buffered H_2O) were measured in a 1 cm pathlength cuvette equipped with a microstirrer.

Light scattering (LS). A DynaPro-801 light scatterer from Protein Solutions was used with the accompanying software. All data points represent the average of > 20 measurements per dilution. Aedamer solutions were made with 50 mM Na phosphate buffer six hours before measurements. Solutions were filtered through a 0.02 mm pore 13 mm Anodisc membrane filter from Whatman with no evidence of clogging or adsorbed compound just before filling a 12 μ L cuvette and measurements taken. It usually took an equilibration time of 5 minutes before the average intensity of light scattered remained sufficiently steady ($\pm 10\%$). Only data taken after this equilibration were used in the analysis. Data of the average intensity of light scattered were reproducible from trial to trial, sizing data though gave high errors and were not considered in this dissertation.

Thermally-triggered gelling. Solutions were placed in a 0.1 cm pathlength cuvette and plugged with a sliver of rubber. The cuvette was placed in the Hewlett Packard 8452A diode array spectrophotometer whose cuvette holder had been heated to 80 °C by a water bath. After 1 minute to heat the cuvette through, measurements were taken every five minutes with manual shaking in between each UV-Vis spectrum taken. The CT band absorbance was monitored and corrected as previously describe (Figure 2 and 3 from Nguyen 1999). In brief, as the solution became more viscous the baseline in the visible region of the spectrum rose indicating increased light scattering of the tangled aggregate. The absorbance at the CT wavelength of the fully gelled material was subtracted from CT band absorbance during the heating.

Fluorometric assay. Material and supplies were purchased from Ambion unless otherwise noted (product numbers included). The bench surface, pipettors, and gloves were treated with *RnaseZap* (#9780). A bunsen burner flame was left running as well. Na phosphate buffer was made with nuclease-free water (non DEPC treated, #9937). Pre-sterilized, 200 μ L size pipet tips from ART Molecular Bioproducts were used. Test compound solutions were made and 40 μ L were pipetted into RNase-free microfuge tubes (#12350). 45 μ L of Na phosphate buffer was added along with 5 μ L of RNase (activity = 0.01 U/mL, included in *RNaseAlert* kit #1964). For heat trials, the microfuge tube was placed in a 80 °C oil bath for 1 hour with strong agitation by vortex and then centrifuged every 20 minutes. For non-heat trials the samples stood at room temperature but were still agitated. Meanwhile the probe (aliquots were lyophilized in microfuge tubes by Ambion) was suspended with 10 μ L of provided buffer (probe and buffer include in *RNaseAlert* kit). The samples were brought to room temperature and pipetted into the probe, agitated, and transferred to a 96 well assay plate from Corning (#3610). Large air bubbles were popped using disposable needles and fluorescence measurements were made at 30-minute time intervals. All samples, including the negative and positive controls contained a total of 100 μ L of solution and concentrations reported in the data figures represent concentrations of these 100 μ L solutions.

CHAPTER 3

Switching the Folding Patterns of Naphthyl Oligomers

3.1 CHAPTER SUMMARY

Introduction. While Chapters 1 and 2 focused on aedamers, which have an alternating sequence of the form (Dan-Ndi)_n, this chapter will describe work with non-alternating naphthyl oligomers of the sequence Dan_{n+1}-Ndi_n (Figure 3.1). These naphthyl oligomers are expected to fold with a different topology than the pleated ribbon folds exhibited by aedamers. Therefore this project represents the group's first attempts to diverge from the original aedamer design in order to explore the strength and specificity of the Dan:Ndi interaction to direct more challenging folding. While natural α -peptides and nucleotides can form different secondary structures based on their primary sequence, β -peptides are the only foldamers that possess this same ability with reported examples of β -peptide helices and turns (Langenhan 2004) in literature. These systems employ hydrogen bonding and though helices have been shown to be stable in water, the reported turn structures are only stable in non-aqueous solvents. The work presented here with naphthyl oligomers demonstrates a strategy to control distinctly different folding patterns *in water*.

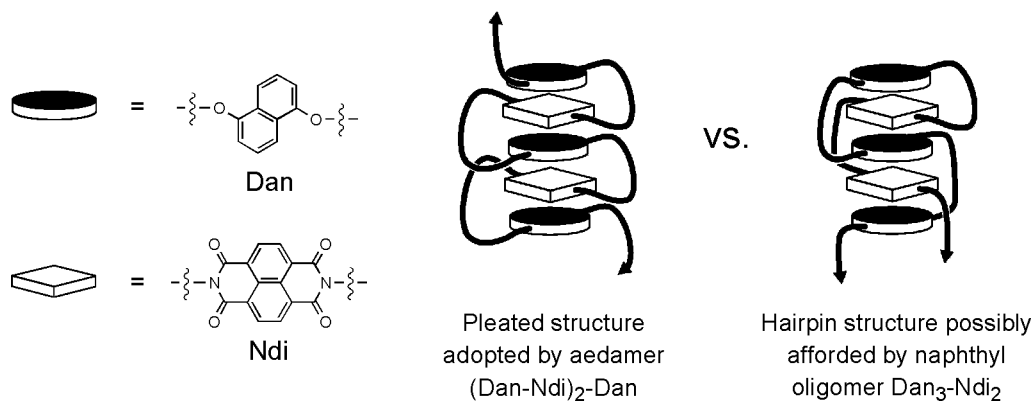


Figure 3.1 Cartoon representation of two different folding patterns. Arrows indicate direction of growth with longer oligomers.

Goals. Experiments described in this chapter aimed to answer the question: *Can naphthyl oligomers be rationally designed to adopt hairpin structures based on directed aromatic stacking?* The short-term goal of this work was to demonstrate the ability of non-alternating naphthyl oligomers to adopt stable folding patterns, in particular turn motifs, as an alternative to the pleated secondary structures of aedamers. The long-term objective of this research is to use various folding patterns to possibly increase the stability of the hydrophobic column and eventually exploit this stability and predictive manipulation of folding to design complex functional molecules.

Approach. Trimers of the type Dan-(X)-Dan-Ndi, varying in linker length (X), were probed by UV-Vis spectroscopy for the formation of a turn motif where the Ndi unit folds back into the trimer and inserts in between the two Dan units. A structural analysis of the best turn candidate, along with control compounds, was then accomplished using 2D NMR techniques and computer modeling.

Results. Overall, the work described in this chapter demonstrated that two simple, but discrete, folding patterns can be created just by changing the sequence of linked Dan and Ndi units (Gabriel 2004b). Data from unfolding investigations, NOESY spectroscopy and computer modeling supported conformational interpretations of a pleated fold for a Dan-Ndi-Dan trimer and an “intercalative” fold for a Dan-Dan-Ndi trimer. Appropriate control compounds were also useful for this investigation. This intercalative trimer was incorporated into a Dan₃-Ndi₂ pentamer to test if the turn motif can aid in templating hairpin-type structures. Preliminary NMR studies were promising and encouraged further use of the predictable and strong Dan:Ndi association to study different binding patterns (Chapter 4). Lastly, the creation of different folding patterns via the facile shuffling of two aromatic monomer types may also provide insights into the general role of aromatic interactions in stabilizing structures.

3.2 BACKGROUND: MIMICS OF BIOLOGICAL HAIRPIN STRUCTURES

The continued pursuit of controlling molecular topology, whether through the development of foldamers, peptidomimetics or other chemical models, may lead to a greater understanding of the folding and binding properties associated with biomolecules (Brandon 1999). One of the key oligomeric conformations in biology is the hairpin structure of a single-stranded biomolecule, which incorporates a U-shaped turn motif. These structures are ubiquitous in oligonucleotides such as DNA loops, ribozymes (catalytic RNA) (Liley 1999), and aptamers, (RNA with molecular recognition properties) (Marshall 1997). Research on hairpin nucleotidomimetics has led to the discovery of extremely

compact DNA fragments (Hirao 1994) and a fuller knowledge of the thermodynamics of DNA folding (Soto 2000).

Concerning peptides, the β -sheet secondary structure found in many proteins is controlled by a collection of hairpin folds. While researchers synthesizing peptidomimetics are actively engaged in using artificial turns to design β -sheet mimics (Kemp 1990, Nowick 2000), researchers designing foldamers have also created synthetic β -sheets and examples were presented in Chapter 1. Also, a comprehensive review on peptide models of β -hairpin structure has been published (Searle 2001). Though there are many noteworthy examples of models of molecular turns, this introduction will touch briefly upon the work of two particular groups, Waters and Li that have specifically utilized aromatic interactions to probe turn conformations.

Waters and co-workers have synthesized structural mimics to investigate β -hairpin peptide stability and to understand how aromatic interactions contribute to peptide structure and binding specificity (Tatko 2002, Butterfield 2002). A substantial data set has been built from which to elucidate the driving forces for folding and molecular recognition of β -hairpin peptides with specific residue substitutions (Figure 3.2). They have also developed models to probe “diagonal” C-H $\cdots\pi$ interactions that are distinct from the noncovalent interactions driven by the hydrophobic effect (Tatko 2004). With rigorous NMR and thermal denaturation experiments they have found interesting geometries of the interacting residues and have parsed the energy of the folding of a β -hairpin peptide into its enthalpic and entropic components.

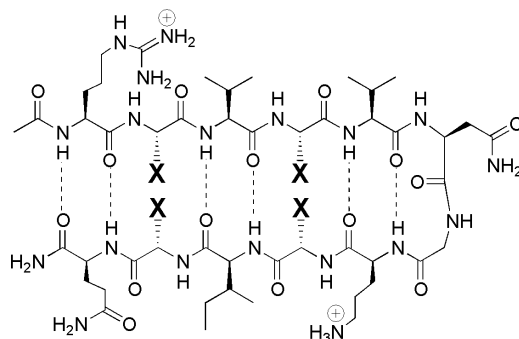


Figure 3.2 Hairpin peptides synthesized by Waters and co-workers (Tatko 2002, 2004). X = various sidechains to explore aromatic-aromatic and C-H $\cdots\pi$ interactions.

Detailed investigations into the energetics of noncovalent interactions are growing in importance since it has been demonstrated that many proteins are stable by only 5-10 kcal per mol over misfolded states (Tatko 2002). So, although isolated noncovalent interactions are weak, the combination of these many subtle attractive forces and their binding geometries can have a pronounced effect on stability and structure, respectively. This information will be significant for *de novo* protein design. As expected, their meticulous studies into the basic science of noncovalent interactions have indeed accelerated the development of functional peptides with tunable properties including ATP recognition (Butterfield 2003) and flavin redox potential modulation (Butterfield 2004).

Li and coworkers have developed δ -peptide foldamers that adopt a turn-type conformation using a donor-acceptor interaction between electron-rich 1,5-dialkoxynaphthalene (identical to the Dan moiety) and an electron-deficient pyromellitic diimide (Pdi) (Zhao 2004). There are two main differences between

δ -peptide foldamers and the naphthyl oligomer foldamers from the Iverson group. One is that δ -peptides present the aromatic rings as side chains projecting along the backbone while the aromatic rings in naphthyl oligomers are incorporated within the backbone. This arrangement is predicted to cause a weaving scenario for naphthyl oligomers (Figure 3.1) rather than a zipper-type situation for the Li system (Figure 3.3). Another important distinction is that the δ -peptide system operates in chloroform and DMF while naphthyl oligomers are water-soluble and are anticipated to fold most stably in aqueous solutions.

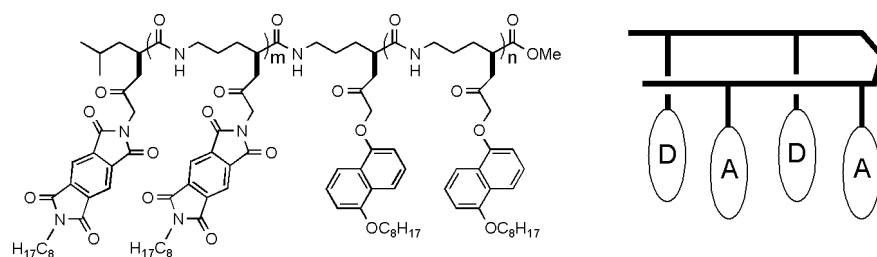


Figure 3.3 Donor-acceptor δ -peptides synthesized by Li and co-workers and a cartoon representation of their asserted “zipper” structure (Zhao 2004).

It is predicted that the Dan:Ndi interaction can be used to design similar turn structures predicated on the idea that the aromatic units will arrange themselves to maximize the number of Ndi:Dan face-to-face contacts, even if it required the chain molecule to fold back on itself. Evidence of this hairpin fold would represent further control of secondary structures through the fairly simple means of shuffling the naphthyl primary sequence.

Also, there is a possibility that hairpin structures will stabilize the naphthyl hydrophobic column further. First, it was postulated that the mechanism of

unfolding a pleated stack of naphthyl units starts at the exposed ends, analogous to DNA fraying (Lokey 1997). Second, work done by Zych has shown that folded conformations go through fairly dynamic motions with aedamers actually surveying many folded states (Zych 2000, 2002). The proposed hairpin naphthyl oligomer has the potential of rigidifying the hydrophobic core due to the weaving of the two halves of the strand. It is also reasonable to expect that for longer oligomers, this weaving pattern, rather than a pleated ribbon pattern, would make it more difficult for the chain to unravel considering the large amount of concerted conformational rearrangements required to fully unfold.

If promising, this initial work would lead an effort toward accessing more intricately folded structures that approach the size and functionality of biomolecules. These architectures should be amenable to substantial functionalization without disruption of structure as well.

3.3 RESULTS AND DISCUSSION

3.3.1 Synthesis of Non-Alternating Naphthyl Trimers

A critical element in a proposed naphthyl pentamer hairpin (Figure 3.4A) is the bend in the middle of the molecule formed by the -Dan-Dan-Ndi- central section, which can be thought of as the minimal turn unit for this hairpin structure. In this portion of the molecule, the Ndi residue is expected to insert itself, in a sense intercalate, in between the two Dan rings to satisfactorily desolvate both of its planar faces.

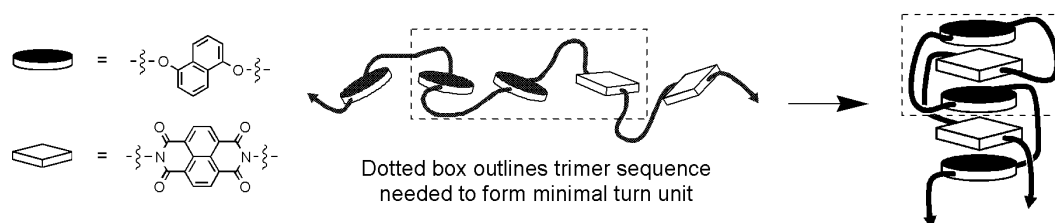
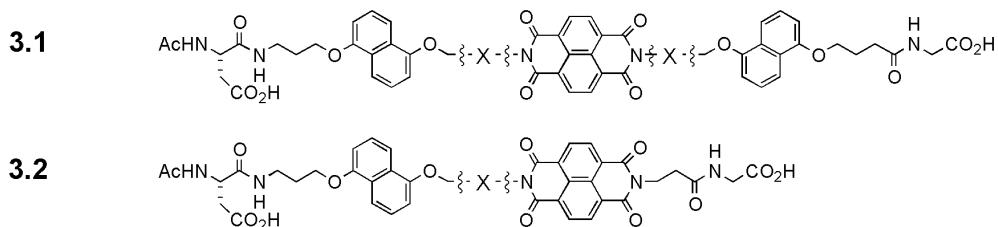


Figure 3.4 Design of a proposed hairpin pentamer.

A set of trimers with different length linkers was therefore synthesized to investigate the feasibility of this, so-called, intercalative-type of fold and to compare it with aedamers, which adopt instead a pleated fold (Figure 3.1, 3.5). Here, the linker between the two Dan units was an important design consideration, and must allow an Ndi unit to lie parallel in between the two Dan rings in order to adopt a Dan/Ndi/Dan face-centered stack. This linker also has to account for the conservative estimate of ~ 3.5 Å as the “thickness” of an Ndi moiety as predicted by computer models. Aedamer **3.1** was synthesized as a suitable control for Dan/Ndi/Dan intramolecular stacking while **3.2** was used as an example of putative Dan/Ndi stacking. (Zych 2002, Lokey 1997). For these compounds, all linkers between each of the naphthalenes were 13 atoms long. Compounds **3.3-3.6** varied the length of the linker connecting the two Dan naphthalenes by 16, 13, 10 and 8 atoms, respectively. Modeling suggested compound **3.6**, the trimer with presumably the most restrictive linker, would be precluded from folding into a trimeric stack due to geometric constraints. Therefore, **3.6**, was considered a potential control compound, specifically a trimer of the same general sequence as **3.3-3.5**, yet unable to form a stable intercalative fold. Modeling indicated that the Dan/Dan linkers for the other three candidates

for the intercalative fold were theoretically long enough but rigorous energy calculations were reserved until UV-Vis studies were performed.

Aedamers with well characterized aromatic stacking



Naphthyl trimers considered for minimal turn unit

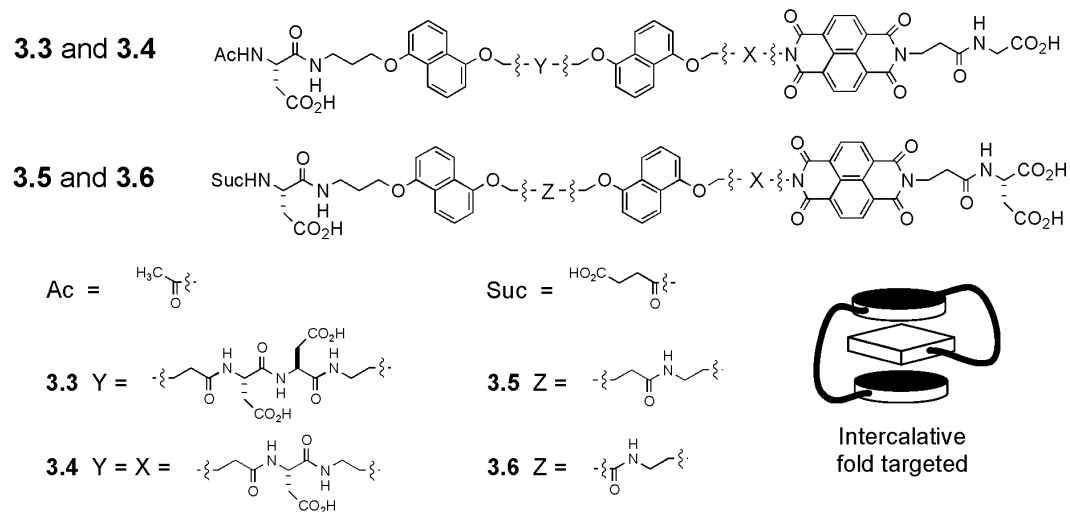


Figure 3.5 Compounds synthesized for folding studies.

The synthesis of these compounds proceeded smoothly using monomers and SPPS protocols previously described in chapter 2. Purification via FPLC (>98% pure judged by HPLC peak area) followed by desalting via a C18 Sep-Pak cartridge and freeze-drying afforded soft pale purple samples.

3.3.2 UV-Vis Spectroscopy

When aedamers were first being developed, Lokey and Iverson identified extremely useful UV-Vis spectroscopic handles to monitor the complexation of the Ndi and Dan moieties in folded oligomers (Lokey 1995). These spectroscopic signatures for interacting Dan/Ndi chromophores included a charge-transfer (CT) band, characteristic extinction coefficients (ϵ) and hypochromism for the naphthyl moieties, all of which changed dramatically upon unfolding of the oligomer by addition of CTAB (Chapter 1). It was envisaged that UV-Vis data would provide a qualitative indication of the types of folding occurring for the previously unexplored non-alternating trimers, **3.3-3.6**. In other words, it was thought that this data might shed light on whether a) these trimers adopt a Dan/Ndi/Dan stack such as aedamer **3.1** or b) their Dan-Dan-Ndi sequences force them into alternative conformations.

UV-Vis data was acquired for solutions of **3.1-3.6** in 50 mM Na phosphate buffer H₂O, pH = 7 (Table 3.1). A CT band appeared for all solutions between 510 and 532 nm, and resulted in a purple color that did not exist with solutions of Dan monomer or Ndi monomer, both of which were colorless. Table 3.1 reports the ϵ of each compound at two wavelengths, at the CT band absorbance and at the Ndi moiety absorbance at 382 nm. The absorbance of the Ndi unit was the more reasonable of the two types of naphthyl units to monitor since **3.1-3.6** had one Ndi moiety each and there was actually very little absorbance overlap between the Dan and Ndi moiety around the maximum Ndi absorbance of 382 nm. Also an Ndi ring flanked on one face by a Dan unit was expected to give distinctive

spectroscopies compared to an Ndi unit with both of its faces in close contact with the Dan ring systems. The ϵ at elevated temperatures (80° C) was measured as well to detect any possible temperature dependence on the UV spectrum which would presumably reflect any ring orientation or oligomer conformation dependence on temperature too. Finally, Table 3.1 reports percent hypochromism at 382 nm, using unstacked monomeric Ndi values for comparison.

Table 3.1 UV-Vis data for **3.1-3.6**.^a

Compound ^b	ϵ_{CT} and (λ_{CT}) ^c	$\epsilon_{382\text{ nm}}$	$\epsilon_{382\text{ nm}} (80^\circ\text{C})$	$\Delta \epsilon_{382\text{ nm}}$ ^d	% Hypo ^e
Alternating trimer and dimer					
3.1 (13)	700 (532)	12200	12400	200	57
3.2 (13)	380 (526)	14600	15300	700	45
Non-alternating trimers					
3.3 (16)	680 (532)	11300	12700	1400	54
3.4 (13)	670 (532)	11200	11800	600	60
3.5 (10)	500 (512)	13000	15100	2100	49
3.6 (8)	490 (510)	13200	15200	2000	48

^a Extinction coefficients (ϵ) reported in $\text{M}^{-1}\cdot\text{cm}^{-1}$, at 25 °C, and using solutions at 40 μM concentrations, unless otherwise noted. ^b Parentheses indicate the number of atoms between the naphthyl units for **3.1** and **3.2** and between the Dan naphthalenes for **3.3-3.6**. ^c Solutions at 1 mM concentrations. ^d $\Delta \epsilon_{382\text{ nm}} = \epsilon_{382\text{ nm}} (80^\circ\text{C}) - \epsilon_{382\text{ nm}} (25^\circ\text{C})$ ^e % Hypo(chromism) = $100\% \times [1 - (\text{absorbance at } 382\text{nm without CTAB} \div \text{with excess CTAB})]$.

3.3.3 Evaluation of UV-Vis Data

Overall, UV-Vis experiments qualitatively showed that all compounds have interacting π -systems arranged in a face-to-face orientation in water (Lokey 1995, Cantor 1980). First, the percent hypochromism, measured at 382 nm, was a

good indication that multiple rings are stacked in a parallel fashion similar to DNA whose bases, within a double helix, display a hypochromism of about 50% (Cantor 1980). Second, solutions of **3.3** and **3.4** gave values of 680 and 670 $\text{M}^{-1}\cdot\text{cm}^{-1}$, respectively for the ϵ of the CT absorbance, both close to the value found for solutions of **3.1** ($700 \text{ M}^{-1}\cdot\text{cm}^{-1}$) that was previously designed to adopt a Dan/Ndi/Dan stack (Lokey 1995, 1997). On the other hand, **3.5** and **3.6** exhibited significantly lower values implicating a ring arrangement deviated from a Dan/Ndi/Dan stack. The Dan-Ndi dimer **3.2** gave a much lower ϵ_{CT} value of 380 $\text{M}^{-1}\cdot\text{cm}^{-1}$ as well. Third, the 532 nm maximum wavelength of the CT band for **3.3** and **3.4**, was identical to **3.1**, which also suggested that their rings arrange in a Dan/Ndi/Dan stack which can reasonably be explained with the proposed intercalative fold conformation while once again **3.5**, and **3.6** deviated from this wavelength and presumably from this trimeric stack arrangement. Thus far it had appeared only **3.3** and **3.4** were promising as non-alternating trimers that can adopt a Dan/Ndi/Dan stacked order analogous to **3.1**.

The ϵ at 382 nm was also useful since for some compounds these measurements changed significantly when the solution was heated. For instance, the $\epsilon_{382\text{nm}}$ of **3.1** was raised by 200 $\text{M}^{-1}\cdot\text{cm}^{-1}$ when heated to 80° C compared to an unusually large increase of 700 units for **3.2**. Besides a likely slight perturbation of intramolecular folding, it was argued that intermolecular aggregates or specifically multimeric stacking might possibly be occurring for **3.2** (Figure 3.6A). This intermolecular stacking could be broken up at elevated temperatures (based on entropy arguments), leaving the presumably stronger intramolecular

interactions relatively unchanged. This multimeric stacking was observed previously with monomers (Cubberley 2001b) and was indeed expected for these chains of nonpolar residues and especially for chain systems that, once folded, still presented opportunities for Dan:Ndi complexation albeit in an intermolecular fashion (Figure 3.6A). The strength of the interaction between separate chains though is expected to become weaker with longer, more unwieldy oligomers as evidenced by multimeric stacking appearing with monomers and dimers but not observed with hexamers (Lokey 1997). Furthermore, it can be argued that trimer **3.1** has a decreased driving force for intermolecular stacking since this situation would require Dan:Dan face-to-face association which has been proven to be relatively unfavorable (Chapter 1, Cubberley 2001b, Figure 3.6B).

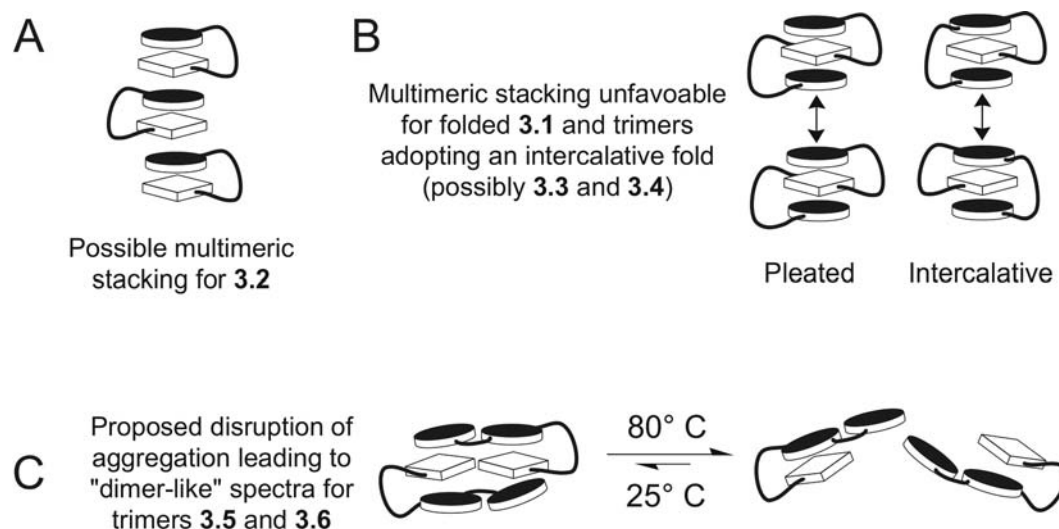


Figure 3.6 Cartoon representation showing A) the likelihood of some type of intermolecular stacking for **3.2** driven by the Dan:Ndi association and B) that intermolecular Dan:Ndi associations are not available if **3.1**, **3.3**, and **3.4** fold in the asserted manner. Double-headed arrows represent repulsion of the electron-rich π -clouds of two Dan units. C) Possible explanation of how trimers **3.5** and **3.6** could afford UV spectra similar to dimers.

As Figure 3.6B shows (right structures), the general non-alternating trimer design was fortunate in the sense that, if folded correctly, the whole structure would be “capped” by two Dan units, just as with the alternating trimer **3.1**, with no exposure of an Ndi surface to propagate intermolecular interactions. Although, if a prohibitively short linker does indeed prevent a stable Dan/Ndi/Dan stack, then it would be possible that significant aggregation may occur. This appeared to be the case for **3.5** and **3.6**, whose $\epsilon_{382\text{nm}}$ increased by around 2100 and 2000 $\text{M}^{-1}\cdot\text{cm}^{-1}$, respectively when their solutions were heated. Figure 3.6C is a cartoon representation of a postulated explanation of this change in UV spectra. Interestingly **3.5**, **3.6**, and dimer **3.2** displayed surprisingly close UV spectra with

$\epsilon_{382\text{nm}}$ (80° C) values of 15100, 15200, and 15300 M⁻¹·cm⁻¹, respectively. Upon heating, it seemed that the UV absorbances of trimers **3.5** and **3.6** become more attributable to just the intramolecular association between the Ndi unit and only one Dan residue giving rise to “dimer-like” spectra (Figure 3.6C). This data provided evidence that the shortened Dan/Dan linker of both **3.5** and **3.6** precluded them from being candidates for intercalative folding but demonstrated their usefulness as negative controls.

Lastly, it was unexpected that the non-alternating trimer with the longest Dan/Dan linker **3.3** also had a relatively large shift in $\epsilon_{382\text{nm}}$ when heated compared to that of **3.4**. It is possible that solutions of **3.3** are conformationally heterogeneous (i.e. different aggregated species exist) due to intermolecular interactions, such as claimed for **3.5** and **3.6**. There could also be distinctly dissimilar intramolecular conformations that are favorable at room and not at elevated temperatures and vice versa due to a longer linker making it possible to survey many different structural orientations dependent on temperature. Examining how heat effects these conformations is a difficult problem and this supposed discrepancy of conformations might make further structure analysis of **3.3** difficult.

Compound **3.4**, on the other hand, displayed comparable values for ϵ_{CT} (λ_{CT}), $\epsilon_{382\text{nm}}$ (at 25 and 80° C), and percent hypochromism as **3.1** without the unusually high, and currently unexplained, $\Delta\epsilon_{382\text{nm}}$ shown by **3.3**. These similarities suggested that **3.4** did exhibit Dan/Ndi/Dan trimeric stacking, as **3.1**, even though it was not biased by a primary sequence of alternating Dan and Ndi

residues. The slight differences in the UV-Vis data between **3.1** and **3.4** likely stemmed from the inherently dynamic nature of folded naphthyl oligomers and the fact that these spectroscopic properties are very sensitive to the stacking orientation of the aromatic rings (Zych 2001, 2002). Also the difference in linker topologies between a pleated fold and an intercalative fold would be expected to alter the ring-to-ring geometries enough to give distinct spectra. Although these UV-Vis measurements by no means gave a crystal clear picture of folding, it did point to compound **3.4** as a reasonable candidate for more comprehensive structural analysis to investigate intercalative folding that would afford a turn-type conformation.

In summary, this initial study determined that trimer **3.4** would be a good candidate for rigorous 2D NMR analysis that could reveal specific aromatic H-H contacts. Also compound **3.1** would be an appropriate “positive” control for Dan/Ndi/Dan stacking. As mentioned previously **3.6** could act as a “negative” control. It was suggested, based on the UV-Vis studies, that the terminal Dan unit of **3.6** is likely energetically prevented from completely “swinging around” to shield the other face of the Ndi ring due to a shortened linker thus preventing a Dan/Ndi/Dan stack (Figure 3.7).

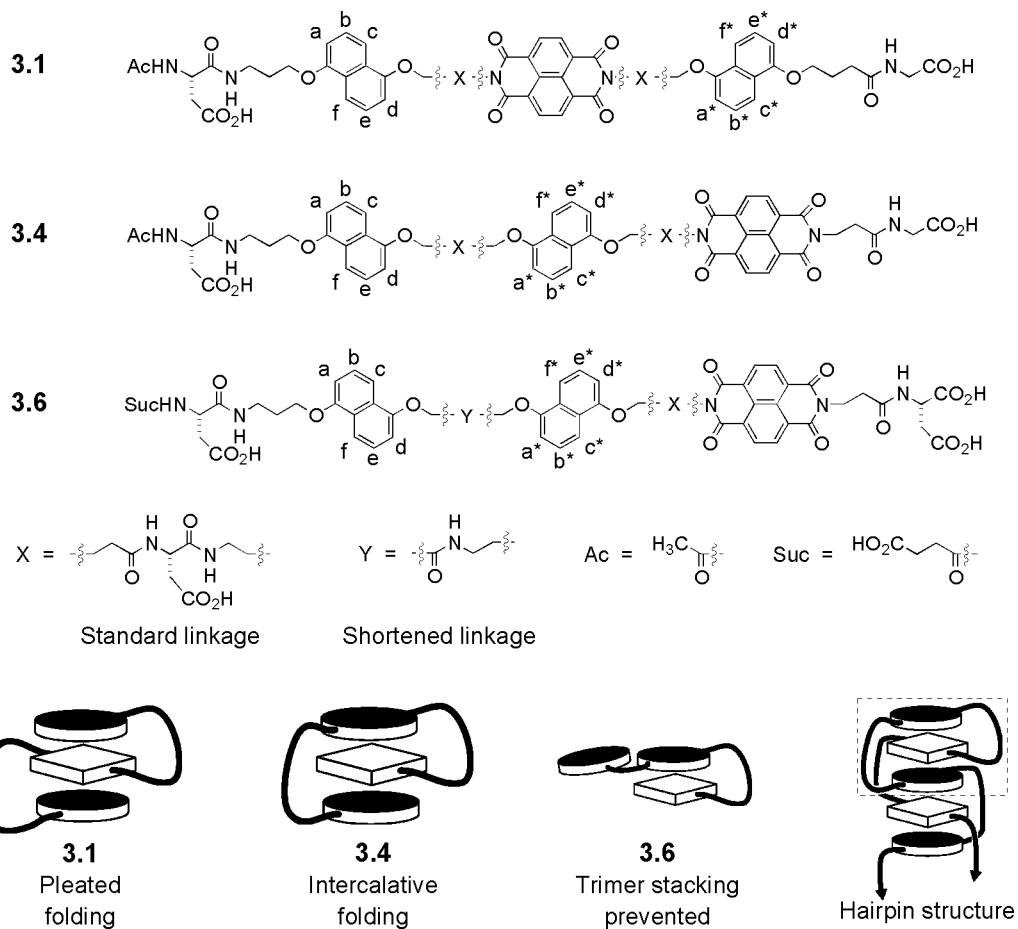


Figure 3.7 Compounds analyzed by 2D NMR and idealized cartoon representations of possible solution conformations. Letter designation for NMR peak assignments for the Dan and Dan* units are given. Also shown is a design of a hairpin structure incorporating an intercalative fold (dotted boxed).

Compounds **3.1**, **3.4**, and **3.6** were chosen for NOESY and modeling studies (Figure 3.7). It was hoped that structural analysis would reveal **3.1** and **3.4** are related by a similar Dan/Ndi/Dan ring stacked arrangement even though the required type of folding to achieve this arrangement would have to be different. Conversely, even though **3.4** and **3.6** are related by an identical Dan-Dan-Ndi

primary sequence, it was anticipated that they would adopt different conformations. Figure 3.7 illustrates these expected folding patterns.

3.3.4 Unfolding Studies by UV Spectroscopy

As alluded to before, more stable structures may be a possible upshot from folding manipulation studies. Obtaining unfolding profiles, shown in Figure 3.8, was a step towards developing a method to analyze the stability of the different folds that have been, and will be, attained in the future. Unfolding traces could also possibly reflect the total number of aromatic units in the stacked hydrophobic core with conformations that have comparable ring arrangements displaying similar curves.

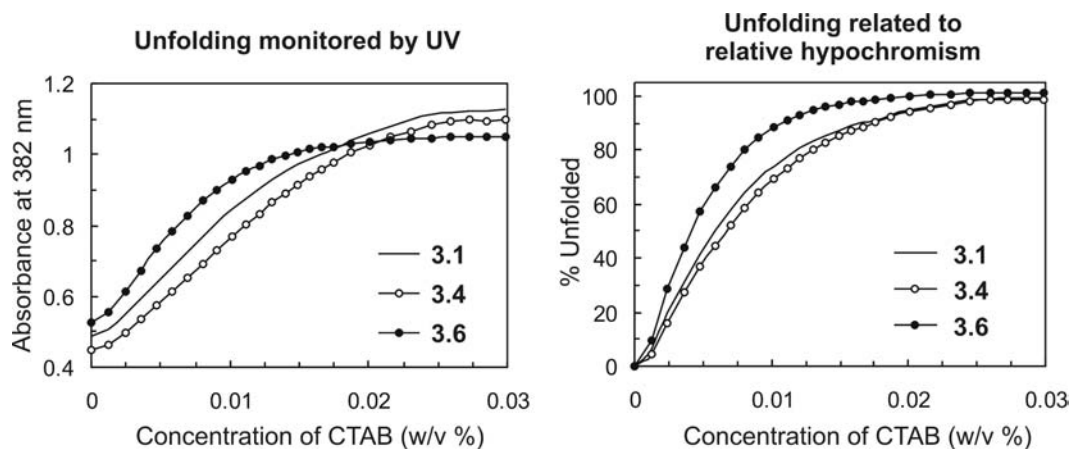


Figure 3.8 Unfolding curves displayed in two different forms.

The unfolding of **3.1**, **3.4**, and **3.6** was monitored via the rise of absorbance with the addition of CTAB, a detergent that was found to denature aedamers (Lokey 1997). Solutions of trimers were initially at 40 μM before the titration of a 2.7 μM (0.1 w/v %) solution of CTAB. Absorbances were adjusted

for volume changes and the concentrations of CTAB reported in w/v %. As more CTAB was added the absorbance increased (same as stating that the hypochromism decreased) as aromatic stacking was disrupted (Figure 3.8, left graph). Complete unfolding appeared at around 0.03 w/v % CTAB. At excess CTAB, the Ndi absorbance for each compound still varied slightly from each other even at identical concentrations. This was expected since different linkers and residue sidechains still affect, in subtle ways, the Ndi absorbance even in the absence of π -stacking (Gabriel 2002). Therefore to visualize the percent of unfolded trimer as CTAB was added, the hypochromism was calculated for each data point and related to the hypochromism of the initial solution (Figure 3.8, right graph). As an example, at 0.01 w/v % CTAB the hypochromism of **3.4** was calculated to be 18% compared to 60% of the initial solution and this translates to about 70% $[1 - (0.18 \div 0.60) \times 100\%]$ unfolded trimer.

It seemed that the unfolding pathways of the three compounds were not overwhelmingly different from each other. However, Figure 3.8 (right graph) did indicate that **3.6** (the trimer that cannot adopt a full Dan/Ndi/Dan stack) was folded slightly less stably than **3.1** and **3.4** under these denaturing conditions. Also, this study provided strong evidence that **3.1** and **3.4** share a similar trimeric-stacked arrangement signified by the near identical stabilities. Indeed, it had been observed earlier that the absorbance traces from detergent-induced denaturation of aedamer dimer, tetramers, and hexamers were near identical (Lokey 1997). So, even as Lokey increased the length of the aedamers, the stability remained unchanged because these molecules had the same pleated structure conformation

and therefore presumably a similar unfolding mechanism. It was encouraging that oligomers with a previously unexplored naphthyl sequence still gave easily interpretable curves (for both **3.4** and **3.6**). Even though the apparent strength of folding was comparable for **3.1** and **3.4**, a hairpin structure (Figure 3.4) may still have potential to give a markedly stable conformation due to the anticipated entwined arrangement of the proposed molecule.

3.3.5 NMR Techniques for Proton Assignment

It was anticipated that the most direct evidence for folding and the specific aromatic-aromatic contacts that guide this folding would come from 2D-NMR experiments. When naphthyl oligomers with linkers greater than eight atoms were modeled in extended conformations, aromatic protons on different rings were at least 10 Å from each other, much too far apart to expect through-space coupling with NOESY spectroscopy. A co-crystal X-ray structure indicated the planes defined by the Ndi and Dan monomer units are separated by approximately 3.5 Å (Lokey 1995). It was reasonable to expect that hydrophobics-driven aromatic stacking would orient these rings close enough to each other, excluding water, and bring particular protons on different aromatic rings within 4-5 Å of each other, a practical range for NOESY spectroscopy.

This NMR technique though becomes truly valuable for these folding systems only if the naphthyl protons can be unambiguously assigned. Unfortunately there was extensive overlap (Figure 3.9) of the two sets of Dan aromatic protons that would complicate matters in differentiating specific aromatic-aromatic contacts between the Ndi and Dan and/or Dan* residue

(Dan/Dan* notation in Figure 3.7). So while the oligomeric nature of our molecules allowed for facile synthesis of a set of foldamers with altered sequences, rigorous assignment of the hydrogens of repeat units (in this case the Dan hydrogens) became quite challenging.

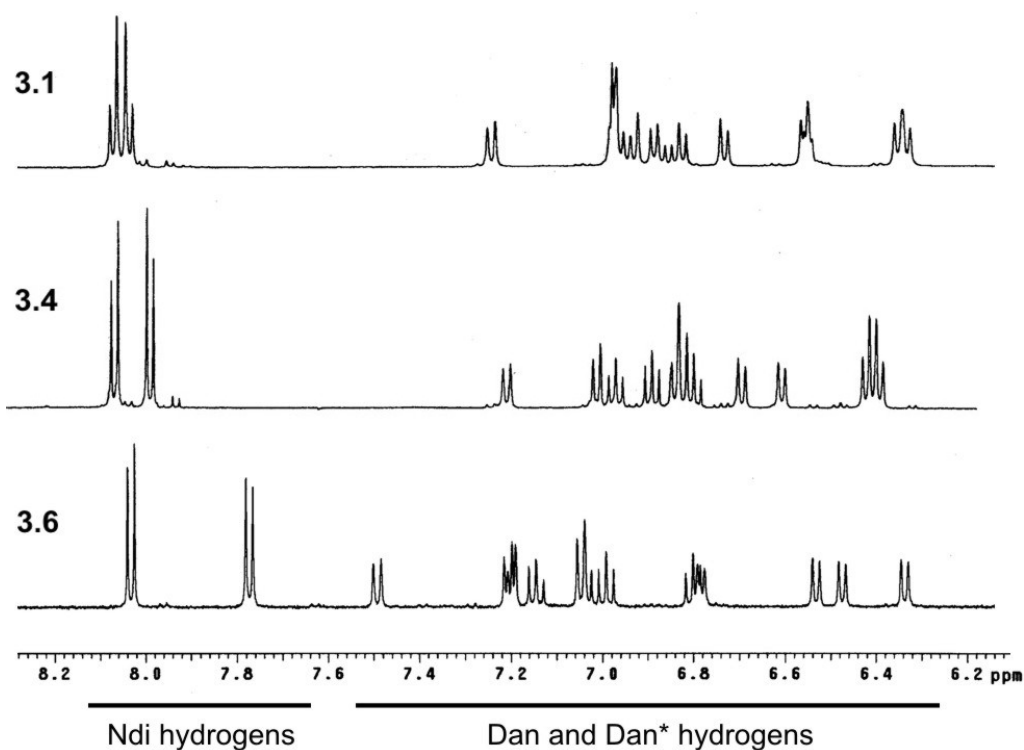


Figure 3.9 Proton NMR spectra of the aromatic region representing 16 hydrogens for each spectrum. Spectra were taken at 1 mM concentrations in 50 mM Na phosphate D₂O.

This general problem is also encountered with the proton assignment of peptides with repeat sequences and has been solved mostly by NOESY experiments ran in 90% H₂O in D₂O, rather than in pure D₂O to keep exchangeable protons observable. These experiments made it possible to “walk”

along the backbone chain using the amide hydrogen to form a continuous correlation across the carbonyls of the amide bond. Naphthyl oligomers though presented a special challenge not seen with peptides. The Ndi and Dan naphthalene moieties essentially were isolated spin systems that “act as insulators along the backbone” (Zych 2001). Fortunately, TOCSY (total correlated spectroscopy) methods, which afforded long-range through-bond correlations for H_a-H_d and H_a-H_f , were previously established for aromatic systems (Martin 1994, Johnston 1989) (Figure 3.10). Zych tested TOCSY methods in the context of our aedamer systems with much success, the details of which have been reported (Zych 2001, 2002). Figure 3.10 summarizes the helpful NOE connections and long-range TOCSY correlations used by this study.

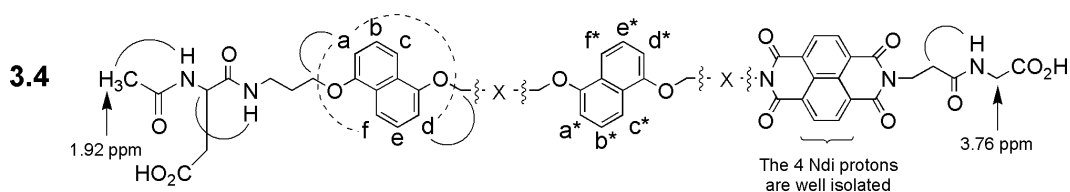


Figure 3.10 Method of “walking” from the terminus of **3.4** in order to assign the Dan and Dan* hydrogen chemical shifts. Examples of key through-space (solid line) and through-bond (dotted line) H-H correlations are marked.

Overall, attaining resonance assignments for the Dan protons of each compound required NOESY or ROESY (rotational nuclear Overhauser effect spectroscopy) spectra taken in 90% H_2O in D_2O and TOCSY spectra taken in 100% D_2O . For some cases, several mixing times had to be tried along with other parameter changes during acquisition and processing performed by Sorey of the

NMR facility at the University of Texas at Austin (Gabriel 2004b). Concentrations were at 1 mM of compound and the solvents were buffered with 50 mM Na phosphate, pH = 7. Sparky v3.85, an online visualization program, facilitated the imaging and interpretation of 2D NMR spectra (Goddard 2000).

Interpretation of these spectra led to the peak assignments for the Dan and Dan* aromatic hydrogens. As Figure 3.10 shows, the four Ndi protons are isolated in that they are more than 5 Å away from the closest methylenes and NOEs were not observed. Also, TOCSY type couplings between these aromatic protons were not observed since these protons are not attached to the same π system as in the case of the Dan residues (Figure 3.10). Therefore the AA'BB' signals in the Ndi region of the spectra (Figure 3.9) could not be assigned to specific protons. Regardless, accurate conformational analysis using the Dan resonances and computer modeling can still be carried out.

3.3.6 NOESY Spectroscopy

Once sufficient assignment of the naphthyl hydrogens was accomplished, NOESY experiments, for the purposes of identifying specific H-H contacts between the aromatic rings, were performed. NOE patterns were considerably different for each compound and NOESY spectra expansions exhibited cross peaks between the Ndi and one or both Dan units (Figures 3.11-3.13). Dan proton signals a-f and a*-f* are labeled and the cross peaks that provided strong evidence of interactions between the Ndi and these Dan aromatic hydrogens are boxed with a dotted line. Interpretations of the observed cross peaks for each NOESY spectrum were discussed in Section 3.3.9.

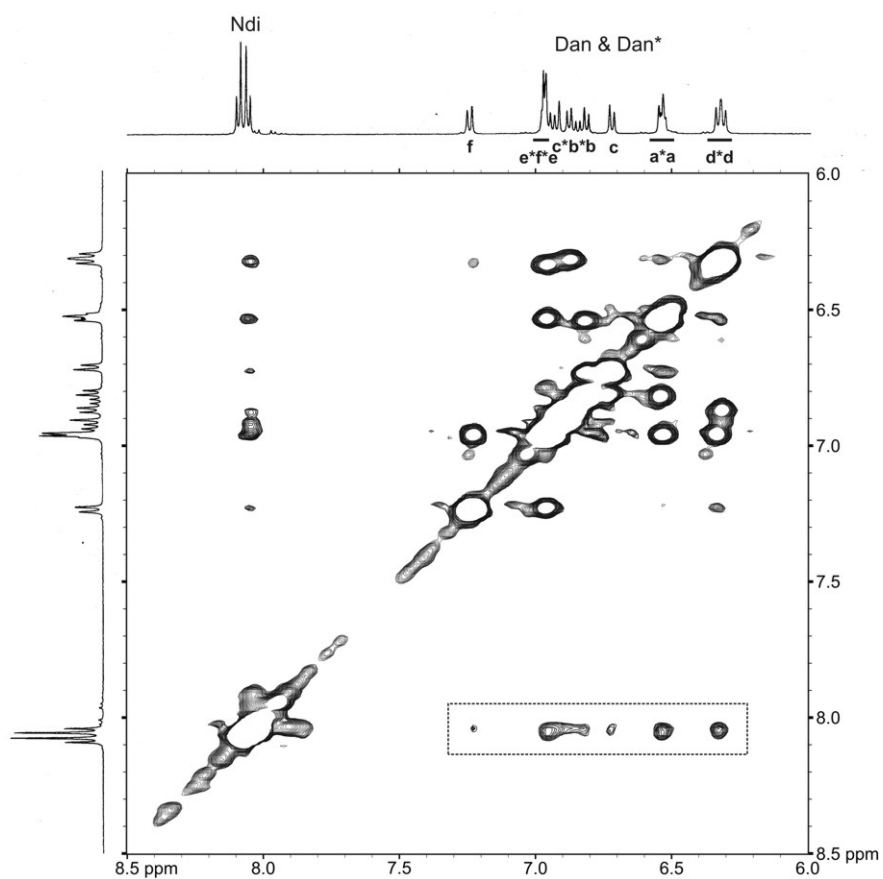


Figure 3.11 Expansion of NOESY spectrum for **3.1**.

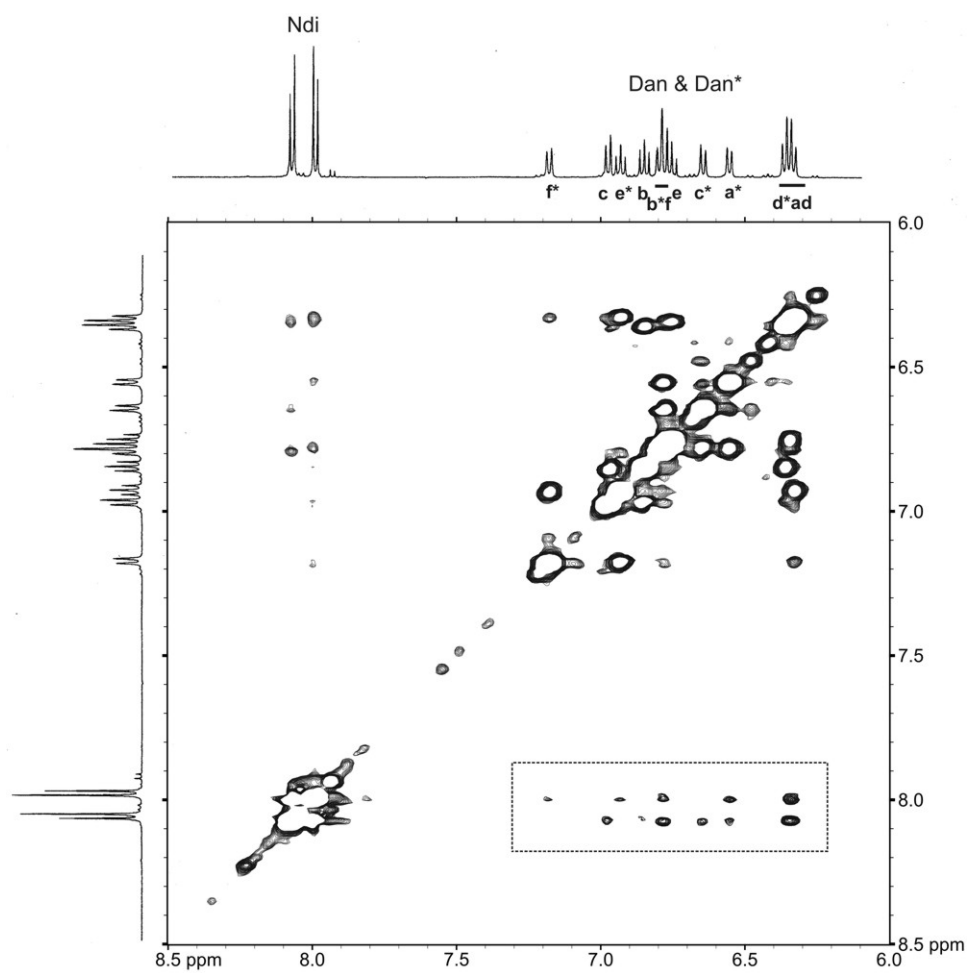


Figure 3.12 Expansion of NOESY spectrum for **3.4**.

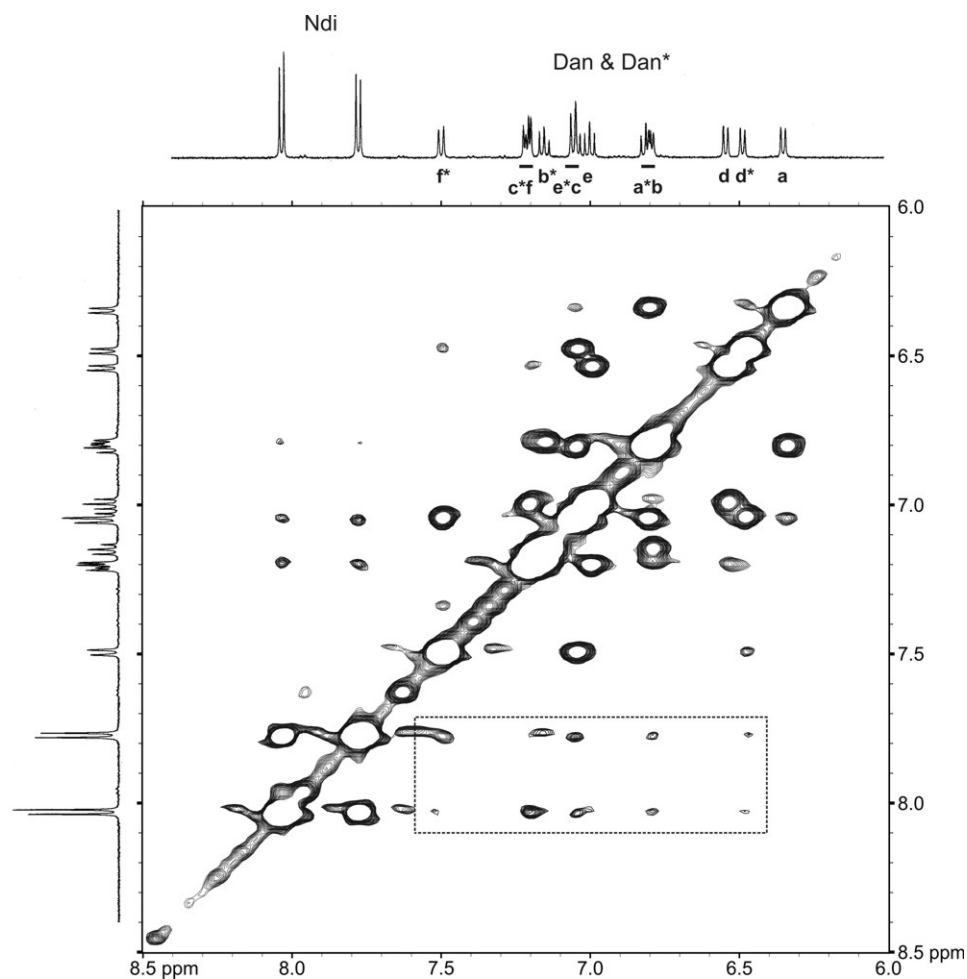


Figure 3.13 Expansion of NOESY spectrum for **3.6**.

3.3.7 Computer Modeling

Fairly conservative procedures were used for computer modeling, taking care not to make unreasonable assumptions. To expedite calculations, models of **3.1**, **3.4**, and **3.6** were used with the side chains removed. It was shown previously that these modifications did not compromise the modeling of naphthyl oligomers where the predominant driving force for folding is the aromatic interactions of the

Ndi and Dan moiety (Zych 2001). Also important to note is that the goal of these computations was not an exhaustive survey of conformational space since there was already strong spectroscopic evidence that the compounds do fold to some extent. The aim of computer modeling was simply to see if energy minimized structures corroborate the general aromatic stacking of a new type of intercalative fold for these naphthyl oligomers.

All modeling simulations and geometry optimizations utilized the HyperChem software bundle (HyperCube, Inc. 1996) set to employ the MM+ force field. Twenty diverse, unfolded conformers were generated for each initial model using molecular dynamics. Each of the twenty structures was then allowed to go through simulated annealing from a temperature of 1000 to 300 K applying weak distance restraints. Lastly and most importantly, each structure was subjected to geometry optimization without any restraints to afford low energy conformers and to probe subtle differences in stacking orientations. This strategy to obtain families of low-energy structures, rather than using prohibitively long molecular dynamics simulations to obtain one assumed lowest energy structure, was proven to be extremely successful for aedamers (Zych 2002).

Since the four Ndi protons of each compound could not be unequivocally assigned, distance restraints for all models were defined from the center of the Ndi ring rather than from a particular hydrogen. For models of **3.1**, a general restraint between the Ndi ring and the center of both Dan naphthalenes was applied that was reasonable based on detailed studies on aedamer trimer structure previously reported (Lokey 1997, Zych 2002). For models of **3.4**, restraints

between the Ndi ring and Dan hydrogens c, c*, and a* (these gave medium strength NOEs with Ndi protons) were used. Finally for models of **3.6**, only two distance restraints were defined, those relating the center of the Ndi ring to protons f* and to d*, again keeping restraints fairly conservative. Only after geometry optimization without restraints would the low-energy conformers be probed for corroboration of the NOE couplings from 2D NMR experiments (Figure 3.14).

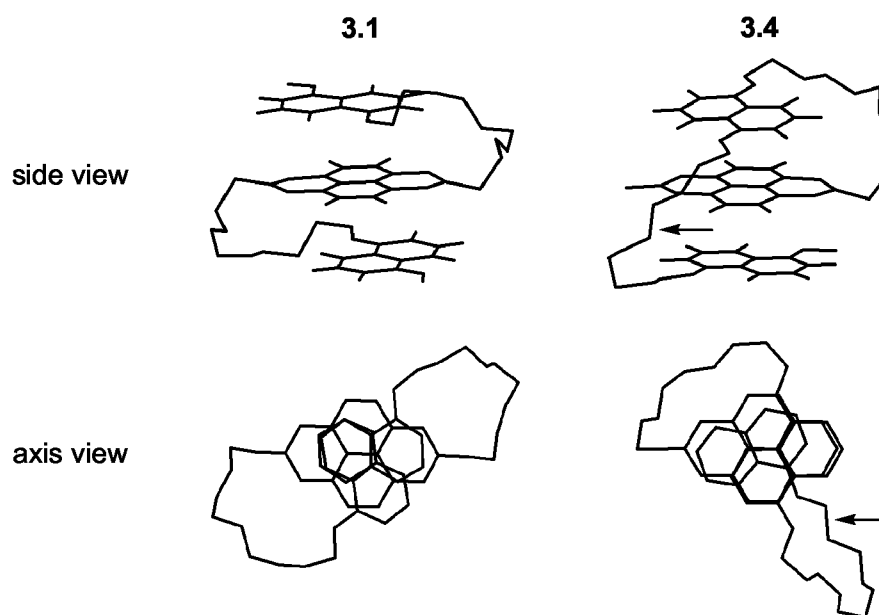


Figure 3.14 Side view of the lowest energy conformers of **3.1** and **3.4** and axis view of the same conformers showing the general topology of the linkers. Arrows indicate the Dan/Dan* linkage. Hydrogens omitted (except for the aromatic of the side views) for clarity.

While most final structures were “folded” with clear face-centered aromatic stacking, it was also satisfying that this computational protocol led to other diverse structures (owing to the relatively unbiased nature of this modeling

strategy) that revealed folding “defects”. Such conformations that deviated from a Dan/Ndi/Dan parallel stack included off-set and non-parallel stacking, Dan/Dan/Ndi stacking and *cis* amide bond orientations, all of which were between 2 and 10 kcal·mol⁻¹ higher in energy than the lowest energy conformer calculated for each compound. In this was families of low-energy conformers could be identified.

3.3.8 Evaluation of NMR Data and Computer Modeling

The spectrum for **3.1** (Figure 3.11) exhibited H_{Dan}-H_{Ndi} cross peaks along the entire range of Dan resonances indicative of the Ndi unit making contacts with both Dan rings. Also, Zych previously showed that when there was only a slight chemical shift difference between the AA' and BB' signals of the Ndi unit, as was the case for **3.1**, it often signified that the Ndi unit is well centered between two Dan units. (Zych 2001, 2002). Additionally, aedamer trimers such as **3.1** have been extensively investigated in several different contexts and all studies including this one supported a pleated fold interpretation of their solution structure (Lokey 1997, Zych 2002).

For compound **3.4**, several unambiguous H-H correlations were observed between the Ndi and both Dan groups as well (Figure 3.12). In the spectra for **3.4** there were explicit Ndi contacts with both Dan and Dan* hydrogens (c, c*, e, and a* - medium intensity; b and f* - weak intensity). These NOEs were consistent with a structure having the Ndi unit insert in between the Dan rings, implicating an intercalative fold. Interestingly, several cross peaks could be attributed to a specific pair of Ndi protons since the AA' and BB' signals were more separated

for **3.4** (Figure 3.12) than seen for **3.1** (Figure 3.11). For instance protons c and c* only had coupling with the Ndi doublet (representing 2 of the 4 Ndi protons) near 8.1 ppm while protons e* and f* showed exclusive coupling with the other doublet near 8.0 ppm. Interpretation of the modeled conformations (presented later) did allow assignment of the Ndi protons thus giving an even clearer picture of **3.4** folding. In sum, the spectrum of **3.4** strongly supported an intercalative fold that forms a Dan/Ndi/Dan stack just as **3.1** but with a different folding topology.

The NOESY spectrum of **3.6** indicated an interaction between the Ndi unit with the Dan* residue only, consistent with the expected interrupted folding pattern of this molecule. It was rather apparent that **3.6** had a significantly different inter-ring geometry from **3.1** and **3.4** especially when inspecting the cross peak(s) near 6.5 ppm and lower in each of the dotted boxes of Figures 3.11-3.13. It can reasonably be assumed based on relative cross peak intensities that protons a, a*, d, and d* of **3.1** and **3.4** coupled to the Ndi unit. On the other hand, there were absolutely no clear cross peaks involving any of the protons of the Dan (non-asterisked) residue of **3.6** and specifically couplings with protons a and d were noticeably absent (Figure 3.13). This spectral interpretation is consistent with **3.6** unable to form a trimeric stack corroborating UV-Vis studies.

While the NOESY spectra were consistent with a pleated fold structure for **3.1** and an intercalative fold for **3.4**, it was important to consider alternative interpretations. For example it is possible to imagine a conformation for **3.4** in which edges of both Dan rings make contacts (and thus NOEs) with the same face of the Ndi unit, in a roughly triangular geometry. Such a scenario was unlikely,

however, in light of the UV-Vis data that strongly supported a face-to-face stacking geometry of the aromatic units. Moreover such a triangular geometry would have had significantly different ring current effects and therefore dramatically different chemical shifts of the aromatic protons for **3.4** compared with **3.1**. Such differences were not observed, and in fact, the chemical shifts for the aromatic regions of the spectra for **3.1** and **3.4** were comparable.

Computer modeling also corroborated the proposed Dan/Ndi/Dan stacking for **3.1** and **3.4** (Figure 3.14). In earlier investigations, Zych and Iverson rejected a rigid two-state unfolded/folded model for aedamers and provided evidence that there exists families of stably folded structures, but importantly, all of these conformers were characterized by face-centered stacking (Zych 2000, 2002). The same was found to be true for trimers **3.1** and **3.4** where all structures within 1 kcal·mol⁻¹ of the most stable conformation assumed a tri-aromatic parallel stack that maximized Dan:Ndi interactions. Although no lone structure satisfied all the NOEs found, when considered together, these low energy conformers representing **3.1** and **3.4** supported the H-H correlations from the NOESY experiments.

For **3.4**, modeling did suggest an assignment of the Ndi protons as postulated above. Low energy conformers helped identify the Ndi doublet at 7.98 ppm, which coupled explicitly with protons f* and e*, as the pair of protons closer to the terminus (H_B in Figure 3.15). The internal pair of Ndi hydrogens (H_A in Figure 3.15), which coupled unmistakably with protons c and c*, were assigned as the doublet at 8.08 ppm based on low energy structures (Figure 3.12, 3.15).

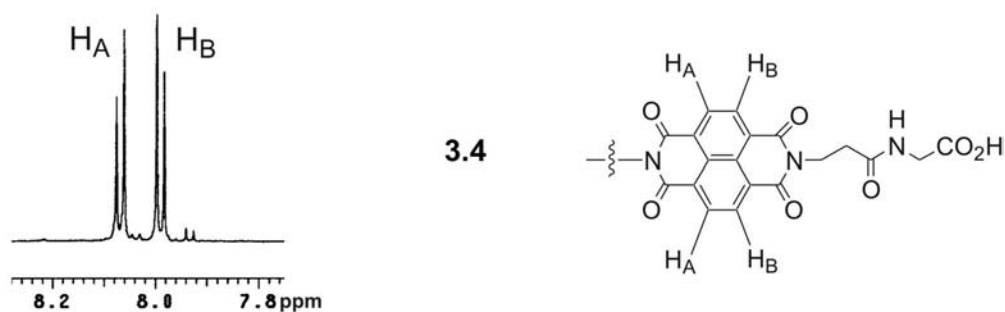


Figure 3.15 The assignment of the AA'BB' Ndi protons shown in a partial spectrum and chemical structure of **3.4**.

Low-energy conformers for **3.6** gave mostly structures having the Ndi and Dan* residues stacked but with the terminal Dan unit in several different positions, sometimes in an edge-to-face orientation but none resulting in face-to-face Dan/Ndi/Dan or even Dan/Dan/Ndi stacking. In fact by inspection of the structures and relative energies, there seemed to be no obvious consensus for the most favorable placement of that Dan residue. As expected for this designed control compound, 2D NMR and modeling indicated that **3.6** did not adopt any conformation even close to a Dan/Ndi/Dan stack.

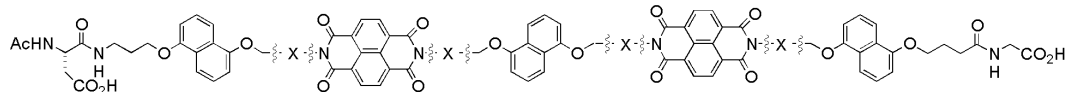
Lastly, it initially seemed unusual that a Dan/Dan* linker length of 13 atoms, equal to that of aedamers, worked so well for **3.4** considering it had to extend over an entire naphthyl ring (Figure 3.7). The axis view of the lowest energy conformers of **3.1** and **3.4** shown in Figure 3.14 plainly displays the topologies of the linkers (all of which were 13 atoms long) compatible for a pleated or an intercalative fold. For **3.1** to stack adjacent Dan and Ndi units, the linker appeared to have to accommodate a quarter turn. This was observed for

both linkers for **3.1** and the Ndi/Dan* linker of **3.4**. The Dan/Dan* linker apparently did not have to provide this turn since the points of attachment were approximately lined up on the same face of the folded structure (Figure 3.14). As a result all linkers spanned similar distances in the folded state even if the two folding patterns of **3.1** and **3.4** were fundamentally different.

3.3.9 Preliminary Studies of a Potential Hairpin Pentamer

Recently, a non-alternating pentamer **3.8** was synthesized incorporating the newly developed intercalative fold of **3.4** to possibly create stable hairpin structures in water. Aedamer pentamer **3.7** was synthesized for future 2D spectral comparisons though the 1D spectrum had comparable shifts with that of **3.8** indicating, at least qualitatively, that **3.8** has significant intramolecular aromatic stacking (Figure 3.16).

3.7



3.8

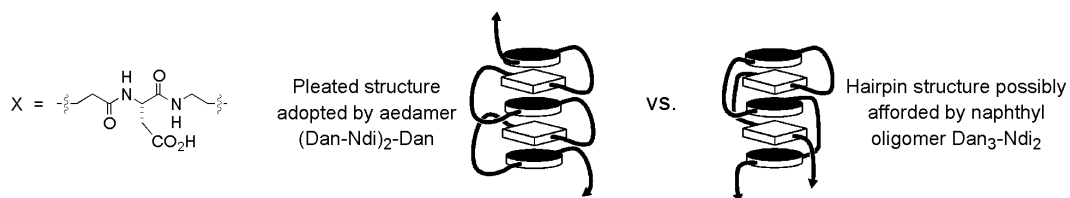
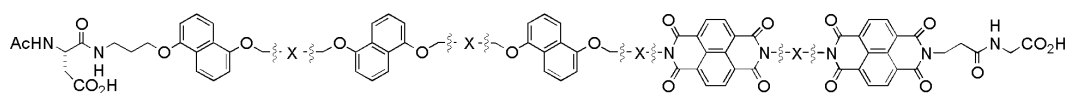


Figure 3.16 Pentamers used for preliminary studies on hairpin structures.

The NOESY spectrum of **3.8** (Figure 3.17) suggests that both Ndi units, make contacts with the Dan units. This was assumed since the resonances of the two Ndi units were *distinguishable from each other* (though not assignable at this point). In other words the Ndi signals at 7.8 and 8.0 ppm could be reasonably attributed to protons on separate Ndi moieties, as denoted in Figure 3.17. Both of these signals were responsible for cross peaks in the Dan region of the spectrum (e.g. $H_{(7.8\text{ppm})}-H_{(6.4,6.2\text{ppm})}$ and $H_{(8.0\text{ppm})}-H_{(6.7,6.2,5.9\text{ppm})}$). This suggests that **3.8** can turn back on itself in solution to allow the terminal Ndi to interact with a Dan unit. Unfortunately overlap of resonances representing 18 Dan hydrogens plus line broadening hampered attempts to assign proton signals. Line broadening is a strong indication that the molecule experienced significant fluctuations in its conformation. Line broadening can also indicate though restricted motion (where low energy conformers do not interconvert quickly), which is indeed expected for the proposed weaving hairpin fold.

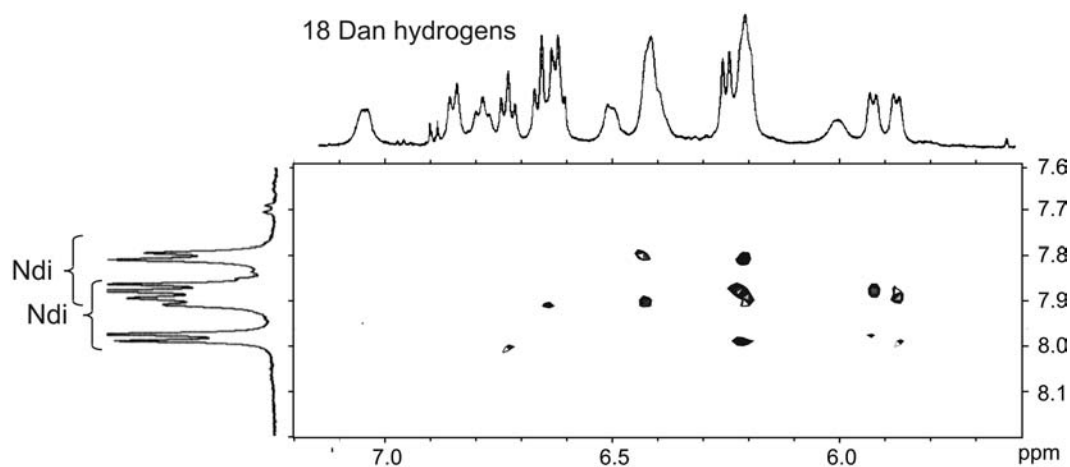


Figure 3.17 Aromatic region of NOESY spectrum.

3.4 CHAPTER CONCLUSIONS

In summary, UV-Vis spectroscopy, unfolding studies, NMR, and modeling investigations are fully consistent with the interpretation that both naphthyl trimers **3.1** and **3.4** adopt a Dan/Ndi/Dan face-to-face stack in aqueous solution. The consequence of this ring arrangement is a pleated fold for **3.1** and an intercalative fold for **3.4**. It thus appears that these folding patterns were predicted by the linear sequence of two residue types owing to the strong directionality of the Dan:Ndi association and the designability of naphthyl oligomers. This work also demonstrates that foldamers for the first time can emulate natural proteins in the sense that significantly different abiotic secondary structures can be accessed with carefully chosen residue substitutions. Lastly, this intercalative fold may represent an alternative to stabilizing turns or bends in water using aromatic interactions an aim of many research groups.

3.5 IDEAS FOR FUTURE INVESTIGATIONS

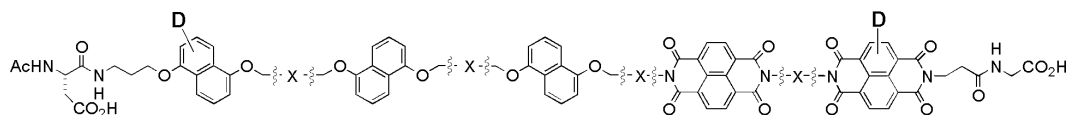
Two research directions are proposed below to address the difficulties in interpreting NMR spectra of naphthyl oligomers longer than trimers.

Deuterated aromatic units as an indispensable tool for proton assignment and structure analysis. The hairpin pentamer conformation can be greatly supported by proving the terminal Dan and Ndi units, which are distant in an extended conformation, end up adjacent to each other in the folded structure. By selective deuteration certain cross peaks found in Figure 3.17 can be eliminated and thus attributed to specific aromatic-aromatic contacts, something

that cannot be easily done currently. The pentamer in Figure 3.18 (top structure) would be one of several compounds that would be synthesized to aid in proton assignment and ultimately structure determination. Interestingly, deuteration of the Dan amino acid (98% conversion) was extremely easy by heating with D₂SO₄ in D₂O/DMF and precipitation with cold H₂O. Unfortunately deuterium is replaced with hydrogen just as easily with TFA under conditions used in the cleavage of oligomer from resin. Cleavage by deuterated TFA would not be useful since all aromatic rings would then be deuterated.

Cyclic naphthyl oligomers with locked structures. Another way to prove that the terminal units of a hairpin structure are close in space is to utilize a cyclization strategy that supposedly would not be efficient if the molecule does not fold in the expected fashion. Cysteine amino acids have been utilized to convert acyclic peptides into cyclic peptides through an easily formed disulfide bond. The oligomer in Figure 3.18 (bottom structure), if cyclized, would effectively lock-in a folded structure. It would be extremely exciting if this resulted in sharpened proton signals and more intense cross peaks as well.

D = Deuterium



C = Handle for cyclization

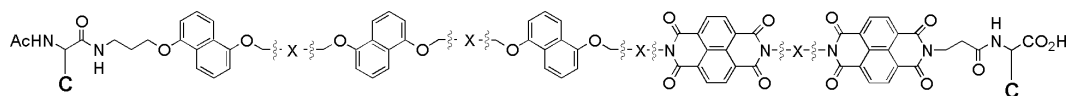


Figure 3.18 Proposed oligomers for future study.

3.6 EXPERIMENTAL SECTION

Synthesis. General methods, full protocols for solid phase peptide synthesis and FPLC/HPLC purification used for oligomers **3.1-3.8** were detailed in chapter 2. Synthesis, followed by purification, desalting, and freeze-drying afforded soft pale purple solids for all compounds.

Compound characterization (1D-NMR general methods). Samples were readily soluble in 50 mM sodium phosphate, pH = 7.0 D₂O. Spectra were recorded on a Varian INOVA 500 MHz spectrometer at 1 mM concentrations of compound and TSP-*d*₄ (3-trimethylsilyl-propionic-2,2,3,3-*d*₄ acid, sodium salt) was used as a reference (δ = 0.00 ppm). Chemical shifts reported in ppm and abbreviations used are singlet (s), doublet (d), doublet of doublet (dd), triplet (t), quartet (q), multiplet (m) and complex multiplet of non-equivalent protons (comp). J coupling constants (*J*) reported in Hz.

“AcHN-AspDanAspNdiAspDan*Gly-OH” (3.1). (SPPS yield = 91%) ¹H NMR (500 MHz, D₂O) δ = 8.04 (q, *J* = 10.0 and 7.6, 4H), 7.22 (d, *J* = 8.4, 2H), 6.97-6.94 (comp, 2H), 6.92 (d, *J* = 8.0, 1H), 6.86 (t, *J* = 7.6, 1H), 6.82 (t, *J* = 7.6, 1H), 6.72 (d, *J* = 8.4, 1H), 6.54-6.53 (comp, 2H), 6.34-6.30 (comp, 2H), 4.72 (dd, *J* = 5.6 and 2.2, 1H), 4.63 (dd, *J* = 5.4 and 2.4, 1H), 4.52 (dd, *J* = 5.0 and 3.8, 1H), 4.37-4.33 (m, 1H), 4.29-4.23 (m, 2H), 4.16-4.13 (m, 1H), 4.02-4.01 (m, 2H), 3.93-3.91 (m, 2H), 3.83-3.52 (comp, 9H), 3.49 (t, *J* = 6.8, 2H), 3.41-3.38 (m, 1H), 2.78-2.74 (m, 2H), 2.72-2.51 (comp, 6H), 2.45 (t, *J* = 7.4, 2H), 2.42-2.37 (m, 2H), 2.10-1.96 (comp, 8H), 1.94 (s, 3H); ESI MS calcd for C₆₉H₇₄N₉O₂₃ [MH]⁺ 1397, found 1395.

“AcHN-AspDanAspNdiGly-OH” (3.2). (93% yield) ^1H NMR (500 MHz, D_2O) δ = 8.33 (q, J = 10.0 and 7.5, 4H), 7.02 (d, J = 8.4, 1H), 6.98 (t, J = 8.4, 1H), 6.93 (d, J = 8.4, 1H), 6.90 (t, J = 7.7, 1H), 6.59 (d, J = 7.0, 1H), 6.29 (d, J = 7.6, 1H), 4.65 (dd, J = 8.1 and 5.2, 1H), 4.40-4.25 (m, 4H), 4.15 (t, J = 5.7, 1H), 4.01 (m, 2H), 3.80-3.70 (m, 2H), 3.73 (s, 2H), 3.63 (m, 3H), 3.52 (m, 1H), 2.78-2.72 (m, 3H), 2.65 (dd, J = 16.0 and 8.2, 1H), 2.51-2.44 (m, 3H), 2.35 (dd, J = 16.0 and 9.2, 1H), 2.08 (m, 4H), 1.89 (s, 3H); ESI MS calcd for $\text{C}_{48}\text{H}_{49}\text{N}_7\text{NaO}_{17}$ $[\text{MH}]^+$ 1019, found 1019.

“AcHN-AspDanAspAspDan*AspNdiGly-OH” (3.3). (80% yield) ^1H NMR (500 MHz, D_2O) δ = 8.00 (d, J = 7.6, 2H), 7.91 (d, J = 7.6, 2H), 7.13 (d, J = 8.3, 1H), 6.89 (d, J = 8.1, 1H), 6.84-6.82 (comp, 2H), 6.80-6.67 (comp, 4H), 6.48 (d, J = 7.5, 1H), 6.30 (d, J = 7.9, 1H), 6.27 (d, J = 7.5, 1H), 6.24 (d, J = 6.9, 1H), 4.61 (dd, J = 5.9 and 1.6, 1H), 4.44-4.39 (m, 2H), 4.24-4.13 (comp, 4H), 3.95 (d, J = 2.1, 1H), 3.91 (d, J = 6.6, 2H), 3.83 (s, 2H), 3.74-3.62 (comp, 7H), 3.48-3.45 (m, 1H), 3.40 (t, J = 6.2, 2H), 3.36-3.32 (m, 2H), 3.06 (dd, J = 5.5 and 0.1, 1H), 2.69-2.63 (m, 3H), 2.58-2.25 (comp 12H), 2.03-2.00 (comp, 4H), 1.97-1.82 (comp 4H); ESI MS calcd for $\text{C}_{73}\text{H}_{78}\text{N}_{10}\text{NaO}_{26}$ $[\text{MH}]^+$ 1534, found 1534.

“AcHN-AspDanAspDan*AspNdiGly-OH” (3.4). (86% yield) ^1H NMR (500 MHz, D_2O) δ = 8.07 (d, J = 7.5, 2H), 7.99 (d, J = 7.5, 2H), 7.18 (d, J = 8.5, 1H), 6.97 (d, J = 8.5, 1H), 6.93 (t, J = 7.9, 1H), 6.85 (t, J = 7.7, 1H), 6.80-6.77 (comp, 2H), 6.75 (t, J = 8.3, 1H), 6.64 (d, J = 8.3, 1H), 6.55 (d, J = 7.5, 1H), 6.36-6.32 (comp, 3H), 4.51 (dd, J = 5.2 and 3.6, 1H), 4.37-4.30 (comp, 3H), 4.27-4.23 (m, 1H), 4.05-4.00 (comp, 3H), 3.91-3.65 (comp, 11H), 3.62-3.58 (m, 1H), 3.47-3.42

(comp, 3H), 2.82-2.44 (comp, 11H), 2.40-2.35 (m, 1H), 2.13-1.95 (comp, 8H), 1.92 (s, 3H); ESI MS calcd for $C_{69}H_{73}N_9NaO_{23}$ $[MH]^+$ 1419, found 1420.

“SucHN-AspDanDan*AspNdiGly-OH” (3.5). (83% yield) 1H NMR (500 MHz, D_2O) δ = 7.90 (d, J = 7.5, 2H), 7.78 (d, J = 7.5, 2H), 7.07 (d, J = 8.3, 1H), 6.96 (d, J = 8.5, 1H), 6.86 (t, J = 8.2, 1H), 6.76-6.65 (comp, 5H), 6.58 (d, J = 7.8, 1H), 6.38 (d, J = 7.5, 1H), 6.12 (d, J = 7.8, 1H), 6.05 (d, J = 7.6, 1H), 4.44 (dd, J = 5.1 and 4.1, 2H), 4.39-4.31 (comp, 2H), 4.24-4.17 (comp 3H), 4.12-4.03 (m, 2H), 3.89 (t, J = 5.2, 2H), 3.74 (m, 1H), 3.63-3.45 (comp, 6H), 3.34 (m, 1H), 3.25 (m, 2H), 2.74-2.65 (comp, 4H), 2.61-2.39 (comp, 6H), 2.34-2.27 (comp, 6H), 2.14-2.07 (comp, 4H), 1.91-1.82 (comp, 4H); ESI MS calcd for $C_{69}H_{72}N_8NaO_{24}$ $[MH]^+$ 1420, found 1420.

“SucHN-AspDan^(8atoms)Dan*AspNdiGly-OH” (3.6). (84% yield) 1H NMR (500 MHz, D_2O) δ = 8.03 (d, J = 7.6, 2H), 7.77 (d, J = 7.4, 2H), 7.49 (d, J = 8.8, 1H), 7.21-7.19 (comp, 2H), 7.14 (t, J = 8.2, 1H), 7.05-7.02 (comp, 2H), 6.99 (t, J = 8.0, 1H), 6.81-6.78 (comp, 2H), 6.53 (d, J = 7.6, 1H), 6.47 (d, J = 7.8, 1H), 6.33 (d, J = 7.4, 1H), 4.63 (dd, J = 5.4 and 2.6, 1H), 4.54 (d, J = 2.2, 2H), 4.48-4.45 (m, 2H), 4.24-4.21 (comp, 6H), 3.79-3.70 (comp, 7H), 3.45-3.43 (m, 1H), 3.36-3.32 (m, 2H), 2.73-2.66 (m, 6H), 2.65-2.56 (m, 2H), 2.45-2.34 (comp, 4H), 2.27-2.18 (m, 2H), 2.00-1.91 (comp, 6H); ESI MS calcd for $C_{67}H_{67}N_8O_{24}$ $[M]^-$ 1368 (negative mode), found 1368.

“AcHN-AspDan(AspNdiAspDan)₂Gly-OH” (3.7). (68% yield) 1H NMR (500 MHz, D_2O) δ = 7.81-7.73 (comp, 8H), 6.86-6.81 (comp, 2H), 6.71-6.58 (comp, 7H), 6.52-6.48 (comp, 3H), 6.33 (d, J = 7.8, 1H), 6.24 (d, J = 7.1, 1H), 6.17 (d, J

= 7.2, 1H), 6.09 (d, $J = 7.8$, 1H), 6.05 (d, $J = 7.9$, 1H), 5.94 (broad d, 1H), 4.59-4.52 (comp, 3H), 4.42 (dd, $J = 4.9$ and 4.0 , 1H), 4.10-4.04 (comp, 7H) 3.96 (m, 1H), 3.82-3.76 (comp, 4H), 3.64-3.26 (comp, 22H), 2.73-2.40 (comp, 14H), 2.33-2.28 (comp, 7H), 1.96-1.82 (comp, 15H); ESI MS calcd for $C_{113}H_{115}N_{15}NaO_{37}$ $[MH]^+$ 2298, found 2298.

“AcHN-(AspDan)₃(AspNdi)₂Gly-OH” (3.8). (61% yield) 1H NMR (500 MHz, D_2O) δ = 7.88 (d, $J = 7.6$, 2H), 7.81-7.77 (comp, 2H), 7.70 (d, $J = 7.2$, 2H), 6.95 (broad, 1H), 6.78-6.63 (comp, 3H), 6.59-6.52 (comp, 3H), 6.44 (broad, 1H), 6.33 (comp, 3H), 6.16-6.11 (comp, 4H), 5.94 (broad, 1H), 5.84 (broad d, 1H), 5.78 (broad d, 1H), 4.62-4.58 (comp, 2H), 4.38 (dd, $J = 5.1$ and 4.0 , 1H), 4.22-3.95 (comp, 8H), 3.85-3.78 (broad, 2H), 3.71-3.42 (comp, 18H), 3.40-3.22 (comp, 4H), 2.70-2.23 (comp, 20H), 1.92-1.78 (comp, 16H); ESI MS calcd for $C_{113}H_{115}N_{15}NaO_{37}$ $[MH]^+$ 2298, found 2298.

UV-Vis spectroscopy. UV-Vis spectra were taken on a temperature regulated Hewlett Packard 8452A diode array spectrophotometer. Concentration of stock solutions used for UV studies was initially determined by NMR integration of a known concentration of TSP- d_4 added to an aliquot. Unfolding studies were carried out by monitoring the increase in the UV absorbance at 382 nm with the addition of cetyltrimethylammonium bromide detergent (CTAB). Solutions of compound (40 μM in buffered H_2O) were measured in a 1 cm pathlength cuvette equipped with a microstirrer as a solution of 0.1 w/v % CTAB in buffered H_2O was added in 0.025-0.050 mL increments. Complete unfolding of

the naphthyl trimers was determined to be around 0.03 w/v % CTAB in the cuvette. When graphed, absorbances were corrected for dilution.

2D-NMR spectroscopy. For proton assignment purposes several 2D-NMR spectra were taken for **3.1**, **3.4**, and **3.6**, all at 1 mM concentrations of compound in sodium phosphate buffered solvents as above. Representative spectra with acquisition parameters are shown in Figures 3.19-3.25. Samples in 90/10 buffered H₂O/D₂O were prepared for 2D NMR spectra which were acquired at different mixing times, 200-800 milliseconds (ms) for NOESY spectra and 50-150 ms for TOCSY spectra. Since the molecular weight of the compounds fell in between the 800-1500 MW range where the negative/positive transition of NOEs may occur, a ROESY, (which give always positive ROESY peaks and negative exchange peaks) was required when NOESY afforded unexpectedly weak NOEs. Depending on the conditions, this switch resulted sometimes in clearer (more intense) cross peaks, other times not. Other considerations for spectra acquisition were solvent suppression methods (1-1 jump-return suppression sequence for ROESY and presaturation for NOESY and TOCSY spectra) and filtering parameters, such as “gf” and “gfs”, during processing.

Only NOESY spectra taken in 100% buffered D₂O with a mixing time of 800 ms was used for structural analysis. SPARKY, an online visualization program, facilitated the imaging and interpretation of 2D-NMR spectra (Goddard 2000).

Molecular modeling. Computations were performed with the HyperChem software using the MM+ force field. A set of twenty random starting

conformations of models for **3.1**, **3.4**, and **3.6** were generated using unrestrained molecular dynamics at 1000 K. Each of the twenty diverse structures was then allowed to anneal with a weak distance restraint as the simulation temperature was lowered from 1000 K to 300 K over 10 ps. After annealing, a final geometry optimization was performed without restraints using Fletcher-Reeves conjugate gradient, 0.01 kcal·mol⁻¹. The lowest energy conformer for both **3.1** (relative energy = -18.97 kcal·mol⁻¹) and its sequence isomer **3.4** (-19.27 kcal·mol⁻¹) afforded a structure that adopts a parallel Dan/Ndi/Dan stack.

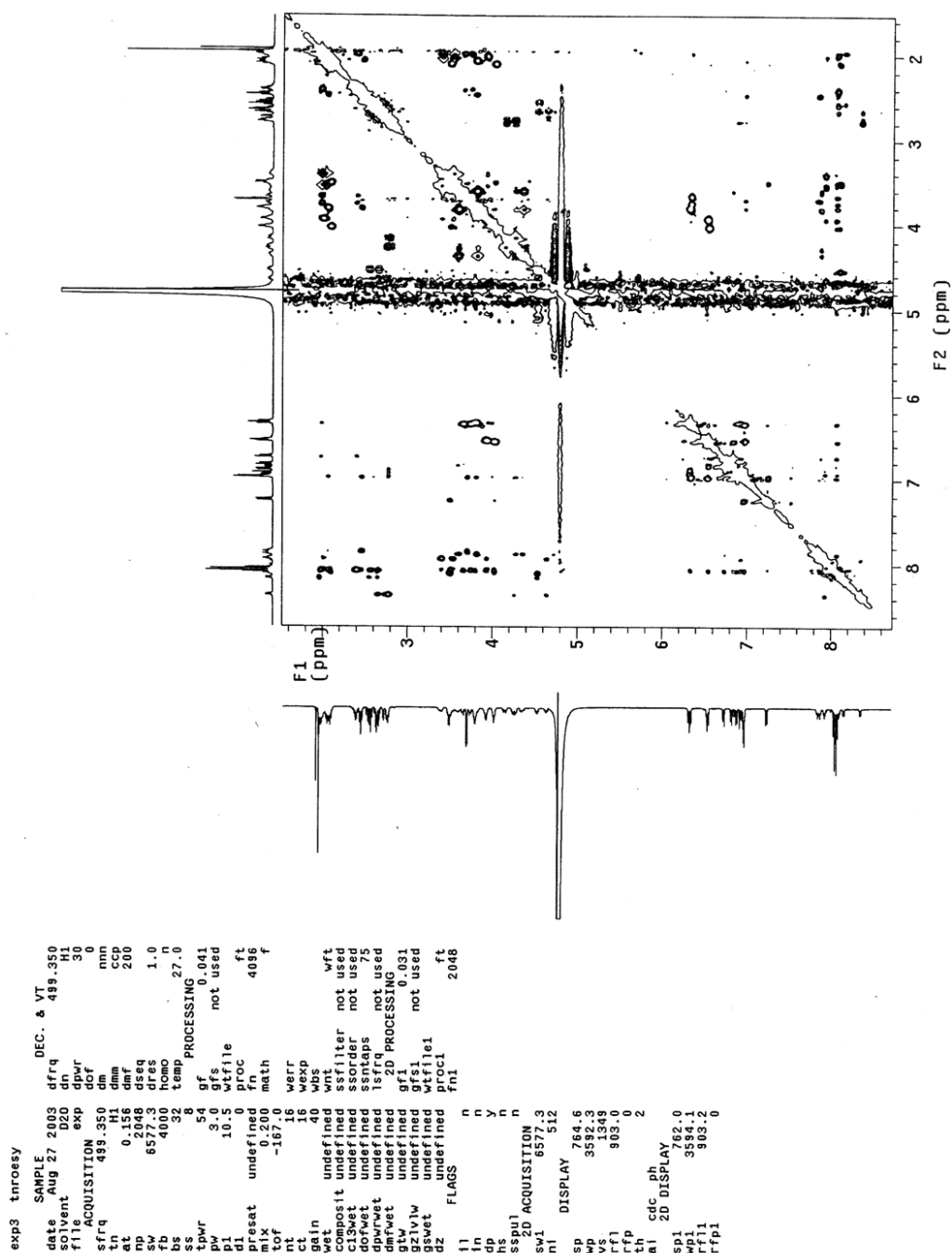


Figure 3.19 “Water” ROESY spectrum of **3.1**.

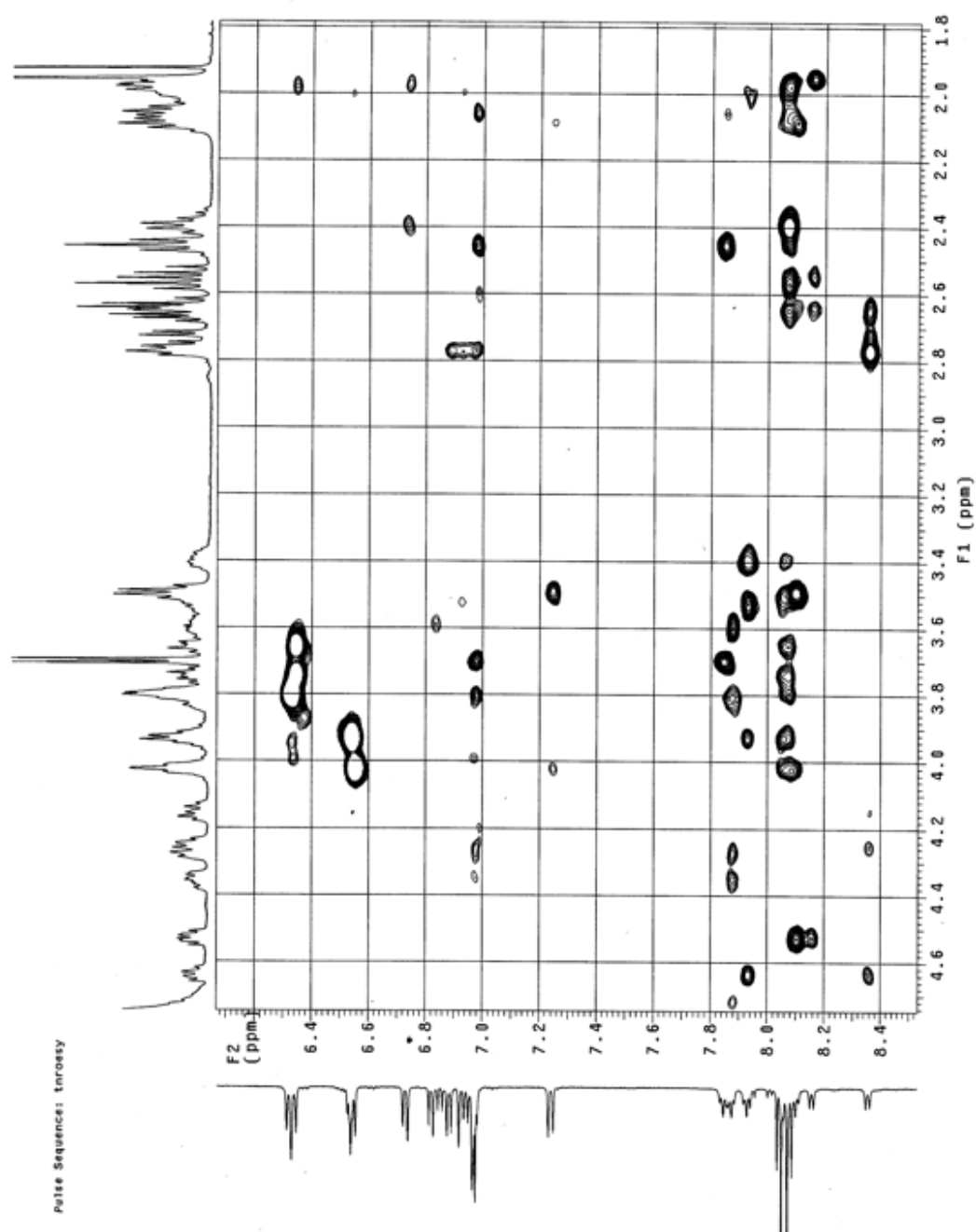


Figure 3.20 Expansion of “water” ROESY spectrum of **3.1**.

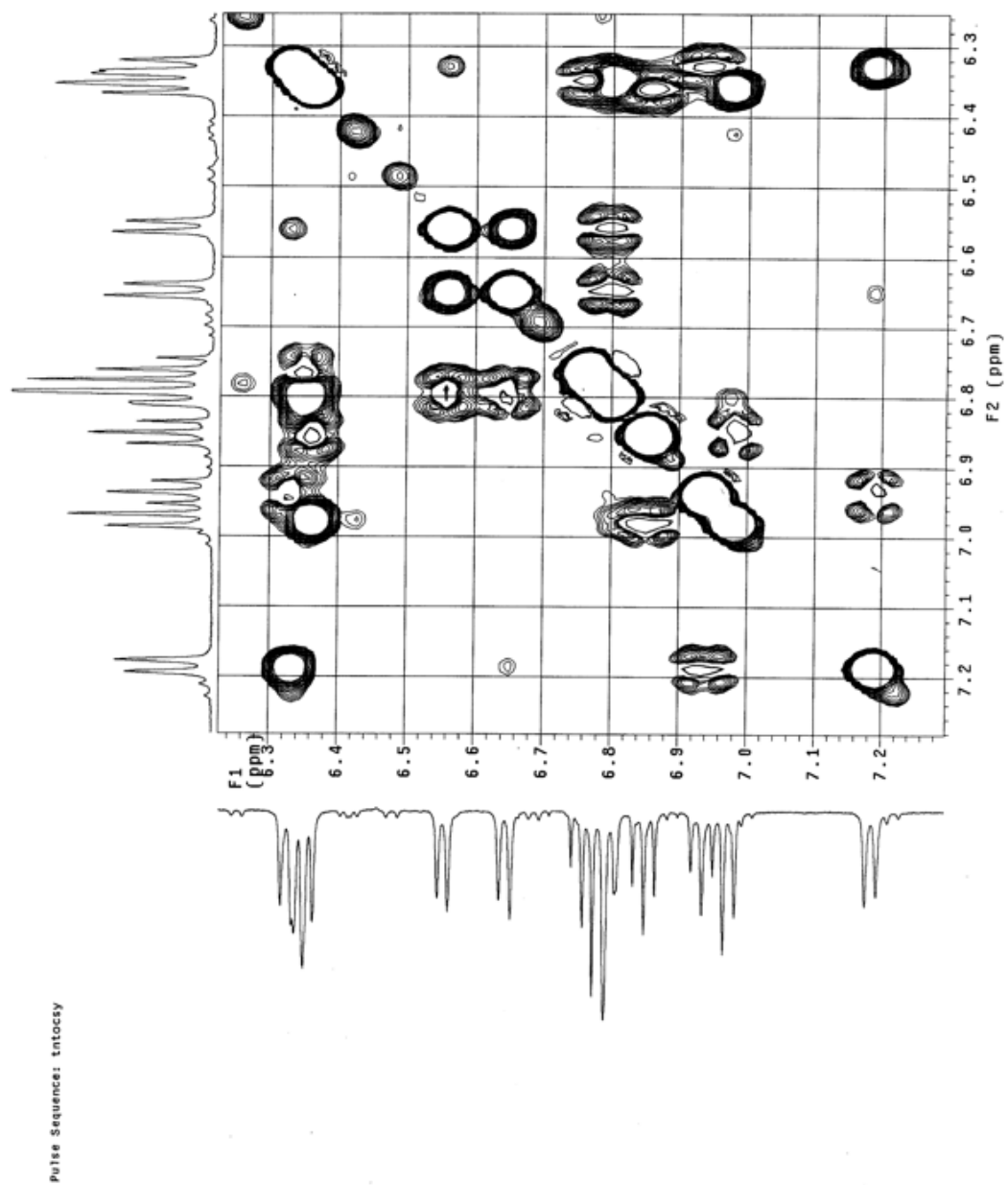


Figure 3.22 Expansion of “water” TOCSY spectrum of **3.4**.

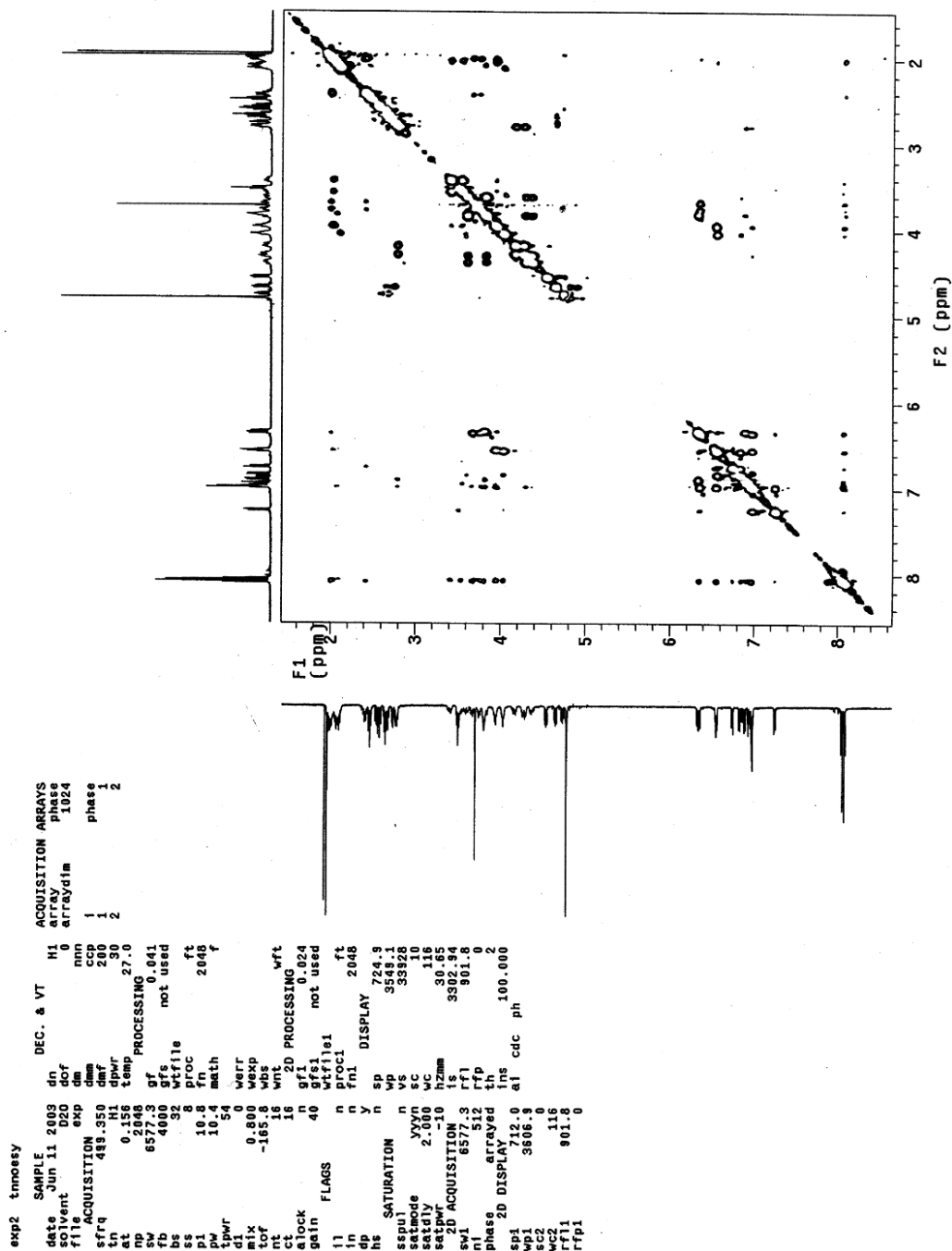


Figure 3.23 NOESY spectrum of **3.1**.

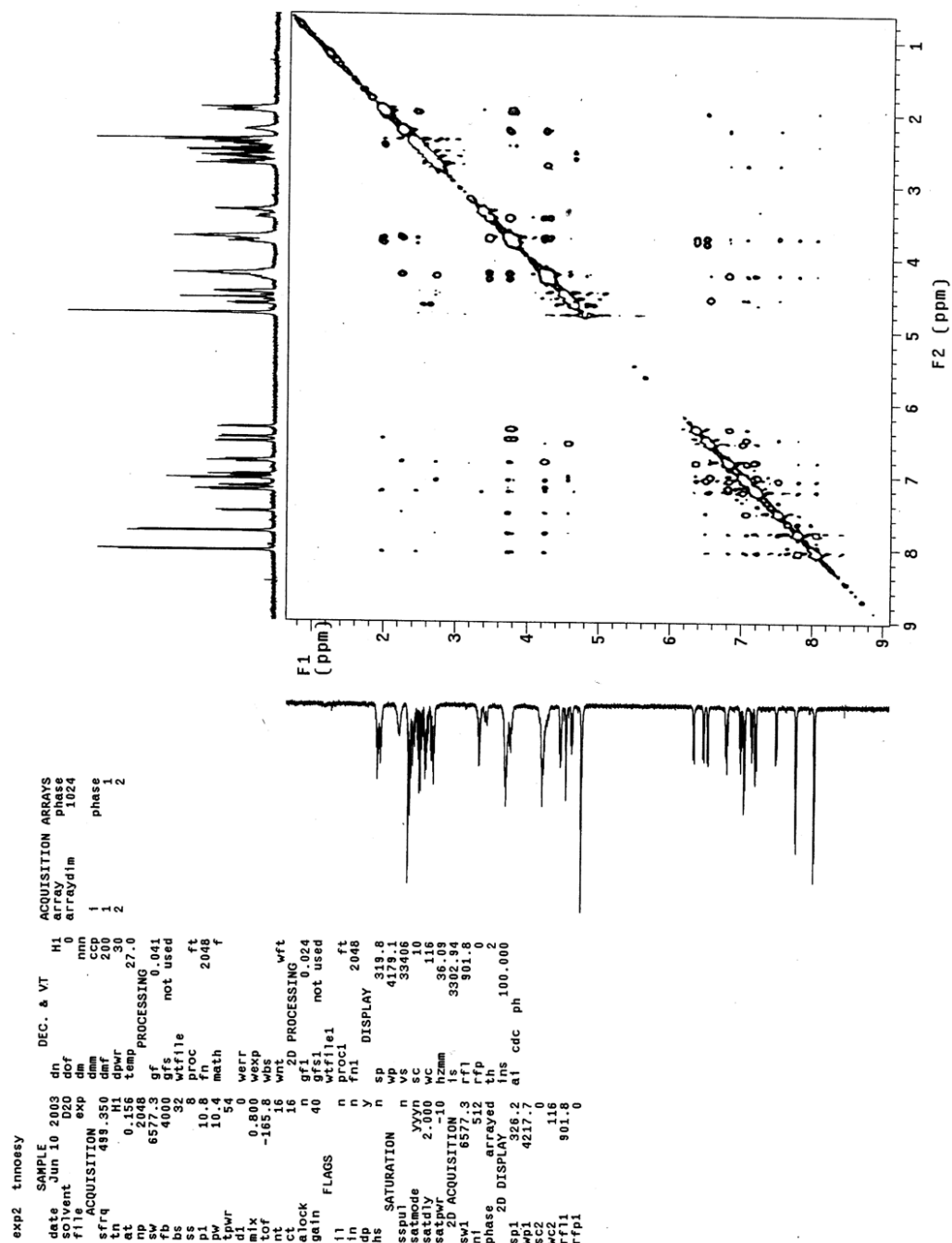


Figure 3.24 NOESY spectrum of **3.4**.

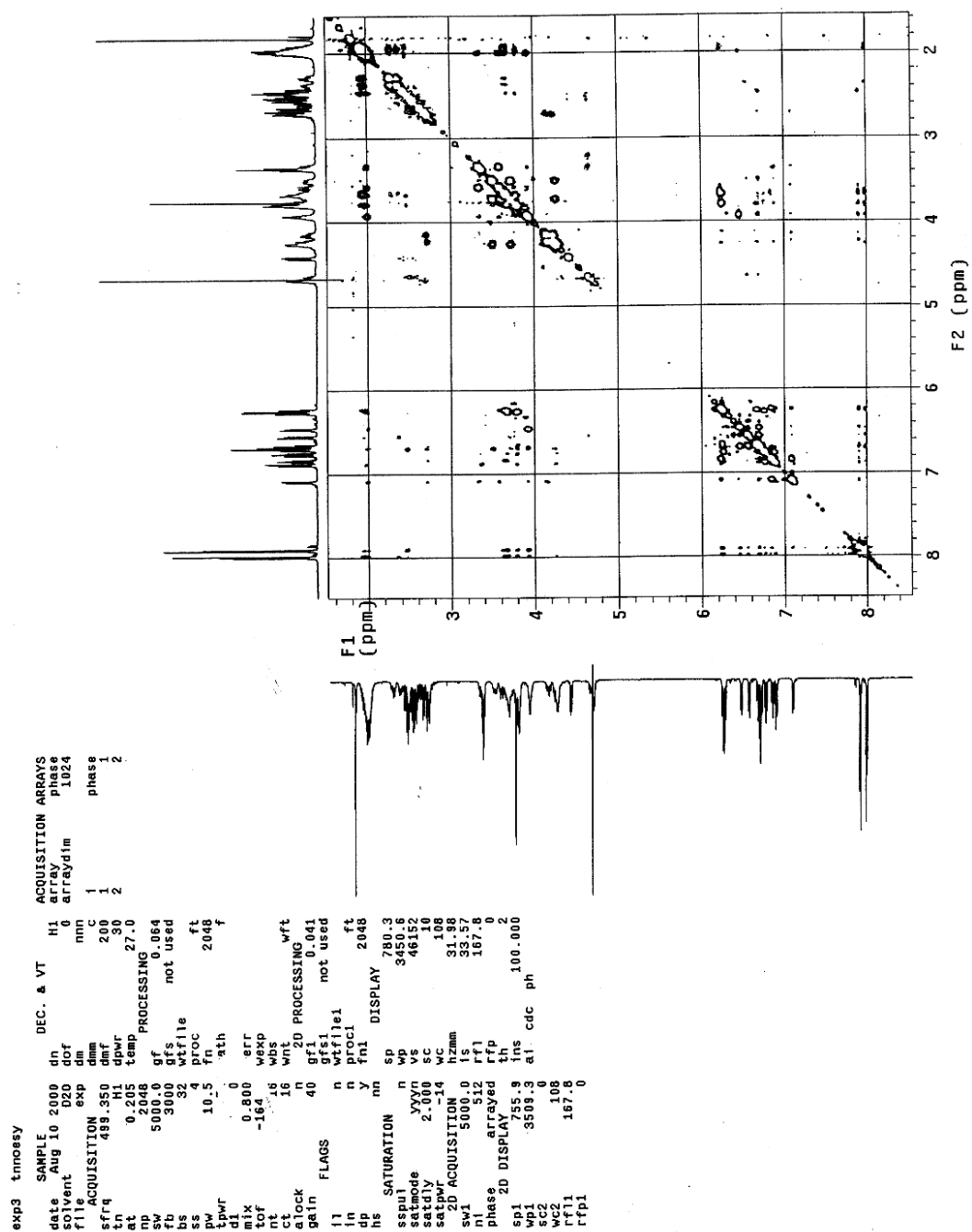


Figure 3.25 NOESY spectrum of **3.6**.

CHAPTER 4

Naphthyl Oligomers that Form Hetero-Duplexes

4.1 CHAPTER SUMMARY

Introduction. The previous chapter illustrated that the Dan:Ndi interaction can dictate *intramolecular* folding of intercalative turns, a more challenging topology than the pleated structures exhibited by aedamers. This chapter will discuss work showing that the Dan:Ndi interaction can also direct *intermolecular* binding and bring together Dan_n and Ndi_n chains to form hetero-duplexes (Figure 4.1). Chemists have utilized, quite successfully, hydrogen bonding and metal-coordination to construct duplex-forming oligomers with desirable properties such as high binding affinities/stabilities and good chain recognition. Examples of duplexes that use predominantly aromatic interactions are few and examples that work in water mainly through aromatic stacking were, to the best of our knowledge, non-existent prior to the system described in this chapter. Synthetic hetero-duplexes that can operate in aqueous solutions could possibly be exploited in a wide range of fields ranging from materials (high strength fibers processible in water, a fairly benign solvent) to medicine (diagnostic kits that require robust biomolecule immobilization). Next-generation duplex systems that can self-sort large chain populations, can exhibit reversible binding triggered by various stimuli, and can operate in a range of solvents and on solid phase would also be very attractive.

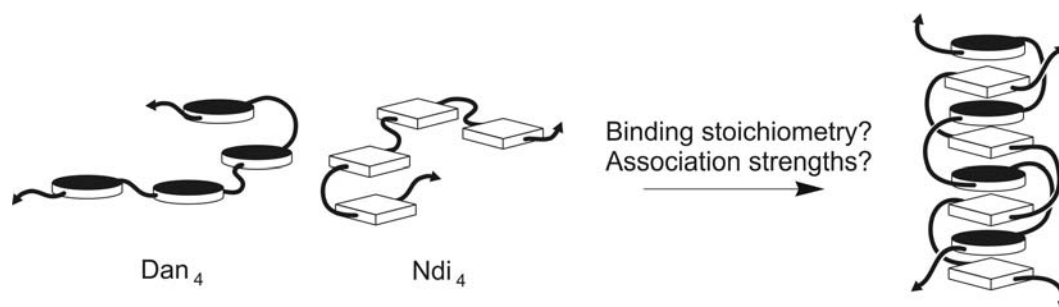


Figure 4.1 Cartoon representation of a proposed hetero-duplex formed to maximize Dan:Ndi associations in an intermolecular fashion and critical questions answered in this project.

Goals. Experiments described in this chapter aimed to answer the question: *Can the Dan:Ndi interaction be exploited in an intermolecular fashion to form stable hetero-duplexes with high affinities and chain recognition?* The short-term goals of this work were to develop a first-generation water compatible hetero-duplex system formed from complementary oligo-Dan and oligo-Ndi molecular strands and to investigate their binding behavior. The long-term objective of this research is to create hetero-duplex systems with affinities and binding selectivities sophisticated enough to be used possibly for building well-defined aedamer assemblies with dramatically larger size domains and for exploring surface patterning applications.

Approach. Binding stoichiometries and association constants were determined by NMR and isothermal titration calorimetry (ITC) at different temperatures. The thermodynamics of binding was also investigated. Size exclusion chromatography (SEC) and polyacrylamide gel electrophoresis (PAGE)

experiments were carried out to further test the robustness of the complexes formed.

Results. Overall, the work described in this chapter demonstrated the assembly of oligo-Dan and oligo-Ndi strands into stable hetero-duplexes (Gabriel 2002). NMR and ITC investigations were consistent with a 1:1 binding ratio. ITC revealed that tetra-Dan and tetra-Ndi chains (tetrameric system) formed hetero-duplexes with a stability constant of $350,000 \text{ M}^{-1}$ at $T = 318 \text{ K}$, three orders of magnitude higher than the binding constant of the monomeric system. Additionally, ITC analysis calculated a heat capacity between -50 and $-94 \text{ cal}\cdot\text{mol}^{-1}\cdot\text{K}^{-1}$ depending on the temperature range studied. Furthermore, duplexation was enthalpically favored and an enthalpy-entropy compensation effect was seen with the dimeric system. SEC chromatographs showed that a 1:1 molar mixture of tetra-Dan:tetra-Ndi resulted in material that eluted approximately when a hetero-dimer would be expected to elute relative to retention times of uncomplexed tetra-Dan and tetra-Ndi chains. Lastly, discrete hetero-duplex formation for the tetrameric system was observed under PAGE conditions even when one component was in slight excess over the other further signifying a strong and discriminating inter-chain interaction.

4.2 BACKGROUND: SELF-ASSEMBLY OF MOLECULAR STRANDS

Natural chain molecules, or biopolymers, possess a range of functions due largely to the organization of linear precursors into defined assemblies such as multistranded complexes for proteins and duplexes in the case of DNA (Venkatraman 2001, Wang 1991). Nearly 10 years after the review “Interlocked

and Intertwined Structures and Superstructures" was published (Amabilino 1995), the field of self-assembly has continued to expand and has led to emerging research programs in "bottom-up engineering" (Stoddart 2001), dynamic covalent chemistry (Rowan 2002), and supramolecular protein assemblies (Yeates 2002).

The development of artificial chains that self-assemble into defined complexes, in particular into duplexes, has drawn active interest recently. Synthetic assemblies, where binding is based on recognition between two complementary chains, could potentially afford capabilities for information storage and transfer, reminiscent of DNA. Strands of protein, which form biological fibers such as muscle (von Kiedrowski 1994) and spider silk (Vollrath 2000, Kubik 2002), have set high standards for materials considered for their mechanical properties. Another protein example is the hetero-dimerization of leucine zipper transcription factors that bind specific sequences of DNA (Glover 1995). Finally, molecular strands with orthogonal binding and self-sorting capacities would nicely complement existing patterning and immobilization technologies (Wilchek 1990).

While certain hydrogen bonding patterns are responsible for the secondary structures of proteins and the base-pairing specificities of DNA, several groups have reported impressive results using significantly different hydrogen bonding strategies for their nonnatural duplex oligomers (Gong 2001, Archer 2000). For instance, Krische and co-workers have synthesized oligomers applying a "covalent casting" strategy to link amino-dichlorotriazines to design duplex oligomers with predefined hydrogen bonding patterns (Archer 2002a, b). These

oligomers exhibited up to nanomolar binding affinities and a strong cooperative effect was observed upon extension from monomer to dimer to trimer. Also at the forefront of hydrogen bonded duplexes, is the work from Gong and co-workers who have established specific recognition with their “hydrogen bonded tapes” through the precise placement of hydrogen bonding donors and acceptors (Zeng 2001, 2002).

The wealth of hydrogen bonding donor and acceptor precursors has no doubt been key for the investigation of a variety of bonding patterns and creative design strategies. Though the use of hydrogen bonds has afforded synthetic duplex systems with high binding strengths and selectivities, a discussion of artificial duplexes would not be complete without referencing complexes based on metal-coordination (Albrecht 2001). In 1987 Lehn introduced the term “double-stranded helicates” for the complexes between oligobipyridine and copper(I) cations that were shown by x-ray crystallography to form double helices (Lehn 1987). Studies with double-stranded helicates continue to this day with recent examples showing special features, for instance, stereoselective self-assembly (Telfer 2004) and synergism of metal coordination and hydrogen bonding effects (Chowdhury 2004).

In close relation to the work presented in this chapter, duplexes having an aromatic interactions component have also been reported. Probably the earliest published report of an aromatic donor-acceptor hetero-duplex system came from Stoddart's group using oligomers of linked hydroquinol and linked bipyridinium units (Figure 4.2). Structure characterization from this pioneering effort was not

conclusive for double-helical conformations, as hoped for by the authors, since low temperature NMR did not seem to significantly freeze out a unique structure. Nonetheless, this groundbreaking study put forth the idea of using aromatic stacking that is, in a sense, less geometrically rigid than hydrogen bonding and metal coordination.

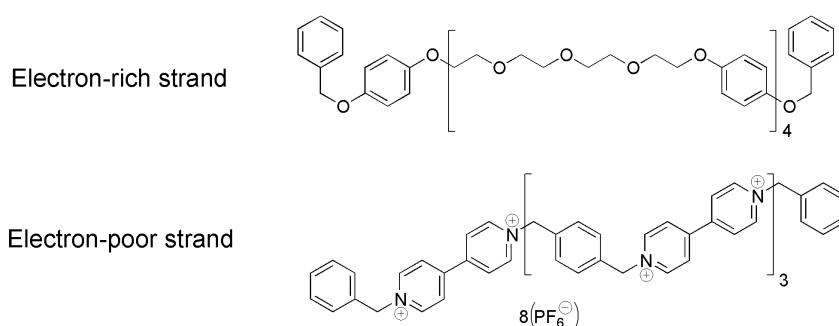


Figure 4.2 Aromatic π - π stacking system from Stoddart's laboratory (Ashton 1992).

The Stoddart group has continued to do important work in the field of supramolecular chemistry (Philp 1996) mainly focusing on the development of aromatic donor-acceptor based catenanes and rotaxanes (rather than hetero-duplexes) for use in nanoscale devices (Stoddart 2001, Feynman 1960). This research program has been tremendously prolific and most recently, in a milestone achievement in molecular topology, they reported the self-assembly of the first wholly synthetic Borromean rings (Chichak 2004, Mao 1997).

The next two examples described used a combination of hydrogen bonding and aromatic interactions. Lehn and co-workers have synthesized a family of oligo(pyridylamide)s that exhibited dynamic exchange between single

and double helices (Berl 2000, 2001). In general, intramolecular hydrogen bonds were responsible for the helical conformations while aromatic stacking stabilized dimerizations (Figure 4.3).

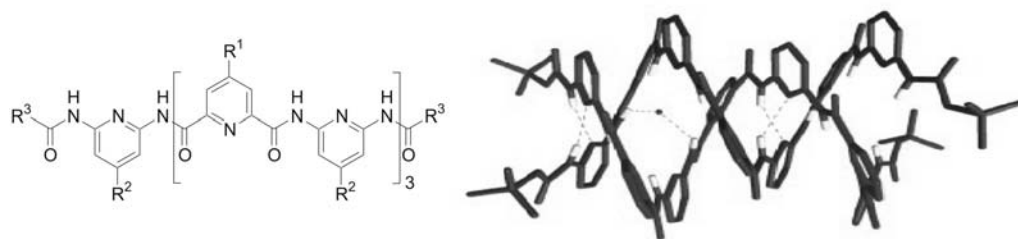


Figure 4.3 X-ray crystal structure of Lehn's oligopyridinecarboxamide ($R^1 = R^2 = \text{H}$, $R^3 = \text{O}^t\text{Bu}$) showing interstrand aromatic stacking and hydrogen bonding which includes two bridging NH-O hydrogen bonds. Crystals grown from $\text{CH}_3\text{CN/DMSO}$. (Berl 2000).

The “molecular zippers” designed by Hunter and co-workers were prepared from isophthalic acid and bisaniline derivatives (Bisson 1994, 2000, Hunter 2003). Hydrogen bonding was determined to be the main driving force for complexation but interestingly aromatic interactions that had edge-to-face orientations also existed (Figure 4.4). For this system, recognition properties between unlike strands seemed to rely simply on the length of the oligomers.

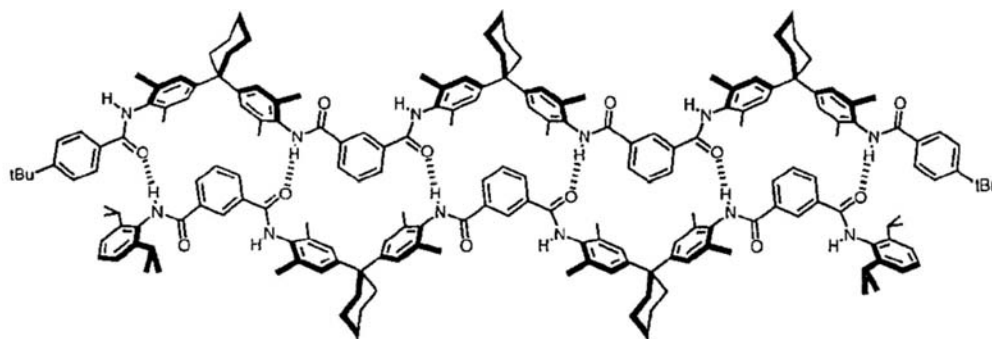


Figure 4.4 Proposed structure of zipper complex between two different aromatic amide oligomers showing hydrogen bonding and edge-to-face aromatic interactions (from Bisson 2000).

Reprinted with permission from Bisson, A. P.; Carver, F. J.; Eggleston, D. S.; Haltiwanger, R. C.; Hunter, C. A.; Livingstone, D. L.; McCabe, J. F.; Rotger, C.; Rowan, A. E. *J. Am. Chem. Soc.* **2000**, *122*, 8856. Copyright 2000 American Chemical Society.

Li and co-workers have reported a π -stacking duplex system that is very similar to the Iverson duplexes (Gabriel 2002) except for a few key design elements (Zhou 2003). First, the electron-deficient pyromellitic diimide (Pdi) ring was used instead of the naphthalene diimide (Ndi) unit. Second, and more interesting, is the comb-type architecture of Li's molecules that projects the aromatic rings *from* the backbone leading to a zipper-like association (Figure 4.5) versus an intertwined association (Figure 4.1) proposed for Iverson's hetero-duplexes whose aromatics are *within* the backbone. How architecture differences affect the entropy and enthalpy components of binding is certainly an intriguing question. Direct comparisons will have to wait though due to the solubility differences of the Iverson duplexes (soluble in water) and the Li duplexes (soluble in chloroform).

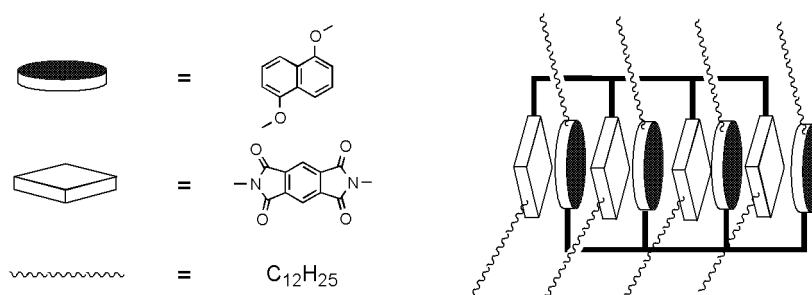


Figure 4.5 A donor-acceptor tetrameric hetero-duplex formed with comb-type naphthyl oligomers (Zhou 2003).

As mentioned above, the hetero-duplexes introduced by the Iverson laboratory were soluble in aqueous solutions and previous studies have shown that the Dan:Ndi interaction was overwhelmingly stronger in water than in organic solvents (Cubberley 2001b). On the other hand, all of the synthetic duplexes presented above were studied in organic solutions in which extremely strong associations were typically obtained. In studies that tested the addition of polar protic solvents such as methanol (Bisson 2000) and water (Berl 2000), duplex formation was disrupted. Structure characterization of most of these systems though has benefited greatly from x-ray quality crystals grown from organic solutions. Attempts to grow crystals of water-soluble naphthyl oligomers have been unsuccessful. Thus the synthesis of organic-soluble analogues is another pursuit of the Iverson laboratory (Cubberley 2000). Nonetheless, the water solubility of the hetero-duplexes presented in the following sections may confer its own advantages (long-term), most promising of which is the possibility to construct duplex foldamers compatible with biological systems.

4.3 RESULTS AND DISCUSSION

4.3.1 Synthesis of Homo-Naphthyl Oligomers

The synthesis of **4.1-4.8** (Figure 4.6) used monomers and SPPS protocols previously described in Chapter 2. While the incorporated aspartate residues provided the much desired solubility in water buffered to pH = 7, consequently, the desired hetero-duplex formation might experience significant charge repulsion involved with the assembly of like-charged chains. Purification via FPLC (>98% pure judged by HPLC peak area) was straightforward for all compounds except **4.7**, which required multiple FPLC runs at 50% longer gradients since a small amount of the **4.5**, formed as a deletion side-product, had similar retention times on the reverse-phase column. Final desalting via a C18 Sep-Pak cartridge and freeze-drying afforded soft solids (white and pale yellow in color for the oligo-Dan and oligo-Ndi series, respectively).

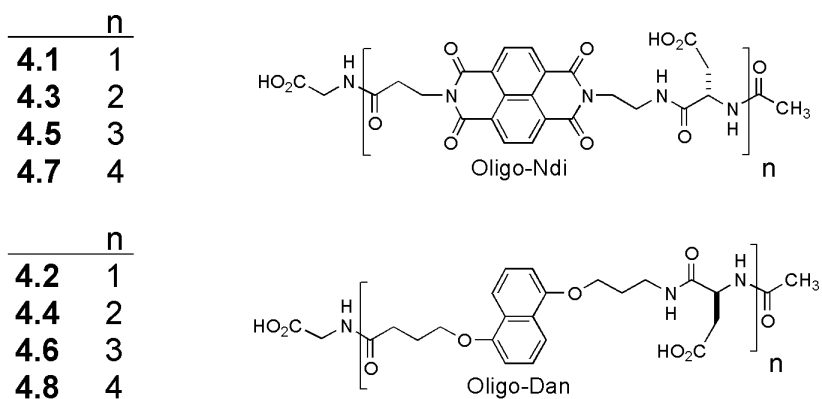


Figure 4.6 Compounds synthesized and studied in Chapter 4. 13-atom linkers between naphthyl moieties were used.

Figure 4.7 shows an idealized model of the dimeric (4.3:4.4) duplex. As previously seen with computer modeling of the intercalative fold topology (Chapter 3, Section 3.3.7), a 13-atom linkage between naphthyl units would allow “sandwiching” of an aromatic ring for intertwining chains also (Figure 4.7). Geometry optimization of a 10-atom linker indicated that it was too short to allow ideal face-centered stacking in which the aromatic rings are parallel and ~ 3.5 Å apart (approximate inter-ring distance based on van der Waals radii. Modeling of dimers with a 16-atom linkage resulted in structures with markedly kinked linkers, which would be expected to lower binding affinities. Although far from rigorous, modeling still provided a good starting point for the design of intertwining strands of oligo-Dan and Ndi chains.

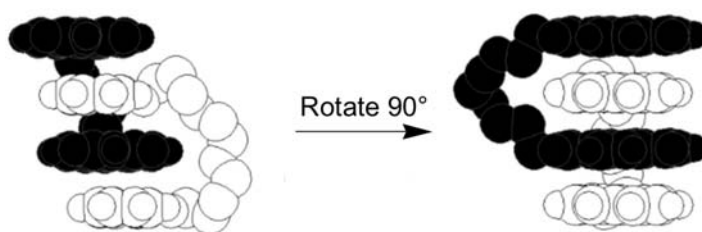


Figure 4.7 Computer generated space-filled model (right structure is rotated by 90°) of the duplex formed from truncated **4.3** (black) and **4.4** (white). Linker atoms not along backbone path omitted for clarity.

4.3.2 NMR Job Plots and Titrations

Foremost, a one-to-one complex between oligo-Dan and oligo-Ndi molecules had to be established. Although detailed complexation studies have been previously performed for uncharged, but aqueous-soluble monomers (Zych

2000, Cubberley 2001b), **4.1** and **4.2** were designed to be multi-charged in water akin to the longer oligomers of this study and thus required their own NMR analysis. NMR experiments were also performed for the dimeric duplex complex **4.3:4.4**. The chemical shifts of the Ndi unit(s) in **4.1** and **4.3** conveniently allowed the determination of binding stoichiometry by the Job's method (Connors 1987, Gil 1990). One can use Job plots to distinguish between one-to-one from higher-order binding simply by inspection (Figure 4.8). The Ndi chemical shifts also permitted calculation of binding constants, $K_a(\mathbf{4.1:4.2})$ and $K_a(\mathbf{4.3:4.4})$, using titration data (Macomber 1992, Figure 4.8). Quantitative analysis of titration data was accomplished using the HOSTEST program developed by Wilcox and Glagovich (Wilcox 1997).

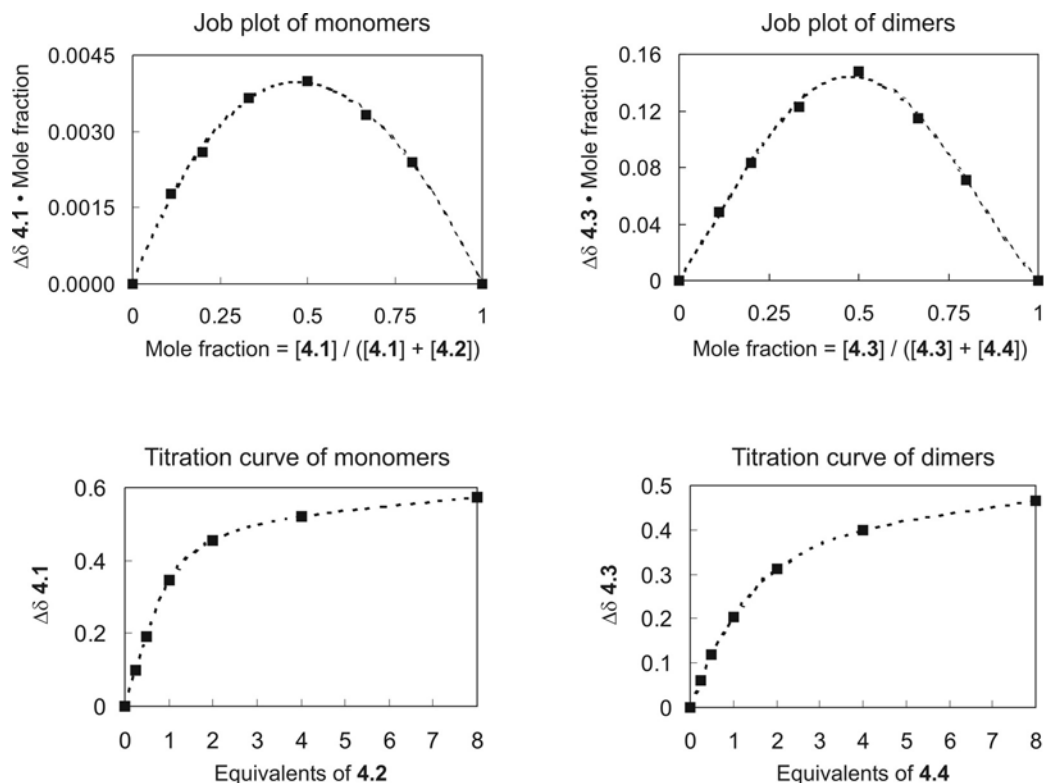


Figure 4.8 NMR Job plots and titration curves for evaluating the complexation of monomers (**4.1:4.2**) and dimers (**4.3:4.4**) at $T = 318$ K.

4.3.3 Evaluation of One-to-One Binding

The Job plots for both the monomeric and dimeric system gave broad maxima at equimolar ratios consistent with a binding stoichiometry that followed a 1:1 mode for **4.1:4.2** and **4.3:4.4** complexation (Figure 4.8). Using a 1:1 binding model to fit NMR titrations resulted in binding constants of $K_a(\mathbf{4.1:4.2}) = 130 \text{ M}^{-1}$ and $K_a(\mathbf{4.3:4.4}) = 2,800 \text{ M}^{-1}$. These values were from NMR experiments carried out at $T = 318$ K for comparison with the trimeric (**4.3:4.4**) and tetrameric (**4.3:4.4**) systems that behaved much better at elevated temperatures as judged by

ITC data (more on this behavior in the following sections). As expected, binding constants increased when the monomeric and dimeric complexes were analyzed at $T = 298\text{ K}$ affording a $K_a(\mathbf{4.1:4.2}) = 300\text{ M}^{-1}$ and $K_a(\mathbf{4.3:4.4}) = 7,500\text{ M}^{-1}$, more than twice the value measured at $T = 298\text{ K}$. Thus the binding stoichiometry and binding constants of the monomeric and dimeric systems were determined and the results are summarized in Table 4.1.

4.3.4 Isothermal Titration Calorimetry (ITC)

Reliable binding analysis of NMR titration data is dependent on tracking a particular proton signal, but this task became increasingly difficult with longer, unit-repeating oligomers due to the shifting of severely overlapped signals. There was little confidence placed in data based on following the intractable Ndi signals for **4.5** and **4.7** in titration experiments. Thus a new method had to be identified to obtain $K_a(\mathbf{4.5:4.6})$ and $K_a(\mathbf{4.7:4.8})$ for trimeric and tetrameric duplexation, respectively.

Analysis of titration data collected with ITC experiments is an attractive alternative on several fronts (Wiseman 1989). ITC measures the heat evolved or absorbed by a system during a titration run and uses these values as its data set rather than chemical shifts. If an injection of titrant results in the system absorbing heat an upward spike is observed indicating the instrument had to add energy to the system to maintain a constant heat signal. If the injection of titrant results in heat being evolved (i.e. an exothermic process) then the heat signals spike downward. ITC provides an efficient means of obtaining K_a , enthalpy (ΔH), and a stoichiometry (N = molar equivalent of titrant) of binding. With equation 1, free

energy (ΔG) and entropy ΔS of binding can be calculated hence the thermodynamic parameters associated with the binding event can be determined in a single titration. For further discussion, a review of the advantages and limitations of ITC has been published (Wadso 1997).

$$\Delta G^\circ = -RT \ln K_a = \Delta H^\circ - T\Delta S^\circ \quad (1)$$

Unfortunately, monomeric complexation of **4.1** with **4.2** was below the sensitivity limit of microcalorimetry (see explanation in Experimental Section, Wiseman 1989). ITC though was carried out appropriately for the dimeric (whose K_a values can be compared with those derived from NMR), the trimeric, and tetrameric systems. A VP-ITC MicroCalorimeter instrument and the analysis software provided with it were used in these experiments (Microcal, Inc. 1999).

When examining the tetrameric system it could be clearly seen that the isotherms collected at $T = 298 \text{ K}$ 1) did not satisfactorily exhibit binding saturation and 2) did not fit any of the Microcal binding models well (Figure 4.9, left isotherm). Comparing the experimental data to a best-fit theoretical curve gave a chi-square fitting analysis of 250,000 (unitless). In personal communications, ITC technicians recommended using data with chi-square values closer to 50,000 or lower (Microcal, Inc 1999). Similar problems were encountered with the trimeric system at this temperature (Isotherm of trimeric system at $T = 298 \text{ K}$ in Experimental Section). Although the average chi-square of 55,000 was better than that calculated for the isotherm of the tetrameric system at identical conditions, the trimer isotherm did not show sufficient saturation

(arbitrary judgment based on the amount of heat still being released at the end of the titration).

Binding of tetramers at different temperatures

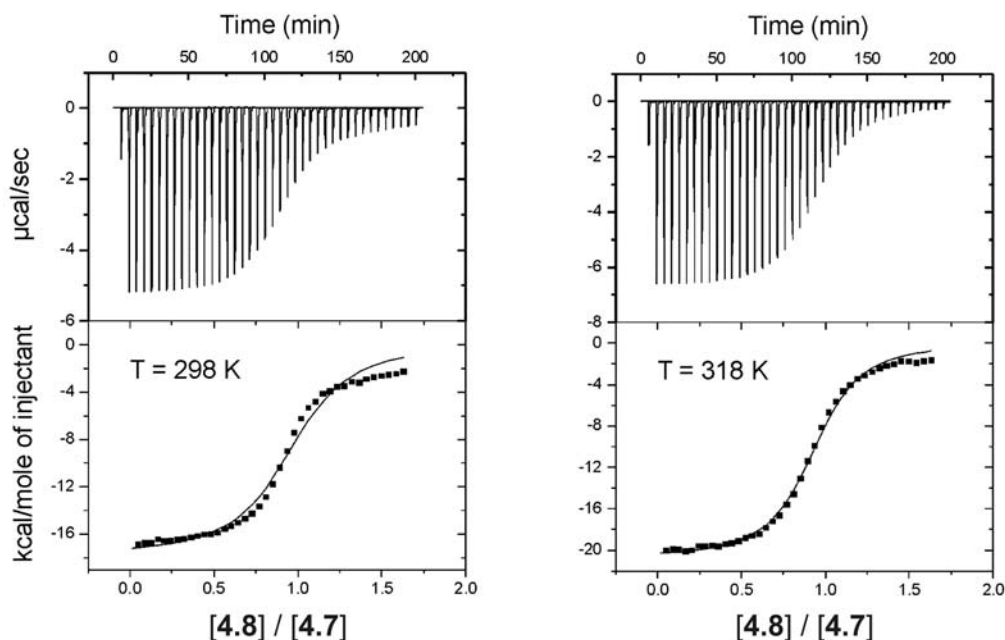


Figure 4.9 Binding isotherms for the titration of **4.7** with **4.8** at two different temperatures. Top panels display, the raw isotherm or the total heat evolved ($\mu\text{cal/sec}$) per injection of **4.8** (40 injections total). Data points in the bottom panels represent the heat evolved (kcal/mol) after correcting for heats of dilution. ITC data collected at $T = 298 \text{ K}$ did not fit theoretical curves (line in bottom panels). Data collected at $T = 318 \text{ K}$ on the other hand fitted predicted curves well according to a chi-square error analysis (Wiseman 1989, Microcal, Inc. 1999).

Faced with these initial difficulties, reverse titrations and sectional titrations where the whole binding isotherm was pieced together from several ITC runs were tried. These setups though were unsuccessful. Fortunately, when

identical runs were performed at $T = 318\text{ K}$ (Figure 4.9, right isotherm), well-behaved, 1:1 binding isotherms were acquired that fit the predicted curves accurately (Chi-square = 35,000 for the tetrameric system and 18,000 for the trimeric system). These results suggested that alternate modes of association, such as 1:2, 2:1 binding and problematic homomeric aggregation, possibly exist at ambient conditions but are disfavored at elevated temperatures. Also more telling is the apparent non-saturation of isotherms obtained at ambient conditions near the end of the titration run where the oligo-Dan is in molar excess which may signal possibly “off-register” binding to provide desolvation of added oligo-Dan. Importantly, results were consistent over multiple trials conducted at $T = 318\text{ K}$ and the fit of the curves, calculated by the analysis software, were entirely acceptable based on chi-square error analysis (Figure 4.9, see Experimental Section for supporting isotherms with corresponding thermodynamic parameters analyses).

With experimental conditions set, isotherms were collected for dimer (4.3:4.4), trimer (4.5:4.6), and tetramer (4.7:4.8) duplexation. Three trials were performed for each system. Figure 4.10 shows representative isotherms. The predicted curves varied the N value and for all cases the best fits were obtained when $N = 1 \pm 0.1$ molar equivalent of titrant.

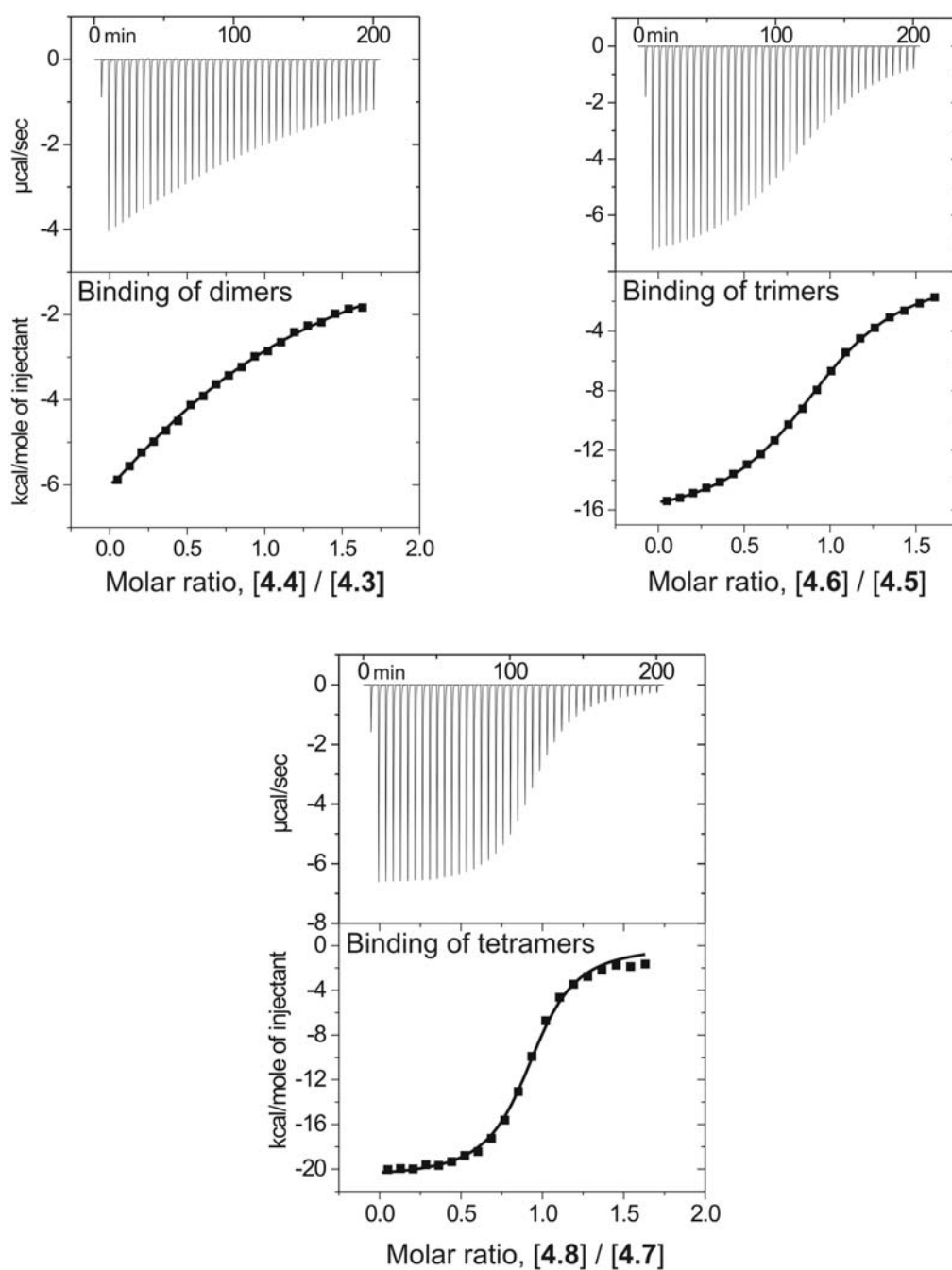


Figure 4.10 Representative binding isotherms at $T = 318 \text{ K}$. Three trials were performed for each system. Fitted line was based on 40 injection data points but only every other point is shown for clarity.

Table 4.1 reports the binding constants and provides a thermodynamic profile for 1:1 binding of each of the pairings. Before a discussion of the binding constants takes place, several points need to be made about the table. First, NMR and ITC values at $T = 298\text{ K}$ are absent for the trimeric and tetrameric systems for reasons mentioned before. Second, only the dimeric system had binding constants within the practical range of both NMR and ITC analysis. These values will be considered shortly. Third, while the binding thermodynamics were parsed into their enthalpy (ΔH) and entropy (ΔS) components for ITC experiments, a published report on the pitfalls of using the van't Hoff method of obtaining ΔH and ΔS from NMR data led to the decision to pass on additional experiments to calculate these thermodynamic parameters (Naghibi 1995). In this report several examples were cited where significant discrepancies were found between enthalpies derived by the van't Hoff method and enthalpies directly measured by ITC. The rule of thumb presented was that ΔH and ΔS should not be derived from NMR data if enthalpy of the system is significantly temperature dependent. This dependence was shown for the dimeric system **4.3:4.4** with ITC experiments conducted at four different temperatures (Figure 4.11, this data is presented in the context of heat capacity discussed in Section 4.3.6).

Table 4.1 Summary of hetero-duplex binding data.^a

Complex ^b	K_a (T=298 K)	ΔG°	ΔH°	ΔS°	N value
4.1:4.2 (Mono-NMR)	3.0×10^2	-3.4	NA	NA	1 ^c
4.3:4.4 (Di-NMR)	7.5×10^3	-5.3	NA	NA	1 ^c
4.3:4.4 (Di-ITC)	7.6×10^3	-5.3	-10.4	-17.2	1.01
K_a (T=318 K)					
4.1:4.2 (Mono-NMR)	1.3×10^2	-3.1	NA	NA	1 ^c
4.3:4.4 (Di-NMR)	2.8×10^3	-5.0	NA	NA	1 ^c
4.3:4.4 (Di-ITC)	2.7×10^3	-5.0	-12.3	-23.0	0.91
4.5:4.6 (Tri-ITC)	4.5×10^4	-6.8	-17.7	-34.2	0.97
4.7:4.8 (Tetra-ITC)	3.5×10^5	-8.1	-19.3	-35.3	0.91

^a K_a (M⁻¹), ΔG° (kcal·mol⁻¹), ΔH° (kcal·mol⁻¹), ΔS° (cal·mol⁻¹·K⁻¹). Complete hetero-duplex binding data and experimental errors for the measured values of K_a , ΔH° , and N can be found in the experimental section. ΔG° and ΔS° were calculated from averaged K_a and ΔH° values, respectively. ^b Size of oligomers used and method of analysis in parentheses. ^c A binding stoichiometry of 1:1 was determined by inspection of Job plots. NA = Not applicable for NMR analysis (see text for explanation).

4.3.5 Summary of Binding Data

Results in Table 4.1 were gratifying for two main reasons. First, binding constants from separate analyses for the dimeric system (**4.3:4.4**) were in agreement. NMR indicated a $K_a^{(T=298K)} = 7,500 \text{ M}^{-1}$ and $K_a^{(T=318K)} = 2,800 \text{ M}^{-1}$ while ITC corroborated these numbers with a $K_a^{(T=298K)} = 7,600 \text{ M}^{-1}$ and $K_a^{(T=318K)} = 2,700 \text{ M}^{-1}$. Also, fitted curves point to discrete one-to-one binding (N values in Table 4.1). Raising the temperature 20 degrees K leads to more than a 50% decrease in association constants for the dimeric system. Even for the trimeric system at 298 K (whose data is just outside of the chi-square error window) the fitting analysis pointed to $K_a(\text{4.5:4.6})$ s above $10,000 \text{ M}^{-1}$ versus $45,000 \text{ M}^{-1}$ at

318 K. It would not be unreasonable to believe that with the proper design adjustments longer oligomer would give discrete hetero-duplexes at ambient conditions with much higher binding constants than those observed at elevated temperatures. Second, association improved with increasing chain length, with free energy (ΔG°) of duplex formation being roughly additive, with a change of -1.3 to -1.9 kcal·mol⁻¹ per additional aromatic unit. Though the increasingly favorable free energy with increasing length is promising, future design improvements are hoped to lead to “cooperative binding effects” (Ercolani 2003) with longer oligomers.

ITC clearly revealed that association was enthalpically favored with $\Delta H^\circ(T=318K)$ values ranging from -12 to -19 kcal·mol⁻¹. Though this data is irrefutable, any explanation as to why a process is enthalpically (and/or entropically) favored has to proceed with caution to avoid confusion.

Typically, favorable changes in solvent-solvent cohesion interactions (presumably an increase in hydrogen bonding in the case where water is the solvent) are ascribed to the favorable enthalpies seen with binding systems operating on desolvation (or the hydrophobic effect). In other words the solvent rather than the binding molecules (or solutes) is mainly responsible for the observed favorable enthalpies (once again in the cases with a strong hydrophobic driving force). The hydrophobic effect though should not automatically be synonymous with an “enthalpy-driven” process. Desolvation in fact has been implemented in entropically favored binding events where there is an entropy gain *by the solvent* since supposedly there is less solute surface required to be

solvated by highly ordered solvent molecules after an apolar binding event. A classic example would be micelle formation in water driven by the desolvation of apolar surfaces. After micelle formation, water is simply more disordered (solvation of more apolar areas means more ordered water molecules) hence this particular process is *entropically* favored. It is this situation most often attributed to the hydrophobic effect (Tanford 1980).

One could imagine that this scenario would also apply to the Iverson duplex system predicated on the hydrophobically-driven interaction between the Dan and Ndi units. ITC though indicated that *entropy was unfavorable* with $\Delta S^{\circ(T=318K)}$ values ranging from -23 to $-35 \text{ cal}\cdot\text{mol}^{-1}$. For comparison, Diederich and co-workers who have studied, in detail, aromatic ring inclusion by cyclophanes in water, have found similar favorable enthalpy values ranging from -8 to $-13 \text{ kcal}\cdot\text{mol}^{-1}$ and unfavorable entropy values ranging from -6 to $-22 \text{ cal}\cdot\text{mol}^{-1}\cdot\text{K}^{-1}$ depending on the nature of the aromatic guests used (Smithrud 1991). Diederich and co-workers characterized these apolar binding processes as being driven by hydrophobic bonding and proposed that the degrees of freedom lost by the bound molecules *masked any positive entropic benefit experienced by the solvent* due to the hydrophobic effect (Smithrud 1991). Therefore, there is no contradiction in stating that tight host-guest complexation in water, which is often observed to be enthalpically favored ($\Delta H^{\circ} \ll 0$, $T\Delta S^{\circ} < 0$) and “less tight” micelle formation, which is often entropically favored ($\Delta H^{\circ} \approx 0$, $T\Delta S^{\circ} > 0$) can *both* be considered hydrophobically-driven processes (Smithrud 1991). The larger entropic cost for the assembly of the Iverson duplexes as compared to the

Diederich cyclophane system is thus expected since the ordering of flexible strands into an entwined duplex likely results in more degrees of freedom lost than when cyclic hosts bind small molecule guests in general.

Returning to the evaluation of binding affinities, it was most satisfying to observe that the hetero-duplex **4.7:4.8** displayed an association constant of $350,000\text{ M}^{-1}$, three orders of magnitude larger than **4.1:4.2**, despite presumably larger charge repulsion between the longer chains. This result emphasizes the relatively strong driving force for duplex formation present in oligo-naphthyl systems. In fact, negative charge along the backbone of both oligomers may confer an important advantage over neutral strands. As is thought for DNA, intramolecular charge repulsion might keep oligomer chains “spread out” and more available to interact with a complementary chain (Benner 2002). Secondly, having like-charged strands, instead of complementary charged chains, kept the final hetero-duplex water-soluble as was required for NMR and ITC binding analysis.

4.3.6 Examination of Heat Capacity

To elucidate the underlying thermodynamic parameters of binding, **4.3:4.4** association was reexamined from $T = 288$ to 318 K (Figure 4.11) to obtain heat capacities. The change in the heat capacity, ΔC_p , ($\Delta C_p = \delta\Delta H^\circ / \delta T$) associated with binding is often reported for biological systems in order to determine the extent of hydrophobic driven recognition (Murphy 1999). There are still questions though whether heat capacity can be correlated accurately with the change in the amount of buried surface area for a binding event (Guinto 1996, Gill 1985).

Notwithstanding this debate, heat capacity still remains an important thermodynamic quantity to measure differences in solvent-solute interactions and can lead to insights into conformational changes of the binding partners (Murphy 1999).

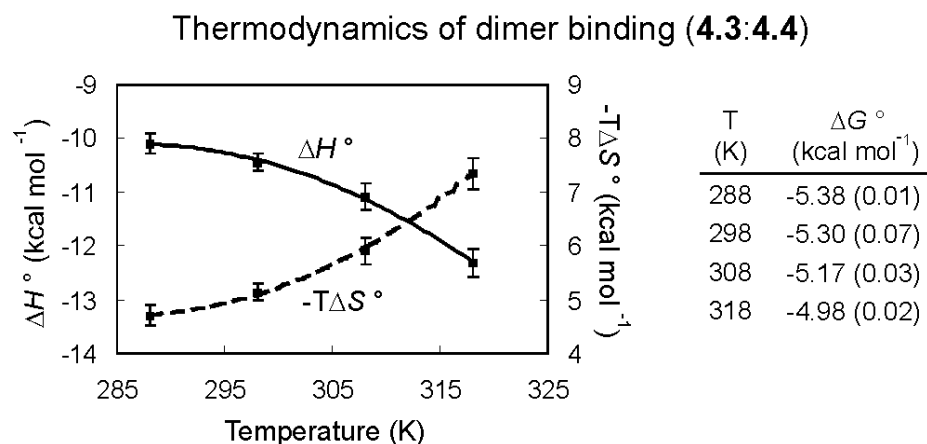


Figure 4.11 Graph of the thermodynamic parameters taken from ITC experiments of 4.3:4.4 binding and table of the corresponding free energies.

A change in heat capacity (ΔC_p) is typically reported in $\text{cal}\cdot\text{mol}^{-1}\cdot\text{K}^{-1}$ and is defined as the amount of heat required to increase the temperature of a substance (or solution) by 1 Kelvin. In essence, it represents a change in the way the solvent solvates the solute. Therefore, ΔC_p is a convenient term to compare not only other different binding systems, but also folding systems. A simple example is when a protein unfolds there is a positive change in the heat capacity. The same effect is seen when hydrophobic solutes are added to water; the observed ΔC_p is positive. The converse is true as well and protein folding,

protein-protein binding, and adding ionic solutes in water almost always afford negative ΔC_p values.

ITC experiments revealed a significant temperature dependence of enthalpy ΔH° (Figure 4.11) that is not linear thus precluding determination of a single ΔC_p value over the whole temperature range investigated (Gill 1985). Linear-fitting over narrower temperature ranges gives ΔC_p values between -50 (at lower temperature ranges) and $-95 \text{ cal}\cdot\text{mol}^{-1}\cdot\text{K}^{-1}$ (at higher ranges). Note, that this does not imply that the overall stability of the duplex is greater at elevated temperatures. It *could* indicate that there exists a larger difference in exposed surface area between unbound single strands and duplexes at higher temperatures versus lower temperatures. The Diederich studies with cyclophane hosts reported ΔC_p values up to $-130 \text{ cal}\cdot\text{mol}^{-1}\cdot\text{K}^{-1}$ for the binding of relatively polar guests (nitrophenol) and smaller negative values ($-20 \text{ cal}\cdot\text{mol}^{-1}\cdot\text{K}^{-1}$) for less polar guest such as *p*-xylene (Ferguson 1991, Smithrud 1991).

Finally, while evaluating data in the context of heat capacity determination, an apparent enthalpy-entropy compensation effect (Liu 2001) was observed with ΔG° values that decrease only slightly with increasing temperature (Figure 4.11). Another way of stating this is $\Delta\Delta G^\circ \approx 0$ while $\Delta\Delta H^\circ$ and $\Delta\Delta S^\circ$ were significant but compensatory. In Figure 4.11 the compensation occurred with one constant system (the dimeric system) studied at various temperatures. Often though the phenomenon of enthalpy-entropy compensation arises in studies that vary the system slightly, such as in the case of rigidification of ligands to possibly improve the entropic component of ligand-protein binding.

Explanations for this compensation have been debated. Some reports simply, and quite reasonably, state, “a stronger intermolecular interaction or bonding (related to enthalpy) will lead to a greater reduction of the configurational freedom...(Liu 2001)” The review written by Liu and Guo give other numerous explanations some choosing to focus on the thermodynamic parameters of the solvent rather than the interlocking molecules (Liu 2001). Counterpoints though exist in such articles entitled, “Entropy-enthalpy compensation: fact or artifact?” (Sharp 2001) and “Enthalpy-entropy compensation: a phantom phenomenon” (Cornish-Bowden 2002). Invariably, more studies will be reported supporting one explanation over the other, but hopefully a working knowledge of how to improve ΔG° of binding through molecular designs that favorably affect both enthalpy and entropy will also come forth from these investigations.

4.3.7 Size Exclusion Chromatography (SEC)

With binding constants and the thermodynamic profiles of hetero-duplex formation well in hand the following two analyses (size exclusion chromatography, SEC, and polyacrylamide gel electrophoresis, PAGE) were carried out to gain further insight as to the robustness of the complexes under other experimental conditions.

A 1:1 solution of **4.7:4.8** resulted in two separate signals when passed through a C18 reverse-phase column using the HPLC conditions that were used to purify naphthyl oligomers. The two signals corresponded to the retention times of pure **4.7** and pure **4.8** indicating that the putative tetrameric duplex did not survive

these conditions. In brief, the HPLC column separates oligomers by hydrophobic interactions with the packing material. Samples are usually loaded onto the column with predominantly water (>9:1 ratio of H₂O:CH₃CN). As the percentage of acetonitrile is increased the solvent (mobile phase) competes with the packing material (stationary phase) for interactions with the compound (duplex) and thus elutes the sample. Most likely the increase in organic solvent disrupts duplex formation. In pure water runs the compound did not migrate at all through the column and in isocratic runs (at a constant H₂O:CH₃CN composition) still only separation of chains was observed.

On the other hand, SEC runs (using a proprietary Bio-Sil column, Bio-Rad Inc., Hercules, CA 94547) afforded a different retention profile for a 1:1 mixture than both pure **4.7** and pure **4.8** (Figure 4.12). SEC, synonymous with gel filtration chromatography, separates compounds based on diffusion in and around highly porous silica beads. Retention is more dependent on the size and shape of the molecules rather than their hydrophobicity and charge, although these properties can play an important role. Since large molecules are sterically excluded and pass around the beads these molecules elute fastest (at lower retention volumes). SEC columns are usually more amenable than HPLC columns to isocratic runs ideal for separating proteins and nucleic acids that have molecular weights of 2,000-1,000,000 g·mol⁻¹.

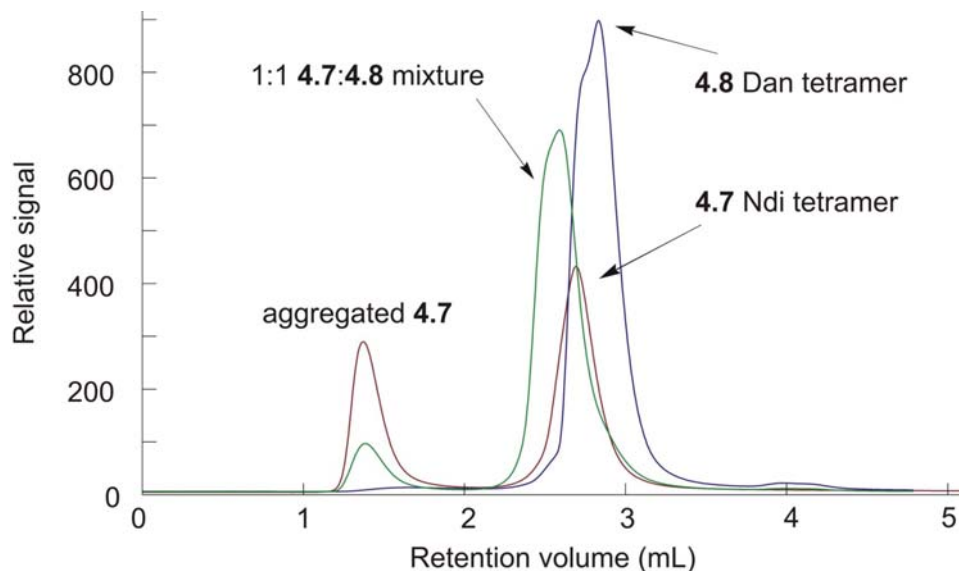


Figure 4.12 UV chromatograph (270 nm) showing that solutions of **4.7** are aggregated (at the SEC conditions) but are effectively broken up by the addition of **4.8** as seen by the trace give the 1:1 molar mixture. Also the 1:1 mixture results in a complex with a distinctly different retention volume than either strand.

Dr. Thomas Mourey from the Eastman Kodak Company (Rochester, NY 14650) performed all the SEC studies discussed with runs using Na phosphate buffered water. The chromatograph in Figure 4.12 indicated that **4.7** was aggregated (retention volume 1.4 mL). The **4.7** species at retention volume 2.7 mL was probably in the monomeric form considering that **4.8** showed no sign of forming large aggregates and its retention volume was similar at 3.0 mL. Most interestingly was that the addition of **4.8** to **4.7** appeared to significantly break up the **4.7** aggregates. It is important to remember that ITC analyses at $T = 318$ K were not hampered by aggregates. If aggregates under these ITC conditions were significant then reproducibility of measurements and curve-fitting to afford N

values near 1 molar equivalent definitely would have been problematic and substantial errors reported. With that being the case, aggregation was not prohibitive to the interpretation of SEC results.

The trace for the 1:1 mixture showed the appearance of one new signal with a lower retention volume (2.5 mL) than either **4.8** or **4.7**. This retention volume is consistent with a complex, larger than either strands, presumed to be a tetrameric **4.7:4.8** duplex. These encouraging SEC results will be evaluated along with the PAGE results presented next.

4.3.8 Polyacrylamide Gel Electrophoresis (PAGE)

Due to the physical similarity of the Iverson duplexes to DNA (both are multianionic unit-repeating duplexes formed by complementary strands containing aromatic units), PAGE was used to separate naphthyl oligomer species of different sizes analogous to DNA. PAGE, in practice, separates DNA pieces based on size (since charge density is constant regardless of length) with smaller strands migrating through the gel faster. For the naphthyl duplexes though it could be expected that the 1:1 complex, if stacked in a relatively compact fashion, might have a higher charge density than unbound single strands that are in a more extended conformation absent of Dan:Ndi stacking. Therefore the duplex, though more massive, may migrate farther than single chains due to a higher charge density.

Figure 4.13 shows both the tetrameric and trimeric system run on the same gel and visualized under a UV lamp after a Coomassie Blue stain/destain treatment (Sambrook 2001). Compounds were loaded in wells atop a vertical gel

(19:1 crosslinker ratio [acrylamide:bis], 20% w/v% acrylamide solution). The photograph in Figure 4.13 is of a 3 cm swath about two thirds of the way down from the top of the gel (height of gel = 11 cm). Each of the 12 lanes loaded with compound had visible bands. Concentrations of solutions in each lane are given (Figure 4.13). For instance Lane 1 was loaded with a solution of 0.4 mM **4.7** while Lane 2 was loaded with a 2:1 **4.7**:**4.8** solution with a final concentration of 0.4 mM **4.7** and 0.2 mM **4.8**.

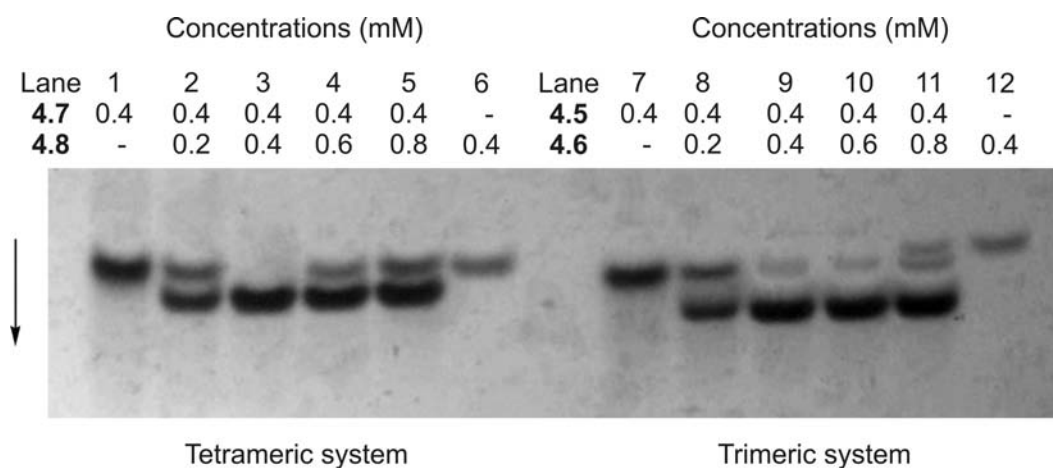


Figure 4.13 Photograph of gel from PAGE experiments. Arrow indicates direction of band migration.

For the trimeric system, Lanes 7-12 in Figure 4.13 indicated good complex formation when **4.5** and **4.6** were mixed. Lane 8, which contained a 2:1 ratio of **4.5**:**4.6**, had two bands one of which correlated with uncomplexed **4.5** (Lane 7) while the band below it was taken to be some type of complex. Lane 9 suggested that this complex was probably a duplex since the 1:1 molar mixture of Lane 9 resulted in essentially a single band with the same migration as the faster

migrating band in Lane 8. There was a bit of a shadow in Lane 9 indicating a band of single-stranded **4.5**, but it was a relatively tiny amount according to the intensity of the band. There should be a small amount of uncomplexed **4.6** as well, but probably this material was not visible since oligo-(Dan)s were observed to stain less intensely than oligo-(Ndi)s.

For the tetrameric system, Lanes 1-6 in Figure 4.13 indicated even better formation of a discrete 1:1 complex. Notice that a 1:1 molar mixture of **4.7** and **4.8** resulted in only one band (with no faint second band present). When one component was in slight excess as in Lane 2 and 4 the duplex still appeared to be formed with the seemingly complete exclusion of the excess strand that remained unbound. This exclusion underscored the high degree of chain discrimination with the tetrameric system and its ability to maintain a hetero-duplex formation in the presence of unbound naphthyl oligomers that one might think would be driven to hydrophobic collapse with the complex. Once again the highly negative charge surrounding the duplex may be fortuitous in this regard.

4.3.9 Discussion of SEC and PAGE Results

SEC data was consistent but not exclusive of a 1:1 complex forming. The absence of standards that are known to mimic the shapes of these proposed complexes makes conclusive sizing determination difficult. It is extremely unlikely though that 2:2, 3:3, and higher complexes with a ratio of 1:1 exists considering the retentions of pure samples of **4.7** and **4.8**.

PAGE studies were also quite persuasive supporting the formation of discrete hetero-duplexes and were successful on other fronts too. The detection of

unbound oligomers in mixtures containing a slight excess of one component was impressive. Even the band intensities seemed to fully support claims of the creation of a high-affinity duplex system. Notice that the duplex bands in lanes 3, 4, and 5 had similar intensities and theoretically under perfect 1:1 complexation the concentration of the duplex should be the same (0.4 mM). Lane 2, which would have a duplex concentration of 0.2 mM, had a duplex band with an intensity, judged by eye, of half that observed for Lanes 3, 4, and 5.

One feature of PAGE is the belief that there is a cage effect where once a complex enters the gel, the gel matrix forms a “cage”. If the complex then dissociates during the running of the gel the components have a better opportunity to rebind than if dissociation had taken place in solution. The opposite effect probably occurs during an HPLC run where once a duplex dissociates, rebinding actually is less likely as the strong resolving abilities of HPLC separates the chains even further. A consequence of the cage effect for gels is that the bands approximate the distribution of bound and unbound species present in solution just before PAGE is performed. Another advantage in using gels to analyze species distributions is that a typical experiment requires about a thousand times less material than NMR, ITC, or SEC.

Based on these results it is expected that both SEC and PAGE analyses will become standard procedures in the Iverson laboratory for characterizing the binding and self-assembly properties of naphthyl oligomers.

4.4 CHAPTER CONCLUSIONS

In general, this study is another example of the attractive designability of naphthyl oligomers due to the predictable association of Dan and Ndi moieties. Specifically, a first-generation duplex system, based on aromatic stacking, has been designed that forms discrete hetero-duplexes in aqueous solutions from complementary oligo-Dan and oligo-Ndi strands. The 1:1 association occurs with strong binding affinities and high chain discrimination according to ITC, SEC, and PAGE analyses. ITC indicated that this binding is enthalpically favored and entropically disfavored and the longer the chains the more stable the formed hetero-duplexes. Though the multi-anionic charge of the oligomers conferred water solubility and probably prevented intra-chain collapse, this investigation sparked ideas of new duplex designs to decrease putative inter-chain charge repulsion. ITC, SEC, and PAGE protocols optimized for the facile analysis of naphthyl oligomers have been devised for future work as well.

In summary, the observed discrimination ability and high affinity between like-charged chains of complementary aromatic donors and acceptors illustrated the potential of this approach for modulating molecular recognition in aqueous solution. This new approach is encouraging for future development of assemblies with highly programmable modes of binding in solution or on surfaces.

4.5 IDEAS FOR FUTURE INVESTIGATIONS

As mentioned before, hetero-duplexes with cooperative binding, triggered reversible binding, and self-sorting capabilities are current pursuits. To draw closer to these goals binding will need to be improved beyond that of the near-

micromolar affinities of these current naphthyl oligomer duplexes. Still, this system is extremely good considering it operates in aqueous solutions and with highly negatively charged strands. With this in mind, ideas for future work can be lumped into the following section.

New compounds for new analyses. The affinities of the tetrameric system place them outside the practical binding constant range for NMR analyses ($1\text{-}10^4\text{ M}^{-1}$). Maybe future systems invented by the Iverson group will exhibit affinities beyond the capabilities of ITC ($10^3\text{-}10^9\text{ M}^{-1}$). One priority, to reach ultra-high affinity duplexes, will be to pin down the true effects of charge repulsion. Unfortunately several oligomers containing positive charges were investigated without success due to possible intramolecular folding and seemingly non-specific aggregation. Another idea would be to synthesize water-soluble comb-architecture versions of the current duplex system. This comb-architecture appears to preorganize the single strand and on the surface, might lead to improved entropies of binding. Speaking of surfaces, biotinylated oligomers can be attached to a surface and be amenable to surface plasmon resonance (SPR) technology used to profile the thermodynamics and the kinetics of extremely strong binding events. Finally, with fluorescently labeled oligomers, fluorescence-activated cell sorting (FACS) could potentially be used for binding affinity studies.

As can be seen many options are available and it would be very interesting to see what research directly falls from this first study dealing with hetero-duplexes formed via directed aromatic interactions. Already, preliminary results

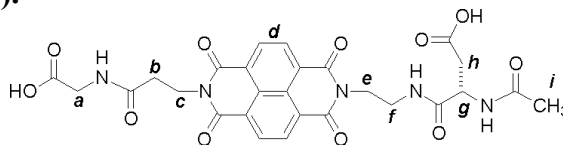
from offshoots of this project dealing with protein-naphthyl oligomer binding (mentioned in Chapter 2) and the assembly of polymers have been intriguing.

4.6 EXPERIMENTAL SECTION

Synthesis. General methods, full protocols for solid phase peptide synthesis and FPLC/HPLC purification used for compounds **4.1-4.8** were detailed in chapter 2. Synthesis, followed by purification, desalting, and freeze-drying afforded soft solids for all compounds.

Compound characterization (1D-NMR general methods). Samples were readily soluble in 50 mM sodium phosphate, pH = 7.0 D₂O. Spectra of monomers were obtained on a Varian UNITY+ 300 MHz spectrometer. Spectra of oligomers were recorded on a Varian INOVA 500 MHz spectrometer at 1 mM concentrations of compound and TSP-*d*₄ (3-trimethylsilyl-propionic-2,2,3,3-*d*₄ acid, sodium salt) was used as a reference (δ = 0.00 ppm). Chemical shifts reported in ppm and abbreviations used are singlet (s), doublet (d), doublet of doublet (dd), triplet (t), quartet (q), multiplet (m) and complex multiplet of non-equivalent protons (comp). Coupling constants (*J*) reported in Hz.

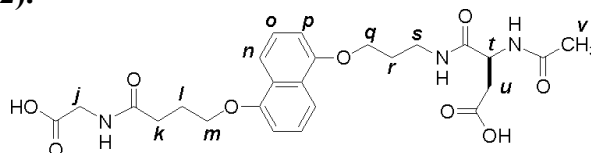
“Ndi monomer” (4.1).



3-acetylamin-*N*-(2,{7-[2-(carboxymethyl-carbamoyl)-ethyl]-[1,3,6,8-tetraoxo-3,6,7,8-tetrahydro-1*H*-benzo[*lmn*][3,8]phenanthrolin-2-yl}]-ethyl)-succinamic acid (4.1). (SPPS yield = 94%). $\epsilon_{(w/o \text{ CTAB})}$ 24700 M⁻¹·cm⁻¹ at λ_{max} 384 nm; $\epsilon_{(w/ \text{ CTAB})}$ 23900 M⁻¹·cm⁻¹ at λ_{max} 382 nm; no hypochromism at 382 nm; ¹H

NMR (300 MHz, D₂O) δ = 8.56 (AA'BB' q, J = 7.6, 5.6, 4H *d*), 4.43 (t, J = 7.1, 2H *c*), 4.36 (dd, J = 4.8, 4.4, 1H *g*), 4.30 (m, 2H *f*), 3.73 (s, 2H *a*), 3.61 (t, J = 5.7, 2H *e*), 2.74 (t, J = 7.1, 2H *b*), 2.45 (dd, J = 4.8, 11.2, 1H *h*), 2.33 (dd, J = 9.2, 6.8, 1H *h*), 1.86 (s, 3H *i*); ¹³C NMR (300 MHz, D₂O) δ = 177.4, 176.4, 173.9, 173.6, 173.2, 163.9, 163.7, 131.1, 131.0, 125.9, 125.8, 125.6, 51.6, 42.3, 39.6, 38.6, 37.3, 33.9, 21.6; CI HRMS calcd for C₂₇H₂₆N₅O₁₁ [MH]⁺ 596.163, found 596.163.

“Dan monomer” (4.2).



3-acetylamino-*N*-(3-{5-[3-(carboxymethyl-carbamoyl)-propoxy]-naphthalen-1-yloxy}-propyl)-succinamic acid (4.2). (91% yield). $\epsilon_{(w/o \text{ CTAB})}$ 8100 M⁻¹·cm⁻¹ at λ_{max} 296 nm; $\epsilon_{(w/ \text{ CTAB})}$ 7900 M⁻¹·cm⁻¹ at λ_{max} 298 nm; no hypochromism at 298 nm; ¹H NMR (300 MHz, D₂O) δ = 7.88 (d, J = 8.4, 1H *n*), 7.84 (d, J = 8.6, 1H *n*), 7.50 (m, 2H *o*), 7.07 (t, J = 7.6, 2H *p*), 4.47 (dd, J = 5.2, 3.4, 1H *t*), 4.29-4.25 (comp, 4H *m* and *q*), 3.69 (s, 2H *j*), 3.50 (t, J = 6.7, 2H *s*), 2.60 (dd, J = 5.2, 7.8, 1H *u*), 2.58 (t, J = 7.0, 2H *k*), 2.50 (dd, J = 8.6, 7.4, 1H *u*), 2.24 (m, J = 6.2, 2H *l*), 2.13 (m, J = 6.1 2H *r*), 1.89 (s, 3H *v*); ¹³C NMR (300 MHz, D₂O) δ = 178.2, 176.5, 174.6, 174.2, 154.5, 126.7, 126.6, 114.8, 114.6, 107.7, 107.3, 52.7, 47.1, 43.9, 39.5, 37.2, 33.6, 28.6, 25.4, 22.3; CI HRMS calcd for C₂₅H₃₂N₃O₉ [MH]⁺ 518.214, found 518.213.

HO-Gly(NdiAsp)₂-NHAc “Ndi dimer” (4.3). (88% yield). $\epsilon_{(w/o \text{ CTAB})}$ 37000 M⁻¹·cm⁻¹ at λ_{max} 364 nm; $\epsilon_{(w/ \text{ CTAB})}$ 53000 M⁻¹·cm⁻¹ at λ_{max} 382 nm; hypochromism ~ 39% at 382 nm; ¹H NMR (500 MHz, D₂O) δ = 8.58 (AA'BB' q, J = 5.1, 2.6,

4H), 8.39 (AA'BB' q, $J = 14.1, 7.9$, 4H), 4.69 (dd, $J = 5.3$ and 3.2 , 1H), 4.47-4.31 (comp, 3H), 4.12 (t, $J = 7.5$, 2H), 4.07-4.01 (m, 2H), 3.90-3.84 (m, 2H), 3.79-3.72 (m, 2H), 3.67 (s, 2H), 3.66 (t, $J = 6.2$, 2H), 3.57 (dd, $J = 9.5$ and 6.4 , 1H), 2.74 (dd, $J = 11.7, 5.1$, 1H), 2.68-2.44 (comp, 6H), 1.88 (s, 3H); ESI MS calcd for $C_{50}H_{44}N_5O_{15}$ $[MH]^+$ 1074.3, found 1074.3.

HO-Gly(DanAsp)₂-NHAc “Dan dimer” (4.4). (79% yield). $\epsilon_{(w/o \text{ CTAB})}$ 18700 $M^{-1} \cdot cm^{-1}$ at λ_{max} 298 nm; $\epsilon_{(w/ \text{ CTAB})}$ 19300 $M^{-1} \cdot cm^{-1}$ at λ_{max} 298 nm; no hypochromism at 298 nm; 1H NMR (500 MHz, D_2O) $\delta = 7.73$ -7.67 (m, 3H), 7.61 (d, $J = 8.4$), 7.40-7.33 (m, 3H), 7.29 (d, $J = 8.1$), 6.90 (d, $J = 7.6$, 1H), 6.85 (d, $J = 7.6$, 2H), 6.73 (d, $J = 7.6$, 1H), 4.58 (t, $J = 6.4$, 1H), 4.48 (dd, $J = 5.2, 3.5$, 1H), 4.07-3.76 (comp, 8H), 3.68 (s, 2H), 3.35 (t, $J = 6.7$, 2H), 3.27-3.23 (m, 1H), 2.97-2.92 (m, 1H), 2.64-2.40 (comp, 6H), 2.35-2.06 (comp, 4H), 2.00-1.85 (comp, 3H), 1.91 (s, 3H), 1.84-1.75 (m, 3H); ESI MS calcd for $C_{46}H_{56}N_5O_{15}$ $[MH]^+$ 918.4, found 918.4.

HO-Gly(NdiAsp)₃-NHAc “Ndi trimer” (4.5). (78% yield). $\epsilon_{(w/o \text{ CTAB})}$ 52800 $M^{-1} \cdot cm^{-1}$ at λ_{max} 364 nm; $\epsilon_{(w/ \text{ CTAB})}$ 79100 $M^{-1} \cdot cm^{-1}$ at λ_{max} 382 nm; hypochromism $\sim 41\%$ at 382 nm; 1H NMR (500 MHz, D_2O) $\delta = 8.59$ (d, $J = 7.7$, 2H), 8.47 (d, $J = 7.5$, 2H), 8.38-8.34 (comp, 6H), 8.29 (d, $J = 7.7$, 2H), 4.56-4.51 (m, 2H), 4.39-4.30 (comp, 3H), 4.25-4.18 (comp, 6H), 4.10 (t, $J = 6.3$, 2H), 3.99 (t, $J = 6.9$, 2H), 3.78 (m, 1H), 3.73 (s, 2H), 3.68-3.64 (m, 2H), 3.56 (t, $J = 5.9$, 3H), 2.68-2.43 (comp, 10H), 2.35 (d, $J = 9.0$, 1H), 2.31 (d, $J = 9.0$, 1H), 1.87 (s, 3H); ESI MS calcd for $C_{73}H_{62}N_{13}O_{27}$ $[MH]^+$ 1552.4, found 1552.4.

HO-Gly(DanAsp)₃-NHAc “Dan trimer” (4.6). (70% yield). $\epsilon_{(w/o \text{ CTAB})}$ 21400 M⁻¹·cm⁻¹ at λ_{max} 298 nm; $\epsilon_{(w/ \text{ CTAB})}$ 22900 M⁻¹·cm⁻¹ at λ_{max} 298 nm; no hypochromism at 298 nm; ¹H NMR (500 MHz, D₂O) δ = 7.61-7.55 (m, 6H), 7.23-7.13 (m, 6H), 6.73-6.63 (m, 4H), 6.53 (d, J = 7.7, 2H), 4.59 (t, J = 6.4, 2H), 4.48 (dd, J = 5.1, 3.8, 1H), 3.90-3.67 (comp, 12H), 3.65 (s, 2H), 3.25 (t, J = 6.2, 2H), 3.20-3.08 (m, 2H), 2.93-2.84 (m, 2H), 2.67-2.44 (m, 6H), 2.35-2.22 (m, 6H), 2.01-1.84 (comp, 8H), 1.90 (s, 3H), 1.68-1.62 (m, 4H); ESI MS calcd for C₆₇H₈₀N₇O₂₁ [MH]⁺ 1318.5, found 1318.6.

HO-Gly(NdiAsp)₄-NHAc “Ndi tetramer” (4.7). (69% yield). $\epsilon_{(w/o \text{ CTAB})}$ 63800 M⁻¹·cm⁻¹ at λ_{max} 366 nm; $\epsilon_{(w/ \text{ CTAB})}$ 113100 M⁻¹·cm⁻¹ at λ_{max} 382 nm; hypochromism ~ 50% at 382 nm; ¹H NMR (500 MHz, D₂O) δ = 8.51-8.37 (comp, 14H), 8.21 (d, J = 6.9, 2H), 4.56-4.50 (m, 2H), 4.41-4.01 (comp, 18H), 3.74-3.52 (comp, 8H), 3.76 (s, 2H), 2.68-2.43 (comp, 14H), 2.33 (d, J = 9.3, 1H), 2.30 (d, J = 9.2, 1H), 1.87 (s, 3H); ESI MS (neg mode) calcd for C₉₆H₇₇N₁₇O₃₅ [M]²⁻ 1014.4 (m/z), found 1014.4.

HO-Gly(DanAsp)₄-NHAc “Dan tetramer” (4.8). (58% yield). $\epsilon_{(w/o \text{ CTAB})}$ 30000 M⁻¹·cm⁻¹ at λ_{max} 298 nm; $\epsilon_{(w/ \text{ CTAB})}$ 32600 M⁻¹·cm⁻¹ at λ_{max} 298 nm; no hypochromism at 298 nm; ¹H NMR (500 MHz, D₂O) δ = 7.59 (d, J = 8.7, 4H), 7.55-7.53 (m, 4H), 7.24-7.22 (m, 4H), 7.12 (t, J = 8.2, 4H), 6.72 (d, J = 8.3, 2H), 6.67-6.65 (m, 3H), 6.52 (t, J = 7.2, 3H), 4.58 (t, J = 7.4, 3H), 4.48, (dd, J = 5.1, 4.5, 1H), 3.99-3.69 (comp, 16H), 3.64 (s, 2H), 3.24 (t, J = 6.4, 2H), 3.17-3.06 (m, 3H), 2.92-2.75 (m, 3H), 2.66-2.43 (m, 8H), 2.34-2.33 (m, 8H), 2.01-1.83 (comp,

10H), 1.89 (s, 3H), 1.68-1.58 (m, 6H); ESI MS (neg mode) calcd for $C_{88}H_{102}N_9O_{27} [M]^-$ 1716.7, found 1716.6.

NMR analysis. Stock solutions were prepared using 50 mM sodium phosphate pH = 7.0 D_2O with TSP- d_4 as a 0.0 ppm reference (Previous experiments showed no indication that trace amounts of TSP affected the stacking of aromatic units.) Concentrations were confirmed by extinction coefficients. A microanalytical syringe was used to transfer aliquots to dry NMR tubes. For both Job plot and titration experiments, at least 7 samples of varying ratios were made. All NMR samples contained a minimum amount of solution (0.75 mL) to avoid excessive convection effects, which were initially problematic at $T = 318$ K and all NMR spectra were acquired on a 300 MHz Varian spectrometer. Chemical shift data is provided in Table 4.2.

Table 4.2. NMR data for Job plots and titrations.

Chemical shift, δ (ppm), data for Job plots ^(T=298 K) . $[4.1] + [4.2] = [4.3] + [4.4] = 0.375$ mM							
Sample	[4.1]	[4.2]	δ of 4.1	Sample	[4.3]	[4.4]	δ of 4.3
1	0.375	0	8.748	8	0.375	0	8.600
2	0.300	0.075	8.745	9	0.300	0.075	8.511
3	0.250	0.125	8.743	10	0.250	0.125	8.428
4	0.188	0.188	8.740	11	0.188	0.188	8.305
5	0.125	0.250	8.737	12	0.125	0.250	8.231
6	0.075	0.300	8.735	13	0.075	0.300	8.184
7	0.042	0.333	8.732	14	0.042	0.333	8.163

Chemical shift, δ (ppm), data for titration curves. $[4.1] = [4.3] = 0.375$ mM for all samples							
Sample	[4.2]	δ of 4.1 ^(T=298 K)	^(T=318 K)	Sample	[4.4]	δ of 4.3 ^(T=298 K)	^(T=318 K)
15	0	8.748	8.764	22	0	8.600	8.598
16	0.094	8.738	8.759	23	0.094	8.501	8.537
17	0.188	8.727	8.753	24	0.188	8.408	8.478
18	0.375	8.708	8.741	25	0.375	8.255	8.393
19	0.750	8.671	8.719	26	0.750	8.144	8.287
20	1.500	8.615	8.684	27	1.500	8.080	8.200
21	3.000	8.544	8.624	28	3.000	8.026	8.133

For Job plots, stock solutions of **4.1-4.4** (0.375 mM) were prepared and mixed in various ratios so that $[4.1] + [4.2] = [4.3] + [4.4] = 0.375$ mM. The most upfield chemical shift of the Ndi unit for each of the 7 samples was tracked.

For NMR titrations, the concentration of the Ndi containing compound for each sample was held constant at 0.375 mM while the concentration of the Dan containing compound ranged from 0.0 mM to 3 mM (0 to 8 molar equivalents). Data was analyzed using the HOSTEST curve fitting program (v5.60) developed

by Glagovich and Wilcox at the University of Pittsburgh, Pittsburgh, PA. The HOSTEST program can apply a number of different models to the chemical shift data. The reported association constants were obtained using a 1:1 binding model as in previous studies (Cubberley 2000). Standard deviations of the association constants, K_a , calculated by the HOSTEST program were reasonable and R^2 for the fitted curves, for all experiments, exceeded a 0.999 value. Examples of the program outputs are in Figure 4.14 (binding between monomers) and 4.15 (between dimers).

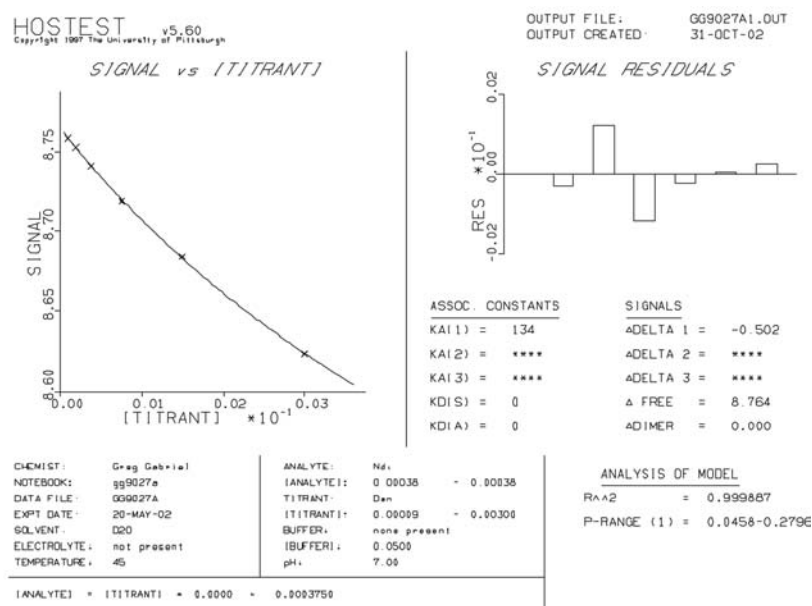


Figure 4.14 Representative HOSTEST output for (4.1:4.2) binding at T = 318 K.

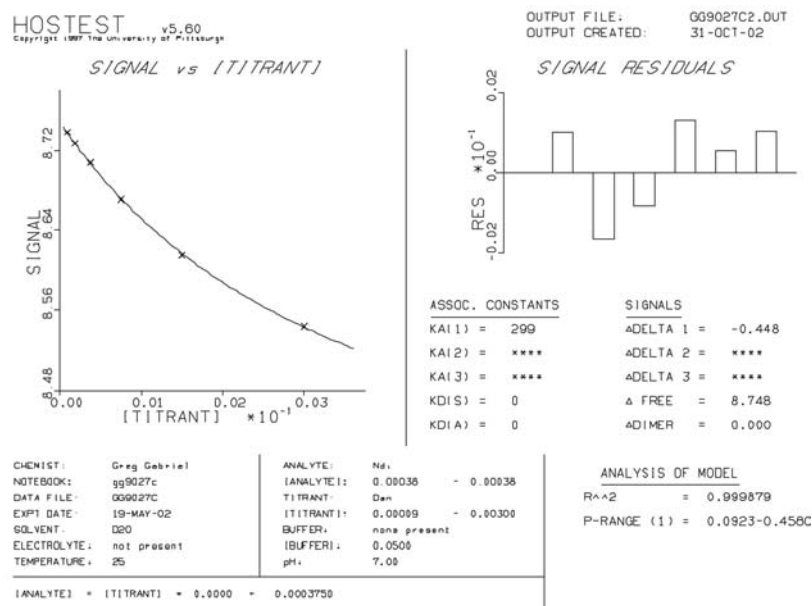


Figure 4.16 Representative HOSTEST output for (4.3:4.4) binding at T = 318 K.

ITC. Experiments were performed on a VP-ITC microcalorimeter from Microcal Inc. (Northhampton, MA 01060) and followed the experimental setups detailed in literature (Wiseman 1998). Three trials were performed for each system. Complete binding data is shown in Table 4.3. All solutions were made in 50 mM sodium phosphate buffer and degassed for 15 minutes and stock solution concentrations were confirmed by extinction coefficients. For a typical experimental run a solution of the Ndi containing compound was placed in the instrument chamber at a relatively dilute concentration (4.3, 0.375 mM; 4.5, 0.250 mM; 4.7, 0.188 mM). Relatively concentrated solutions of the Dan containing compound were taken up in the 250 μ L injection syringe (4.4, 3.21 mM; 4.6, 2.11 mM; 4.8, 1.59 mM). After a 10 minute equilibration time injections were started

with the first being 2.0 μL and the next 39 being 6.3 μL with 5 minutes between each injection. After the final injection the molar ratio ($[\text{oligo-Dan}] / [\text{oligo-Ndi}]$) reached greater than 1.5 and this was sufficient for analysis by the *ORIGIN* software provided with the ITC instrument. Each experiment was performed three times and the first data point (injection # 1) of each trial was not considered in the analyses. Also for each experiment, blanks were run where oligo-Dan was injected into buffer and buffer was injected into oligo-Ndi. Although heats of dilution were near zero these were still subtracted from raw titration data to account for any slight heat effects from dilution. Integrated data from titration runs were fit using a single site model with K_a , ΔH° allowed to vary. The stoichiometry of binding (N) was not assumed and this value was allowed to vary as well during the fitting process. In all cases N indicated 1:1 binding with values within 10 % of 1.00. The c value, as defined in the Wiseman article, fell within the acceptable range for the determination of accurate binding constants (Wiseman 1998). As mentioned before the monomeric system (4.1:4.2) could not be analyzed by ITC due to sensitivity limits. The c value dictated that concentrations needed to be prohibitively high to achieve an acceptable signal to noise ratio for heat measured.

Table 4.3. Complete hetero-duplex binding data.^a

Complex	T	Conc ^d	K _a	N value ^e	ΔG°	ΔH°	ΔS°
4.1:4.2 ^b	318	0.375	1.3 (0.1) × 10 ²	1	-3.2 (0.01)	NA	NA
4.3:4.4 ^b	318	0.750	2.8 (0.3) × 10 ³	1	-5.1 (0.02)	NA	NA
4.3:4.4 ^c	318	0.750	2.7 (0.1) × 10 ³	0.91 (0.01)	-5.0 (0.02)	-12.3 (0.3)	-23.0 (0.9)
4.5:4.6 ^c	318	0.750	4.5 (0.1) × 10 ⁴	0.97 (0.02)	-6.8 (0.02)	-17.7 (0.1)	-34.2 (0.3)
4.7:4.8 ^c	318	0.750	3.5 (0.1) × 10 ⁵	0.91 (0.01)	-8.1 (0.03)	-19.3 (0.2)	-35.3 (0.6)
4.1:4.2 ^b	298	0.375	3.0 (0.1) × 10 ²	1	-3.2 (0.02)	NA	NA
4.3:4.4 ^b	298	0.750	7.5 (0.5) × 10 ³	1	-5.3 (0.03)	NA	NA
4.3:4.4 ^c	288	0.750	1.2 (0.1) × 10 ⁴	0.98 (0.01)	-5.4 (0.01)	-10.1 (0.2)	-16.4 (0.6)
4.3:4.4 ^c	298	0.750	7.6 (0.1) × 10 ³	1.01 (0.04)	-5.3 (0.07)	-10.4 (0.2)	-17.2 (0.5)
4.3:4.4 ^c	308	0.750	4.7 (0.1) × 10 ³	0.99 (0.01)	-5.2 (0.03)	-11.1 (0.2)	-19.2 (0.1)

^a Units are T (K), K_a (M⁻¹), ΔG° (kcal·mol⁻¹), ΔH° (kcal·mol⁻¹), ΔS° (cal·mol⁻¹·K⁻¹). For NMR data, errors represent standard deviations calculated by the *HOSTEST* program (Wilcox 1997). For ITC data, errors represent the standard deviation of three trials. ^b Analyzed by NMR. ^c Analyzed by ITC. ^d This is the initial concentration (mM), pre-titration, of the Ndi *unit* as oppose to the concentration of the Ndi containing compound. ^e For titrations analyzed by NMR, a binding stoichiometry of 1:1 was determined by inspection of Job plots. For ITC analysis the N values represents the best fit stoichiometry of binding (oligo-Dan:oligo-Ndi ration) calculated by the *ORIGIN* software (Microcal, Inc. 1999). NA = Not Applicable since 1:1 fitting model was used and goodness of fit was used to judge accuracy of calculated binding constants. NA = Not applicable. ΔH° and ΔS° derived from the van't Hoff equation is not applicable since enthalpy for our system was shown to be significantly temperature dependent. (Naghibi 1995).

Figures 4.17-4.22 are representative isotherms showing additional important ITC data collected during these studies. These are meant to give a general idea of the curve shapes, trends, chi-square values, and thermodynamic quantities for these oligomers and may provide a helpful reference as to the magnitude of heats absorbed or evolved that one could expect when studying future naphthyl oligomers.

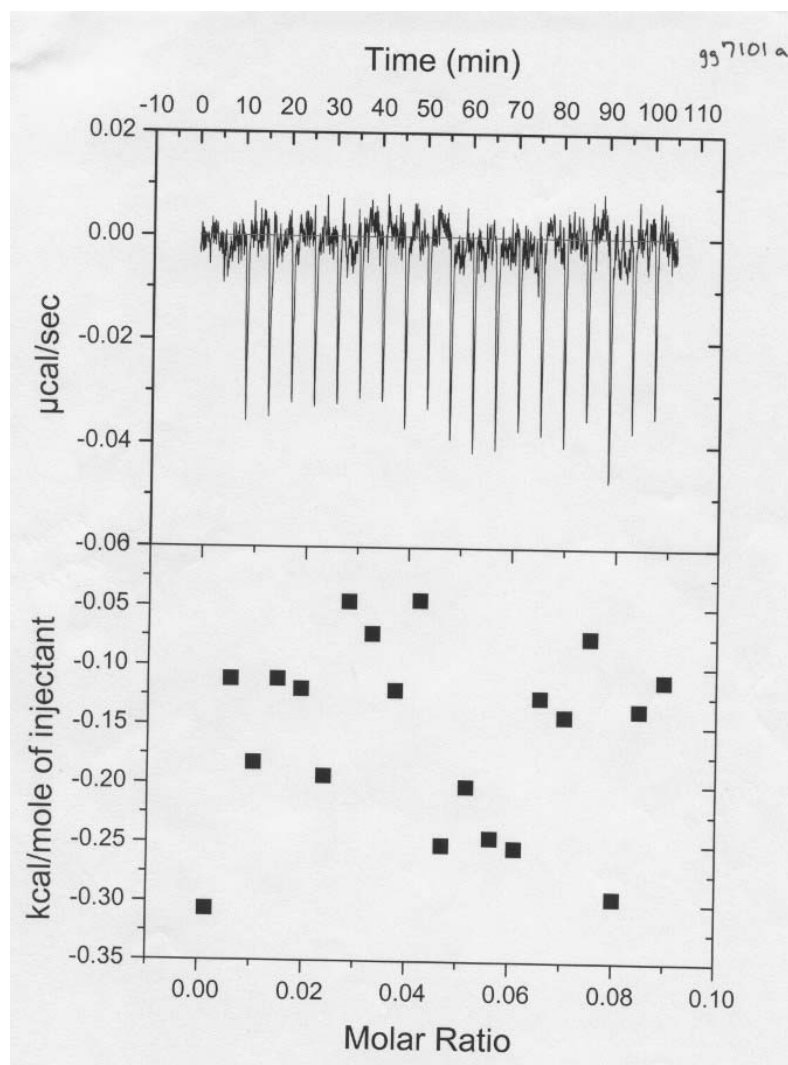


Figure 4.16 Typical buffer into buffer titration that results in extremely small heats (0.05-0.30 kcal/mole) released per injection. For comparison the first couple of injections (same volume) in a tetramer run released 20 kcal/mole of heat.

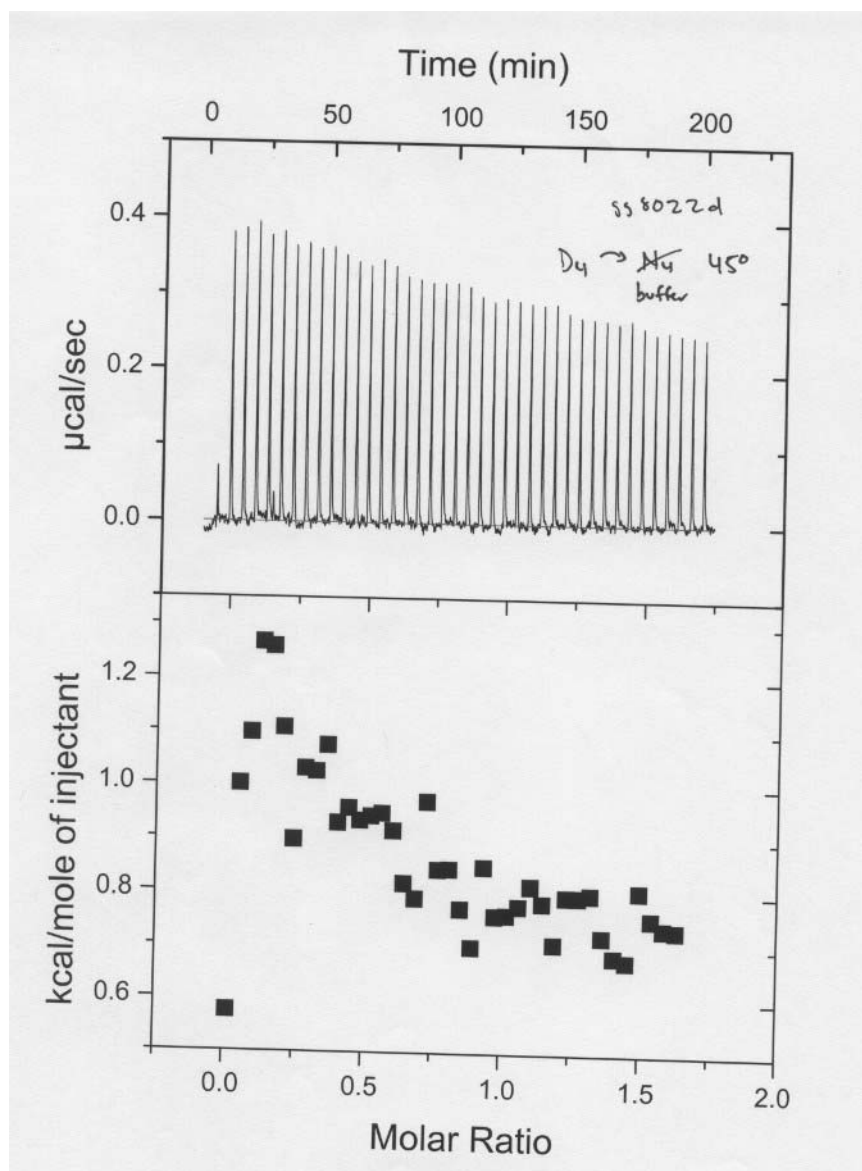


Figure 4.17 Typical tetra-Dan injections into buffer. The small heats absorbed were taken into account when processing the tetramer runs where tetra-Dan **4.8** was injected into tetra-Ndi **4.7**. For all ITC data reported, heats of dilutions were subtracted from the titration runs to afford the heats associated with binding.

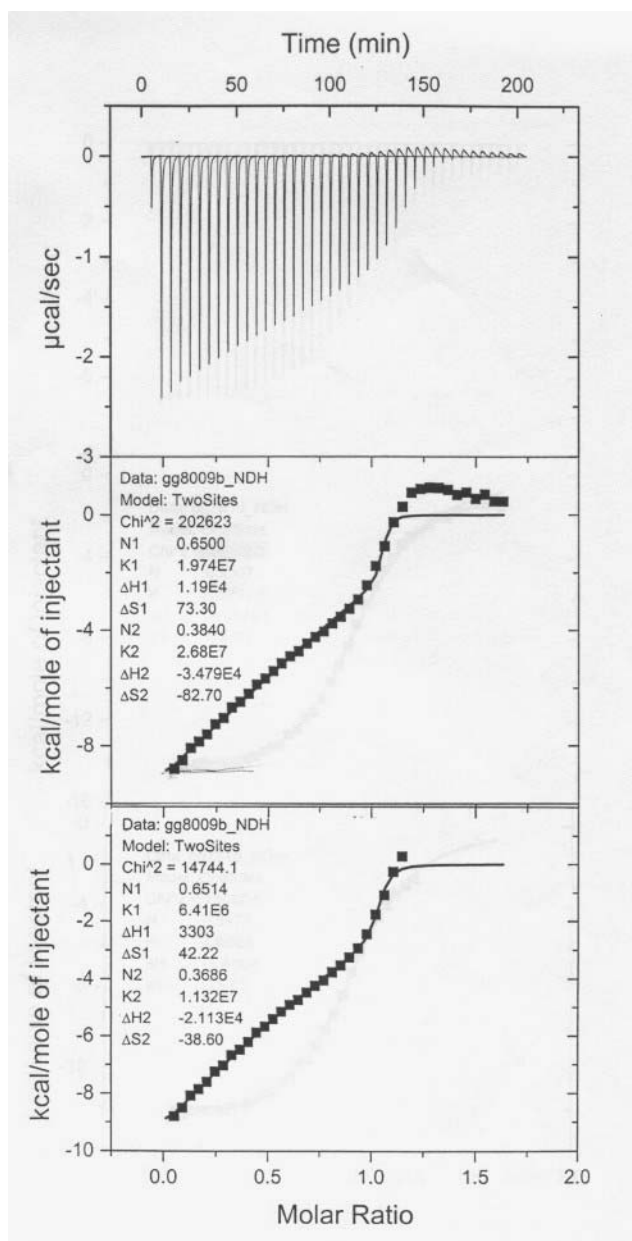


Figure 4.18 Unsuccessful reverse titration at $T = 298\text{ K}$ where tetra-Ndi **4.7** was injected into tetra-Dan **4.8**. Even a two-sites binding model could not accurately describe the experimental data. All reported ITC data used a one-site binding model where the N value was allowed to vary.

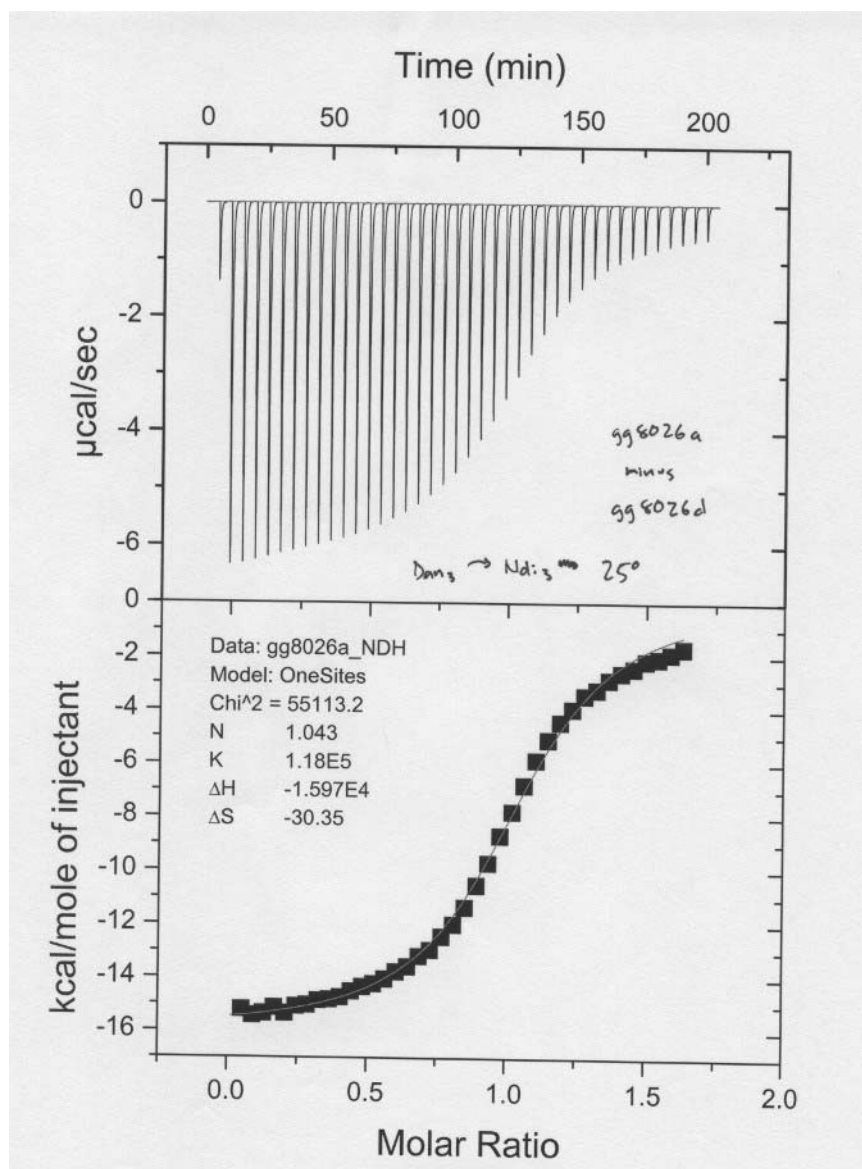


Figure 4.19 A representative trimeric system run at $T = 298$ K. Though the chi-square value is 55,000 the fit appeared to be fairly accurate. On average the $K_a(4.5:4.6)$ was $1.1 \times 10^5 \text{ M}^{-1}$ for the trimeric system at $T = 298$ K, more than twice as large as that measured at $T = 318$ K.

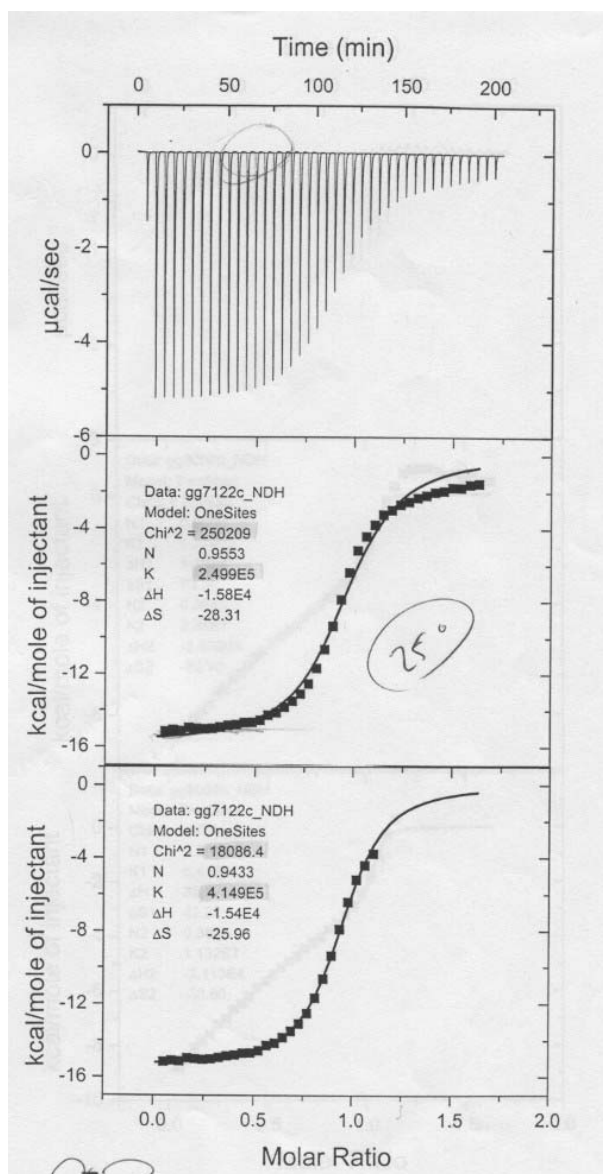


Figure 4.20 A tetrameric system run at $T = 298\text{ K}$. A chi-square value of 250,000 indicated an inability to describe the binding with a one sites model. Only about three-fourths of the curve fit the model possibly indicating a switch in binding stoichiometry at excess titrant (tetra-Dan 4.8) at room temperature.

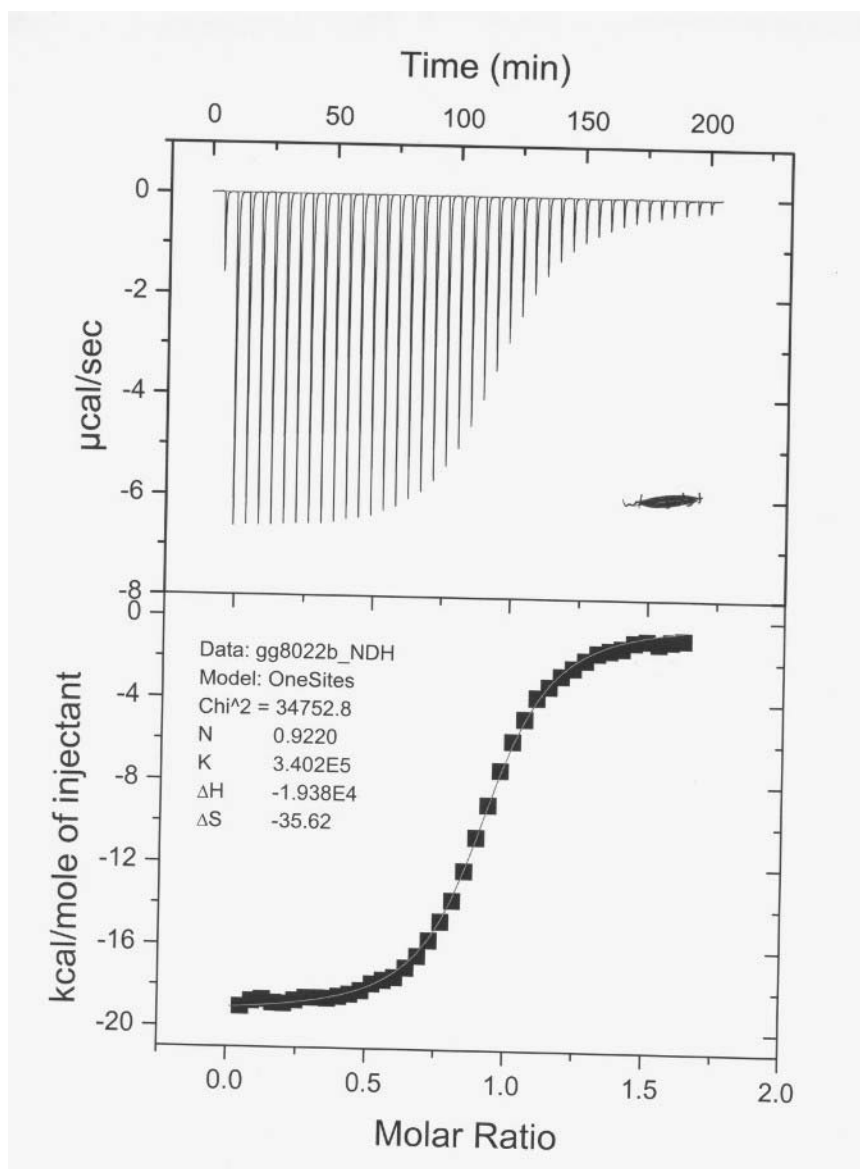


Figure 4.21 Representative isotherm that afforded excellent results for the tetrameric system ($T = 318\text{ K}$). Notice the chi-square value was below 50,000 and the N value was within a 10% error of 1.0.

SEC. All of the SEC runs were performed by Dr. Thomas Mourey from the Eastman Kodak Company (Rochester, NY 14650). Initially, samples of tetraNdi, **4.7**, were tested on glycerol propyl bonded-phase Synchropak columns (4000, 1000, 500 and 100 Angstrom pore size). Though this type of column is silica-based and usually works well for small anionic polymers, samples did not elute after 3 injections. A 60 Angstrom 7.8 x 80 mm Bio-Sil guard column (just the guard column) was ultimately chosen for SEC runs, which provided minimal size separation but near complete sample elution. UV (270 nm) and light scattering (90 degrees) were used for detection. Injections were 0.22 mM in concentration for each strand and mixtures were heated at 60 °C for 15 minutes and injected 10 minutes later.

Additional chromatographs (with figure captions by Dr. Mourey) is included here for future reference should SEC become a standard analytical tool in the investigations of water-soluble naphthyl oligomers and possibly polymers. The author thanks his labmate, Joseph Reczek for initiating the correspondence with Dr. Mourey. In the following chromatographs compound 4a = tetraNdi **4.7** and 4b = tetraDan **4.8**.

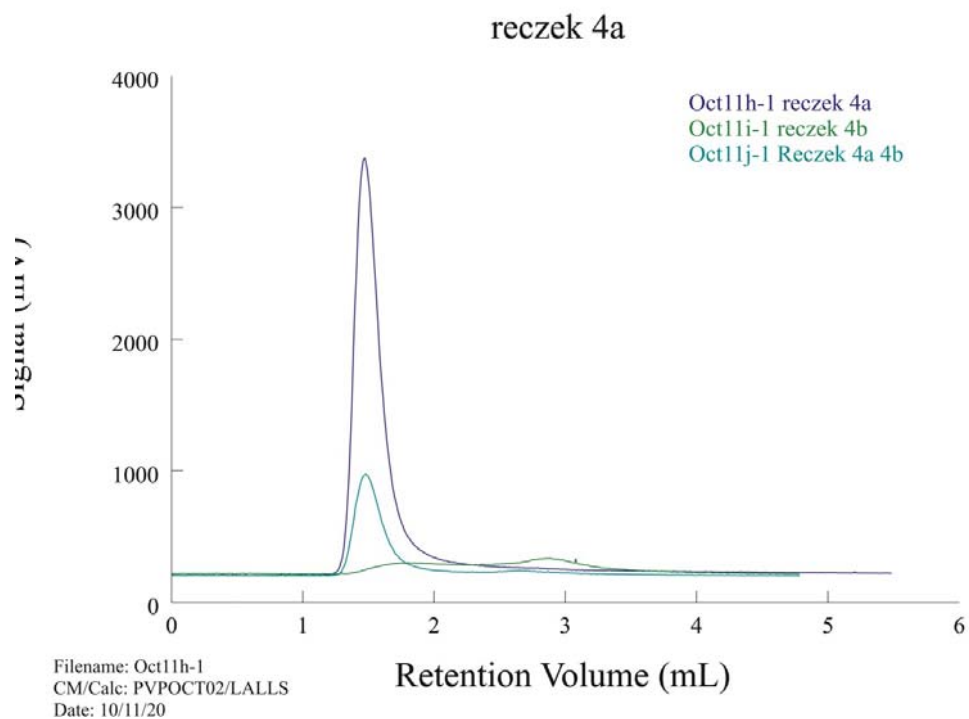


Figure 4.22 90 degree light scattering chromatograms of individual components and 1:1 molar mixture. Note that the intensity of the aggregate peak (1.5 mL) for the 1:1 mixture is less than half that of sample 4A, implying that some of the aggregates are broken during complex formation.

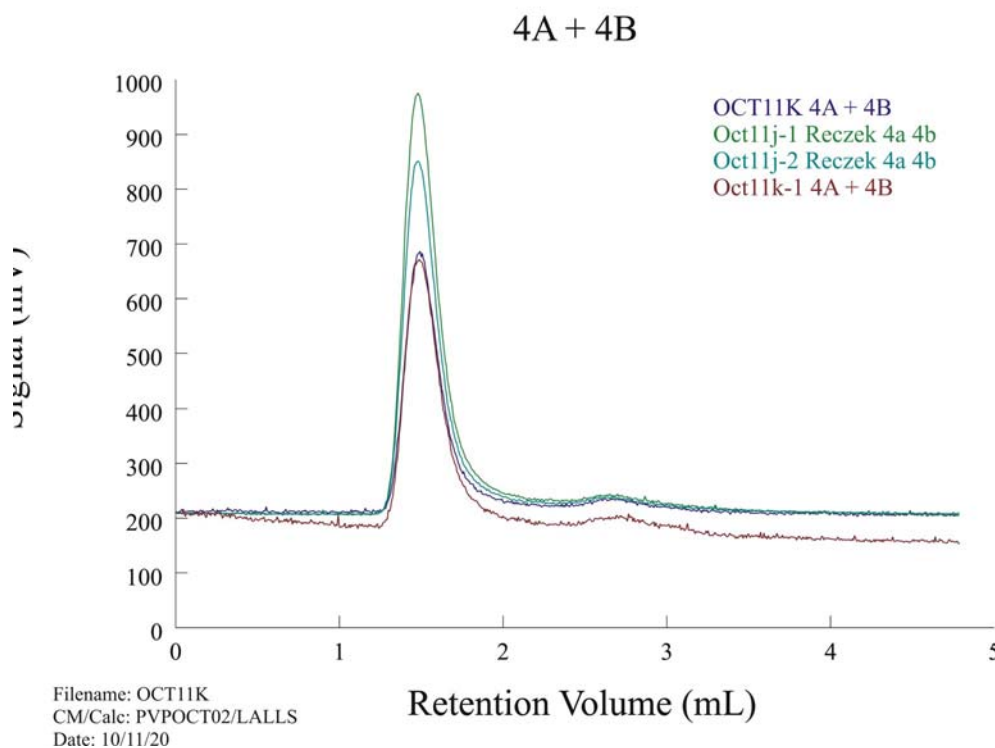


Figure 4.23 90 degree light scattering chromatograms of 1:1 molar complex 10 minutes after preparation (15 minute of heating, 60°C) (green), 24 min (cyan), 79 min (red), 93 min (blue). The peak at 1.5 mL is attributed to aggregates; peak at 2.7 mL is from the complex. (Author's comments – magnitude of 90 degree light scattered is dependent on size of aggregate or complex. See Figure 4.12 for a better quantitative idea of the amount of presumed 1:1 complex to aggregate.)

PAGE. Compounds were dissolved in 50 mM Na phosphate buffer, pH = 7.0, and the duplexes were heated for 5 minutes at 45° C and then left at room temperature before loading into lanes. Non-denaturing polyacrylamide gels were made (19:1 crosslinker ratio [acrylamide:bis], 20% w/v% acrylamide solution from Bio-Rad Inc., Hercules, CA 94547). The gel measured 11 cm in vertical height, with a 1 mm spacer between glass plates. 12 µL of oligomer solution was

loaded into each well along with 3 μ L of 30% glycerol and gels were run vertically at 300V for approximately 2 hr leading to migrations down approximately two-thirds the length of the gel. Bands were only faintly visible by UV so the gel was subjected to standard Coomassie staining/destaining followed by visualization with UV shadowing over a fluorescent TLC plate.

CHAPTER 5

Final (Personal) Remarks

*You see things; and you say, "Why?"
But I dream things that never were; and I say, "Why not?"*
-George Bernard Shaw

After the groundbreaking, lab-making work of R. Scott Lokey creating the first aedamer and after the preliminary study of their gelling properties by John Nguyen, a good deal of foresight was shown by Mark Cubberley and Andy Zych who took it upon themselves to study the fundamental reasons of why and how linked Dan and Ndi units “become” aedamers. Though the paths of combinatorial library synthesis and supramolecular chemistry must have been tempting them to synthesize a whole host of super-sized aedamer derivatives, instead they looked towards more modest sized, but ultimately invaluable molecules.

While Mark found out why aedamers fold, elucidating the driving forces of Dan:Ndi monomer association, Andy probed the minimal folding unit to uncover how dimers truly look like when folded. The results of these meticulous basic science type of projects still impresses. These studies have expanded our thinking of aromatic interactions and revealed that chemists have tremendous opportunities to control, more so than previously believed, these noncovalent interactions for use in molecular assembly. Due to their conclusions, many

aedamer projects were being workshopped shortly after their graduation as we were only limited by our imagination and not the properties of our molecules.

After the studies of Cubberley and Zych there was a promise of “designablility” based on their rules of association (Chapter 1). In this dissertation it was shown that the same interaction that caused a string of beads to zig-zag could also weave the string into a turn (designed folding) and unite two different strings together (designed binding). Even the gelling properties (folding) and enzyme refolding inhibition (binding) may be revealed, with better analyses, to be dependant on (and possibly controllable by) directed aromatic interactions.

Alas, the subtleties of how to fully manipulate these particular properties have thus far eluded us. Keep in mind though that this was the lab’s first pass at trying to take advantage of the designability of naphthyl oligomers. Though the rules of aromatic association have served me well, true mastery of these systems will likely require constant revision of these rules and several leaps of faith; into mindsets contrary to previous thinking, into experiments that none of your labmates believe will work, and into areas where no one in the group has ventured.

*Waiting for the time when I can finally say
That this has all been wonderful but now I'm on my way.
But when I think it's time
To leave it all behind
I try to find a way
But there's nothing I can say
To make it stop.
-Lyrics by Tom Marshall*

References

- Aamer, K. A.; Sardinha, H.; Bhatia, S. R.; Tew, G. N. "Rheological studies of PLLA-PEO-PLLA triblock copolymer hydrogels" *Biomaterials* (2003), 35, 1087.
- Albrecht, M. "Let's twist again - Double-stranded, triple-stranded, and circular helicates" *Chem. Rev.* (2001), 101, 3457.
- Amabilino, D. B.; Ashton, P. R.; Brown, C. L.; Cordove, E.; Godinez, L. A.; Goodnow, T. T.; Kaifer, A. E.; Newton, S. P.; Pietraszkiewicz, M.; Philp; Raymo, F. M.; Reder, A. S.; Rutland, M. T.; Slawin, A. M. Z.; Spencer, N.; Stoddart, J. F. "Molecular meccano. 2. Self-assembly of [n]catenanes" *J. Am. Chem. Soc.* (1995), 117, 1271.
- Amabilino D. B., Stoddart J. F. "Interlocked and intertwined structures and superstructures" *Chem. Rev.* (1995), 95, 2725.
- Anfinsen, C. B. In "Molecular Organization and Biological Function" Allen, J. M., Ed.; Harper and Row: New York, (1967), 1-19.
- Appella, D. H.; Christianson, L. A.; Karle, I. L.; Powell, D. R.; Gellman, S. H. "β-Peptides foldamers: Robust helix formation in a new family of β-amino acid oligomers" *J. Am. Chem. Soc.* (1996), 118, 13071.
- Appella, D. H.; Christianson, L. A.; Klein, D. A.; Powell, D. R.; Huang, X.; Barchi, J. J., Jr.; Gellman, S. H. "Residue-based control of helix shape in β-peptides oligomers" *Nature* (1997), 387, 381.
- Appella, D. H.; LePlae, P. R.; Raguse, T. L. Gellman, S. H. "(R,R,R)-2,5-Diaminocyclohexanecarboxylic acid, a building block for water-soluble, helix-forming β-peptides" *J. Org. Chem.* (2000), 65, 4766.
- Archer, E. A.; Gong, H.; Krische, M. J. "Hydrogen bonding in noncovalent synthesis: Selectivity and the directed organization of molecular strands" *Tetrahedron* (2001), 57, 1139.
- Archer, E. A.; Krische, M. J. "Duplex oligomers defined via covalent casting of a one-dimensional hydrogen-bonding motif" *J. Am. Chem. Soc.* (2002a), 124, 5074.

- Archer, E. A.; Cauble, D. F.; Lynch, V.; Krische, M. J. "Synthetic duplex oligomers: Optimizing interstrand affinity through the use of a noncovalent constraint" *Tetrahedron* (2002b), 58, 721.
- Benner S. A; Hutter D. "Phosphates, DNA, and the search for nonterrean life: A second generation model for genetic molecules" *Bioorg. Chem.* (2002), 30, 62.
- Berl, V.; Huc, I.; Khoury, R. G.; Krische, M. J.; Lehn, J.-M. "Interconversion of single and double helices formed from synthetic molecular strands" *Nature* (2000), 407, 720.
- Berl, V.; Huc, I.; Khoury, R. G.; Lehn, J.-M. "Helical molecular programming: supramolecular double helices by dimerization of helical oligopyridine-dicarboxamide strands" *Chem.-Eur. J.* (2001), 7, 2810.
- Bisson, A. P.; Carver, F. J.; Hunter, C. A.; Waltho, J. P. "Molecular zippers" *J. Am. Chem. Soc.* (1994), 116, 10292.
- Bisson, A. P.; Carver, F. J.; Eggleston, D. S.; Haltiwanger, R. C.; Hunter, C. A.; Livingstone, D. L.; McCabe, J. F.; Rotger, C.; Rowan, A. E. "Synthesis and recognition properties of aromatic amide oligomers: Molecular zippers" *J. Am. Chem. Soc.* (2000), 122, 8856.
- Brandon, C.; Tooze, J. "Introduction to Protein Structure" 2nd ed; Garland: New York, (1999).
- Brenner, M.; Seebach, D. "Synthesis and CD spectra in MeCN, MeOH, and H₂O of γ -oligopeptides with hydroxy groups on the backbone" *Helv. Chem. Acta* (2001), 84, 1181.
- Butterfield S. M.; Waters, M. L. "Contribution of aromatic interactions to α -helix stability" *J. Am. Chem. Soc.* (2002), 124, 9751.
- Butterfield S. M.; Waters, M. L. "A designed β -hairpin peptide for molecular recognition of ATP in water" *J. Am. Chem. Soc.* (2003), 125, 9580.
- Butterfield S. M.; Goodman, C. M.; Rotello, V. M.; Waters, M. L. "A peptide flavoprotein mimic: Recognition and redox potential modulation in water by a designed β hairpin" *Angew. Chem. Int. Ed.* (2004), 43, 724.
- Buxbaum, J. N.; Tagoe, C. E. "The genetics of amyloidosis" *Annu. Rev. Med.* (2000), 51, 543.

- Cantor, C. R.; Shimmel, P. R. "Biophysical Chemistry, part II: Techniques for the study of biological structure and function" W. H. Freeman: New York, (1980).
- Chan, W. C.; White, P.D. eds. "Fmoc solid phase synthesis: A practical approach" Oxford University Press: New York (2000).
- Cheng, R. P.; Gellman, S. H.; DeGrado, W. F. " β -Peptides: From structure to function" Chem. Rev. (2001), 101, 3219.
- Chichak, K. S.; Cantrill, S. J.; Pease, A. R.; Chiu, S.-H.; Cave, G. W. V.; Atwood, J. L.; Stoddart, J. F. "Molecular Borromean rings" Science (2004), 304, 1308.
- Chowdhury, S. "An overlooked dicopper(I) helicate" J. Ind. Chem. Soc. (2004), 81, 153.
- Connors, K. A. "Binding constants" Wiley: New York, (1987).
- Cozzi, F. Cinquini, M.; Annunziata, R.; Dwyer, T.; Siegel, J. S. "Polar/ π interactions between stacked aryls in 1,8-diarylnaphthalenes" J. Am. Chem. Soc. (1992), 114, 5729.
- Cubberley, M. S.; Iverson, B. L. "Models of higher-order structure: Foldamers and beyond" Curr. Opin. Chem. Biol. (2001a), 5, 650.
- Cubberley, M. S.; Iverson, B. L. " ^1H NMR investigation of solvent effects in aromatic stacking interactions" J. Am. Chem. Soc. (2001b), 123, 7560.
- Cubberley, M. S. Ph.D. thesis, "Investigation of solvent effects in aromatic electron donor-acceptor interactions" The University of Texas at Austin (2000).
- Ercolani, G. "Assessment of cooperativity in self-assembly" J. Am. Chem. Soc. (2003), 125, 16097.
- Ferguson, S. B.; Sanford, E. M.; Seward, E. M.; Diederich, F. "Cyclophane-arene inclusion complexation in protic solvents
- Feynman, R. P. "There's Plenty of Room at the Bottom" Transcript of a talk given on December 29, 1960 at the annual meeting of the American Physical Society. (1960), From <http://clsdemo.caltech.edu/archive/00000047/>.

- Frackenhohl, J.; Arvidsson, P. I.; Schreiber, J. V.; Seebach, D. "The outstanding biological stability of β - and γ -peptides toward proteolytic enzymes: an in vitro investigation with fifteen peptidases" *ChemBioChem* (2001), 2, 445.
- Gabriel, G. J.; Iverson, B. L. "Aromatic oligomers that form hetero duplexes in aqueous solutions" *J. Am. Chem. Soc.* (2002), 124, 15174.
- Gabriel, G. J.; Iverson, B. L. "Refolding inhibition by an amphiphilic foldamer" (2004a, in preparation).
- Gabriel, G. J.; Sorey, S.; Iverson, B. L. "Switching the folding patterns of naphthyl trimers" *J. Am. Chem. Soc.* (2004b, submitted).
- Gellman, S. H. "Foldamers: A manifesto" *Acc. Chem. Res.* (1998), 31, 173.
- Ghosh, S.; Ramakrishnan, S. "Aromatic donor-acceptor charge-transfer and metal-ion-complexation-assisted folding of a synthetic polymer" *Angew. Chem., Int. Ed.* (2004), 43, 3264.
- Gil, V. M. S.; Oliveira, N. C. "On the use of the method of continuous variations" *J. Chem. Educ.* (1990), 67, 473.
- Gill, S. J.; Dec, S. F.; Olofsson, G.; Wadso, I. "Anomalous heat capacity of hydrophobic solvation" *J. Phys. Chem.* (1985), 89, 3758.
- Gin, M. S.; Yokozawa, T.; Prince, R. B.; Moore, J. S. "Helical bias in solvophobic folded oligo(phenylene ethynylene)s" *J. Am. Chem. Soc.* (1999), 121, 2643.
- Glover, J. N.; Harrison, S. C. Crystal structure of the heterodimeric bZIP transcription factor c-Fos-c-Jun bound to DNA. *Nature* (1995), 373, 257.
- Goddard, T. D.; Kneller, D. G. SPARKY 3 (Version 3.85), University of California, San Francisco (2000).
- Gong, B. "Specifying non-covalent interactions: Sequence-specific assembly of hydrogen-bonded molecular duplexes" *Synlett* (2001), 582.
- Guelev, V.; Sorey, S.; Hoffman, D.W.; Iverson, B. L. "Changing DNA grooves - A 1,4,5,8-naphthalene tetracarboxylic diimide bis-intercalator with the linker (β -Ala) $_3$ -Lys in the minor groove" *J. Am. Chem. Soc.* (2002), 124, 2864.

- Guelev, V. M.; Cubberley, M. S.; Murr, M. M.; Lokey, R. S.; Iverson, B. L. "Design, synthesis, and characterization of polyintercalating ligands" *Methods in Enzymology* (2001a), 340, 556.
- Guelev, V.; Lee, J.; Ward, J.; Sorey, S.; Hoffman, D. W.; Iverson, B. L. "Peptide bis-intercalator binds DNA via threading mode with sequence specific contacts in the major groove" *Chem. Biol.* (2001b), 8, 415.
- Guelev, V. M. Ph.D. thesis, "Peptide-based DNA intercalators" The University of Texas at Austin (2001c).
- Guelev, V. M.; Harting, M. T.; Lokey, R. S.; Iverson, B. L. "Altered sequence specificity identified from a library of DNA-binding small molecules" *Chem. Biol.* (2000), 7, 1.
- Guinto, E. R.; Di Cera, E. "Large heat capacity change in a protein-monvalent cation interaction" (1996), *Biochemistry*, 35, 10300.
- Hill, D. J.; Mio, M. J.; Prince, R. B.; Hughes, T. S.; Moore, J. S. "A field guide to foldamers" *Chem. Rev.* (2001), 101, 3893.
- Hirao, I.; Kawai, G.; Yoshizawa, S.; Nishimura, Y.; Ishido, Y.; Watanabe, K.; Miura, K.-I. "Most compact hairpin-turn structure exerted by a short DNA fragment, d(GCGAAGC) in solution: an extraordinary stable structure resistant to nucleases and heat" *Nuc. Acid Res.* (1994), 22, 576.
- Hunter, C. A.; Sanders, J. K. M. "The nature of π - π interactions" *J. Am. Chem. Soc.* (1990), 112, 5525.
- Hunter, C. A.; Lawson, K. R.; Perkins, J.; Urch, C. J. "Aromatic interactions" *Chem. Soc., Perkin Trans. 2*, (2001), 651.
- Hunter, C. A.; Jones, P. S.; Tiger, P. M. N.; Tomas, S. "New building blocks for the assembly of sequence selective molecular zippers" *Chem. Comm.* (2003), 14, 1642.
- HyperCube, Inc. HyperChem Computational Chemistry Manual. (Gainesville, FL, 32601) (1996) HyperChem 5.1.
- Ilhan, F.; Gray, M.; Blanchette, K.; Rotello, V. M. "Control of polymer solution structure via intra- and intermolecular aromatic stacking" *Macromolecules* (1999), 32, 6159.

- Johnston, M. D., Jr.; Martin, G. E. "Establishing long-range connectivities in polynuclear aromatics through the use of two-dimensional MLEV-17-based isotropic mixing" *Mag. Reson. Chem.* (1989), 27, 529.
- Jourdan, M.; Griffiths-Jones, S. R.; Searle, M. S. "Folding of a β -hairpin peptide derived from the N-terminus of ubiquitin" *Eur. J. Biochem.* (2000), 267, 3539.
- Junquera, E.; Nowick, J. S. "Folding of an artificial β -sheet in competitive solvents" *J. Org. Chem.* (1999), 64, 2527.
- Kawano, S.-I.; Fujita, N.; Shinkai, S. "A coordination gelator that shows a reversible chromatic change and sol-gel phase-transition behavior upon oxidative/reductive stimuli" *J. Am. Chem. Soc.* (2004), 126, 8592.
- Kirshenbaum, K.; Barron, A. E.; Goldsmith, R. A.; Armand, P.; Bradley, E. K.; Truong, K. T. V.; Dill, K. A.; Cohen, F. E.; Zuckermann, R. N. "Sequence-specific polypeptoids: a diverse family of heteropolymers with stable secondary structure" *Proc. Natl. Acad. Sci. U. S. A.* (1998), 95, 4303.
- Kubik, S. "High-performance fibers from spider silk" *Angew. Chem., Int. Ed.* (2002), 41, 2721.
- Kuehl, C.J.; Tabellion, F. M.; Arif, A. M.; Stang, P. J. "Single- and double-stranded chains assembled via concomitant metal coordination and hydrogen bonding" *Organometallics* (2001), 20, 1956.
- LaBrenz, S. R.; Kelly, J. W. "Peptidomimetic host that binds a peptide guest affording a β -sheet structure that subsequently self-assembles" A simple receptor mimic. *J. Am. Chem. Soc.* (1995), 117, 1655.
- Langenhan, J. M.; Gellman, S. H. "Effects of alternative side chain pairings and reverse turn sequences on antiparallel sheet structure in β -peptide hairpins" *Org. Lett.* (2004), 6, 937.
- Langer, R.; Peppas, N. A. "Advances in biomaterials, drug delivery, and bionanotechnology" *AIChE J.* (2003), 49, 2990.
- Lehn, J.-M.; Rigault, A.; Siegel, J.; Harrowfield, J.; Chevrier, B.; Moras, D. "Spontaneous assembly of double-stranded helicates from oligobipyridine ligands and copper(I) cations: structure of an inorganic double helix" *Proc. Natl. Acad. Sci. U.S.A.* (1987), 84, 2565.

- Lee, J.-Y. Guelev, V.; Sorey, S.; Hoffman, D. W.; Iverson, B. L. "NMR structural analysis of a modular threading tetra-intercalator" *J. Am. Chem. Soc.* (2004 submitted).
- Liao, M.-J.; Prestegard, J. H. "Fusion kinetics of phosphatidylcholine-phosphatidic acid mixed lipid vesicles" *Biochim. Biophys. Acta.* (1980), 599, 81.
- Lilley, D. M. J. "Folding and catalysis by the hairpin ribozyme" *FEBS Lett.* (1999), 452, 26.
- Liu, D.; DeGrado, W. F. "De novo design, synthesis, and characterization of antimicrobial β -peptides" *J. Am. Chem. Soc.* (2001), 123, 7553.
- Lokey, R. S.; Iverson, B. L. "Synthetic molecules that fold into a pleated secondary structure in solution" *Nature* (1995), 375, 303.
- Lokey, R. S. Ph.D. thesis, "Aedamers: A synthetic approach to higher-order structure" The University of Texas at Austin (1997).
- Macomber, R. S. "An introduction to NMR titration for studying rapid reversible complexation" *J. Chem. Educ.* (1992), 69, 375.
- Mao, C.; Sun, W.; Seeman, N. C. "Assembly of Borromean rings from DNA" *Nature* (1997), 386, 137.
- Marshall, K. A.; Robertson, M. P.; Ellington, A. D. "A biopolymer by any other name would bind as well: a comparison of the ligand-binding pockets of nucleic acids and proteins" *Structure (London)* (1997), 5, 729.
- Martin, G. E.; Crouch, R. C. in "Two-Dimensional NMR Spectroscopy: Applications of Chemists and Biochemists" Croasmum, W. R.; Carlson, R. M., Eds; VCH Publishers: New York, (1994).
- Menger, F. M.; Peresypkin, A. V. "Strings of vesicles: Flow behavior in an unusual type of aqueous gel" *J. Am. Chem. Soc.* (2003), 125, 5340.
- Meyer, E. A.; Castellano, R. K.; Diederich, F. "Interactions with aromatic rings in chemical and biological recognition" *Angew. Chem., Int. Ed.* (2003), 42, 1210.
- Microcal Inc. VP-ITC MicroCalorimeter user's manual. ORIGIN software package included. Northhampton, MA 01060, (1999). Personal communications with technicians there were also helpful.

- Miller, C. T.; Weragoda, R.; Izbicka, E.; Iverson, B. L. "The synthesis and screening of 1,4,5,8-naphthalenetetracarboxylic diimide-peptide conjugates with antibacterial activity" *Bio. Med. Chem.* (2001), 9, 2015.
- Mio, M. J.; Prince, R. B.; Moore, J. S.; Kuebel, C.; Martin, D. C. "Hexagonal packing of oligo(m-phenylene ethynylene)s in the solid state: Helical nanotubules" *J. Am. Chem. Soc.* (2000), 122, 6134.
- Murphy, K. P. "Predicting binding energetics from structure: Looking beyond ΔG " *Med. Res. Rev.* (1999), 19, 333.
- Murphy, J. E.; Uno, T.; Hamer, J. D.; Cohen, F. E.; Dwarki, V.; Zuckermann, R. N. "A combinatorial approach to the discovery of efficient cationic peptoid reagents for gene delivery" *Proc. Natl. Acad. Sci. U. S. A.* (1998), 95, 1517.
- Murr, M. M.; Harting, M. T.; Guelev, V.; Ren, J.; Chaires, J. B.; Iverson, B. L. "An octakis-intercalating molecule" *Bio. Med. Chem.* (2001), 9, 1141.
- Naghibi, H.; Tamura, A.; Sturtevant, J. M. "Significant discrepancies between van't Hoff and calorimetric enthalpies" *J. Proc. Natl. Acad. Sci. USA*, (1995), 92, 5597.
- Nassar, N.; Horn, G.; Herrmann, C.; Scherer, A.; McCormick, F.; Wittinghofer, A. "A crystal structure of the Ras-binding domain of the serine/threonine kinase c-Raf1 in complex with Rap1A and a GTP analogue" *Nature* (1995), 375, 554.
- Nelson, J. C.; Saven, J. G.; Moore, J. S.; Wolynes, P. G. "Solvophobically driven folding of nonbiological oligomers" *Science* (1997), 277, 1793.
- Nguyen, J. Q.; Iverson, B. L. "An amphiphilic folding molecule that undergoes an irreversible conformational change" *J. Am. Chem. Soc.* (1999), 121, 2639.
- Nolan, S. L.; Phillips, R. J.; Cotts, P. M.; Dungan, S. R. "Light scattering study on the effect of polymer composition on the structural properties of PEO-PPO-PEO micelles" *J. Coll. Inter. Sci.* (1997), 191, 291.
- Nowick, J. S.; Powell N. A.; Martinez, E. J.; Smith, E. M.; Noronha, G. "Molecular scaffolds. 1. Intramolecular hydrogen bonding in a family of di- and triureas" *J. Org. Chem.* (1992), 57, 3763.

- Nowick, J. S.; Holmes D. L.; Mackin, G.; Noronha, G.; Shaka, A. J.; Smith, E. M. "An artificial β -sheet comprising a molecular scaffold, a β -strand mimic, and a peptide strand" *J. Am. Chem. Soc.* (1996), 118, 2764.
- Nowick, J. S. "Chemical models of protein β -sheets" *Acc. Chem. Res.* (1999), 32, 287.
- Newcomb, L. F.; Gellman, S. H. "Aromatic stacking interactions in aqueous solutions: Evidence that neither classical hydrophobic effects nor dispersion forces are important" *J. Am. Chem. Soc.* (1994), 116, 4993.
- Pecora, R. "Dynamic light scattering: Applications of photon correlation spectroscopy" Plenum Press: New York, (1985).
- Perez-Rodriguez, M.; Prieto, G.; Rega, C.; Varela, L. M.; Sarmiento, F.; Mosquera, V. "A comparative study of the determination of the critical micelle concentration by conductivity and dielectric constant measurements" *Langmuir* (1998), 14, 4422.
- Petka, W. A.; Harden, J. L.; McGrath, K. P.; Wirtz, D.; Tirrell, D. A. "Reversible hydrogels from self-assembling artificial proteins" *Science* (1998), 281, 389.
- Philp, D.; Stoddart, J. F. "Self-assembly in natural and unnatural systems" *Angew. Chem. Int. Ed. Engl.* (1996), 35, 1154.
- Pochan, D. J.; Schneider, J. P.; Kretsinger, J.; Ozbas, B.; Rajagopal, K.; Haines, L. "Thermally reversible hydrogels via intramolecular folding and consequent self-assembly of a de novo designed peptide" *J. Am. Chem. Soc.* (2003), 125, 11802.
- Prince, R. B.; Brunsveld, L.; Meijer, E. W.; Moore, J. S. "Twist sense bias induced by chiral side chains in helically folded oligomers" *Angew. Chem., Int. Ed.* (2000a), 39, 228.
- Prince, R. B.; Barnes, S. A.; Moore, J. S. "Foldamer-Based Molecular Recognition" *J. Am. Chem. Soc.* (2000b), 122, 2758.
- Quinn, T. P.; Tweedy, N. B.; Richardson, J. S.; Williams, R. W.; Richardson, D. C. "Betadoublet: de novo design, synthesis, and characterization of a β -sandwich protein" *Proc. Natl. Acad. Sci. U. S. A.* (1994), 91, 8747.

- Raguse, T. L.; Lai, J. R.; LePlae, P. R.; Gellman, S. H. "Toward β -peptide tertiary structure: Self-association of an amphiphilic 14-helix in aqueous solutions" *Org. Lett.* (2001), 3, 3963.
- Ramachandran, G. N.; Sasisekharan, V. In "Advances in Protein Chemistry" Anfinsen, C. B. J., Anson, M. L., Edsall, J. T., Richards, F. M., Eds.; Academic Press: New York, (1968), Vol. 23.
- Reczek, J. J. X-ray quality crystals of the bis(diethylene glycol) Dan in figure 1.7B could only be obtained by sublimation at 180° C at vacuum pump pressures (2002).
- Robertson, A. D.; Murphy, K. P. "Protein structure and the energetics of protein stability" *Chem. Rev.* (1997), 97, 1251.
- Rouhi, M; "Intriguing behavior of a folded polymer" *Chem. Eng. News* (March 29, 1999), 8.
- Rowan, S. J.; Cantrill, S. J.; Cousins, G. R. L.; Sanders, J. K. M.; Stoddart, J. F. "Dynamic covalent chemistry" *Angew. Chem., Int. Ed.* (2002), 41, 899.
- Ruso, J. M.; Attwood, D.; Taboada, P.; Mosquera, V.; Sarmiento, F. "Light scattering and NMR studies on the self-aggregation of sodium n-hexyl sulfate in aqueous electrolyte solution" *Langmuir* (2000), 16, 1620.
- Sambrook, J.; Russell, D. W.; "Molecular cloning: A laboratory manual, 3rd edition" Cold Spring Harbor Laboratory Press: New York, (2001).
- Searle, M. S. "Peptide models of protein β -sheets: design, folding and insights into stabilizing weak interactions" *J. Chem. Soc. Perkin Trans. 2* (2001), 1011.
- Seebach, D.; Abele, S.; Gademann, K.; Guichard, G.; Hintermann, T.; Jaun, B.; Matthews, J. L.; Schreiber, J. V.; Oberer, L.; Hommel, U.; Widmer, H. " β 2- and β 3-peptides with proteinaceous side-chains. Synthesis and solution structures of constitutional isomers, a novel helical secondary structure, and the influence of solvation and hydrophobic interactions on folding" *Helv. Chim. Acta* (1998), 81, 932.
- Seebach, D.; Abele, S.; Gademann, K.; Jaun, B. "Pleated sheets and turns of β -peptides with proteinaceous side-chains" *Angew. Chem., Int. Ed.* (1999), 38, 1595.

- Seidler, J.; McGovern, S. L.; Doman, T. N.; Shoichet, B. K. "Identification and prediction of promiscuous aggregating inhibitors among known drugs" *J. Med. Chem.* (2003), 46, 4477.
- Simon, R. J.; Kania, R. S.; Zuckermann, R. N.; Huebner, V. D.; Jewell, D. A.; Banville, S.; Ng, S.; Wang, L.; Rosenberg, S.; Marlowe, C. K.; Spellmeyer, D. C.; Tan, R.; Frankel, A. D.; Santi, D. V.; Cohen, F. E.; Bartlett, P. A. "Peptoids: A modular approach to drug discovery" *Proc. Natl. Acad. Sci. U.S.A.* (1992), 89, 9367.
- Smithrud, D. B.; Diederich, F. "Strength of molecular complexation of apolar solutes in water and in organic solvents is predictable by linear free energy relationships: a general model for solvation effects on apolar binding" *J. Am. Chem. Soc.* (1990), 112, 339.
- Smithrud, D. B.; Wyman, T. B.; Diederich, F. "Enthalpically Driven Cyclophane-Arene Inclusion Complexation: Solvent-Dependent Calorimetric Studies" *J. Am. Chem. Soc.* (1991), 113, 5420.
- Soto, A. M.; Kankia, B. I.; Dande, P.; Gold, B.; Marky, L. A. "Incorporation of a cationic aminopropyl chain in DNA hairpins: thermodynamics and hydration" *Nuc. Acid Res.* (2001), 29, 3638.
- Stoddart, J. F. "Molecular machines" *Acc. Chem. Res.* (2001), 34, 410.
- Stojanovic, M. N.; DePrada, P.; Landry, D. W. "Fluorescent sensors based on aptamer self-assembly" *J. Am. Chem. Soc.* (2000), 122, 11547.
- Stone, M. T.; Moore, J. S. "A water-soluble m-phenylene ethynylene foldamer" *Org. Lett.* (2004), 6, 469.
- Tanatani, A.; Mio, M. J.; Moore, J. S. "Chain length-dependent affinity of helical foldamers for a rodlike guest" *J. Am. Chem. Soc.* (2001), 123, 1792.
- Tanatani, A.; Yamaguchi, K.; Azumaya, I.; Fukutomi, R.; Shudo, K.; Kagechika, H. "N-methylated diphenylguanidines: Conformations, propeller-type molecular chirality, and construction of water soluble oligomers with multilayered aromatic structures" *J. Am. Chem. Soc.* (1998), 120, 6433.
- Tanford, C. "The hydrophobic effect: Formation of micelles and biological membranes" 2nd ed.; Wiley: New York (1980).

- Tatko, C. D.; Waters, M. L. "Selective aromatic interactions in β -hairpin peptides" *J. Am. Chem. Soc.* (2002), 124, 9372.
- Tatko, C. D.; Waters, M. L. "Comparison of C-H $\cdots\pi$ and hydrophobic interactions in a β -hairpin peptide: Impact on stability and specificity" *J. Am. Chem. Soc.* (2004), 126, 2028.
- Telfer, S. G.; Sato, T.; Kuroda, R. "Noncovalent ligand strands for transition-metal helicates: The straightforward and stereoselective self-assembly of dinuclear double-stranded helicates using hydrogen bonding" *Angew. Chem., Int. Ed.* (2004), 43, 581.
- Tsai, J. H.; Waldman, A. S.; Nowick, J. S. "Two new β -strand mimics" *Bioorg. Med. Chem.* (1999), 7, 29.
- Varela, L. M.; Rega, C.; Suarez-Fillooy, M. J.; Ruso, J. M.; Prieto, G.; Attwood, D.; Sarmiento, F.; Mosquera, V. "Self-association of penicillin V in aqueous solution" *Langmuir* (1999), 15, 6285.
- Venkatraman, J.; Shankaramma, S. C.; Balaram, P. "Design of folded peptides" *Chem. Rev.* (2001), 101, 3131.
- Vollrath, F. "Strength and structure of spiders' silk" *Rev. Mol. Biotech.* (2000), 74, 67.
- von Kiedrowski, G.; Sievers, D. "Self-replication of complementary nucleotide-based oligomers" *Nature* (1994), 369, 221.
- Wadso, I. "Trends in isothermal microcalorimetry" *Chem. Soc. Rev.* (1997), 26, 79.
- Waters, M. L. "Aromatic interactions in model systems" *Curr. Opin. Chem. Biol.* (2002), 6, 736.
- Wang, J. C. "DNA topoisomerases: Why so many?" *J. Biol. Chem.* (2001), 266, 6659.
- Weigard, H.; Wirz, B.; Schweitzer, A.; Camenisch, G. P.; Perez, M. I. R.; Gross, G.; Woessner, R.; Voges, R.; Arvidsson, P. I.; Frackenpohl, J.; Seebach, D. "The outstanding metabolic stability of a ^{14}C -labeled β -nonapeptide in rats - *in vitro* and *in vivo* pharmacokinetic studies" *Biopharmaceutics & Drug Disposition* (2002), 23, 251.

- Werder, M.; Hauser, H.; Abele, S.; Seebach, D. "β-Peptides as inhibitors of small-intestinal cholesterol and fat absorption" *Helv. Chem. Acta* (1999), 82, 1774.
- Whitford, D.; Concar, D. W.; Williams, R. J. P. "The promotion of self-association of horse-heart cytochrome C by hexametaphosphate anions" *Eur. J. Biochem.* (1991), 199, 561.
- Wilchek, M.; Bayer, E. A. "Methods in enzymology: Avidin-biotin technology" vol 184. Academic Press: San Diego, (1990).
- Wilcox, C. S.; Glagovich, N. M. HOSTEST program v.5.60. Department of Chemistry, The University of Pittsburgh; Pittsburgh, PA. (1997).
- Wiseman, T.; Williston, S.; Brandts, J. F.; Lin, L. N. "Rapid measurement of binding constants and heats of binding using a new titration calorimeter" *Anal. Biochem.* (1989), 179, 131.
- Yeates, T. O.; Padilla, J. E. "Designing supramolecular assemblies" *Curr. Opin. Struct. Biol.* (2002), 12, 464.
- Zeng, H.; Ickes, H.; Flowers, R. A., II; Gong, B. "Sequence specificity of hydrogen-bonded molecular duplexes" *J. Org. Chem.* (2001), 66, 3574.
- Zeng, H.; Yang, X.; Flowers, R. A., II; Gong, B. "A noncovalent approach to antiparallel β-sheet formation" *J. Am. Chem. Soc.* (2002), 124, 2903.
- Zhang, W.; Horoszewski, D.; Decatur, J.; Nuckolls, C. "A folded, secondary structure in step-growth oligomers from covalently linked, crowded aromatics" *J. Am. Chem. Soc.* (2003), 125, 4870.
- Zhao, X.; Jia, M.-X.; Jiang, X. K.; Wu, L.-Z.; Li, Z.-T.; Chen, G.-J. "Zipper-featured δ-peptide foldamers driven by donor-acceptor interaction. Design, synthesis, and characterization" *J. Org. Chem.* (2004), 69, 270.
- Zhou, Q.-Z.; Jiang, X. K.; Shao, X.-B.; Chen, G.-J.; Jia, M.-X.; Li, Z.-T. "First zipper-featured molecular duplexes driven by cooperative donor-acceptor interaction" *Org. Lett.* (2003), 5, 1955. [Addition/Correction; (2003), 5, 2763.]
- Zutshi, R.; Franciskovich, J.; Shultz, M.; Schweitzer, B.; Bishop, P.; Wilson, M.; Chmielewski, J. "Targeting the dimerization interface of HIV-1 protease:

inhibition with cross-linked interfacial peptides” J. Am. Chem. Soc. (1997), 119, 4841.

Zych, A. J.; Iverson, B. L. “Synthesis and conformational characterization of tethered, self-complexing 1,5-dialkoxynaphthalene / 1,4,5,8-naphthalenetetracarboxylic diimide systems” J. Am. Chem. Soc. (2000), 122, 8898.

Zych, A. J. Ph.D. thesis, “Conformational characterization of non-natural secondary structures based on aromatic stacking” The University of Texas at Austin (2001).

Zych, A. J.; Iverson, B. L. “Conformational modularity of an abiotic secondary-structure motif in aqueous solution” *Helv. Chim. Acta* (2002), 85, 3294.

Vita

Gregory John Gabriel was born on November 16, 1975 in New York City, the first of three sons of Dr. Juan B. Gabriel Jr. and Connie Monroy Gabriel. He grew up mostly in New York (in the neighborhood of Astoria) and Emporia, KS. He attended Northern Valley Regional High School in Demarest, NJ and graduated in 1994. Crossing the GW Bridge to return to the city, he attended New York University. In Professor Jim Canary's group he initiated experiments to measure association constants of ternary systems modeled after zinc enzymes. After graduating in 1998 with a BS in Chemistry, he joined Professor Iverson's group at the University of Texas at Austin to pursue his PhD degree. At UT he explored the controlled self-assembly of artificial folding molecules (by making unusual structures with interlocking building blocks). So, although he has no endearing stories of childhood scientific curiosities nor has he ever owned a chemistry set, his days as a kid playing with Legos (making unusual structures with interlocking building blocks) seemed to have had a lasting effect.

Permanent Address: 46 County Rd., Demarest, NJ 07627

This dissertation was typed by the author.